REPORT DOCUMENTATION PAGE

AFRL-SR-AR-TR-03-

0261

1. AGENCY USE ONLY *(Leave blank)*	2. REPORT DATE	3. REPORT TYPE AND DATES COVERED
	27-JUN-03	FINAL (01-JAN-2003 TO 31-DEC-2002)

4. TITLE AND SUBTITLE
OXIDE/OXIDE CERAMICS AND COMPOSITES MEETING

5. FUNDING NUMBERS
F49620-02-0088

6. AUTHOR(S)
PROFESSOR A. SAYIR

7. PERFORMING ORGANIZATION NAME(S) AND ADDRESS(ES)
CASE WESTERN UNIVERSITY
10900 EUCLID AVENUE
CLEVELAND, OH 44108-7204

8. PERFORMING ORGANIZATION REPORT NUMBER

9. SPONSORING/MONITORING AGENCY NAME(S) AND ADDRESS(ES)
AFOSR/NA
4015 WILSON BOULVARD
ARLINGTON, VA 22203

10. SPONSORING/MONITORING AGENCY REPORT NUMBER

11. SUPPLEMENTARY NOTES

12a. DISTRIBUTION AVAILABILITY STATEMENT

Approved for public release;
distribution unlimited.

13. ABSTRACT *(Maximum 200 words)*

Advanced materials are usually composite materials for structural components to carry loads and/or functional components to accomplish specific tasks. Oxide ceramic, oxide fiber reinforced ceramic composites and in-situ composites stand out as those which provide best properties in oxidizing environment. The oxide materials are essential to withstand severe loads in the oxidizing environment a severe conditions. The oxide ceramics and oxide composites is a crucial research area because it's importance to air breathing engine technology of US Air Force, Department of defense and US civilian industry. The components of the oxide ceramics and their composites are essential for the future aerospace industry and the information of their behavior is critical to understand the response of composites. Three focused topical session on the Oxide ceramics and Composites has been organized at the 27~ Annual Cocoa Beach Conference and Exposition on Advanced Ceramics & Composites meeting. These sessions were:

(i) Intrinsic Properties of Oxides (Magnetic, Electrical, Optical, Mechanical),
(ii) Microstructures and Mechanical Behavior
(iii) Novel Processing Techniques.

The proposed meeting provided a forum for discussing the essential scientific issues involved in the development and use of high temperature materials.

14. SUBJECT TERMS			15. NUMBER OF PAGES
			16. PRICE CODE
17. SECURITY CLASSIFICATION OF REPORT	18. SECURITY CLASSIFICATION OF THIS PAGE	19. SECURITY CLASSIFICATION OF ABSTRACT	20. LIMITATION OF ABSTRACT
UNCLASSIFIED	UNCLASSIFIED	UNCLASSIFIED	

Final Report

F49620-02-1-088

Focused Topical Session: Oxide/Oxide ceramics and Composites Meeting At the 27th Annual Cocoa Beach Conference and Exposition on Advanced Ceramics & Composites

by

A. Sayir

CASE WESTERN RESERVE UNIVERSITY

June 15, 2003

Abstract

Focused Topical Session: Oxide/Oxide ceramics and Composites Meeting

At the 27th Annual Cocoa Beach Conference and Exposition on Advanced Ceramics & Composites

Cocoa Beach, FL

(1/26/2003 - 1/31/2003)

Advanced materials are usually composite materials for structural components to carry loads and/or functional components to accomplish specific tasks. Oxide ceramic, oxide fiber reinforced ceramic composites and *in-situ* composites stand out as those which provide best properties in oxidizing environment. The oxide materials are essential to withstand severe loads in the oxidizing environment an severe conditions. The oxide ceramics and oxide composites is a crucial research area because it's importance to air breathing engine technology of US Air Force, Department of defense and US civilian industry. The components of the oxide ceramics and their composites are essential for the future aerospace industry and the information of their behavior is critical to understand the response of composites. Three focused topical session on the Oxide ceramics and Composites has been organized at the 27th Annual Cocoa Beach Conference and Exposition on Advanced Ceramics & Composites meeting. These sessions were:

(i) **Intrinsic Properties of Oxides (Magnetic, Electrical, Optical, Mechanical),**
(ii) **Microstructures and Mechanical Behavior**
(iii) **Novel Processing Techniques.**

The proposed meeting provided a forum for discussing the essential scientific issues involved in the development and use of high temperature materials.

Focused Topical Session: Oxide/Oxide ceramics and Composites Meeting

High performance materials are usually composite materials. Oxide and oxide fiber reinforced composites stand out as those which provide the best properties in oxidizing environment. The fibers, matrices and the interfaces are the essential components in these materials and knowledge of their behavior is crucial to understand the response of composites as well as to develop new design strategies which optimize their use. The organization of three focused topical sessions on Oxide Ceramics and Composite at the 27th Annual Cocoa Beach Conference and Exposition on Advanced Ceramics & Composites (January 26/2003 through January 31/2003) was successful. The papers of the invited speakers are attached as an appendix and list of the presentation of these three sessions also included.

The purpose of this focused sessions was to bring scientists and engineers from all over the world together in order to gain an international perspective on new developments in the high temperature oxide ceramics field. There were two invited speakers from the United States, two from France, and one from Spain. The invited speakers are selected from esteemed university and research organizations on their respective continents. The list of invited speakers and the title of their papers are listed below:

1. Dickey, Elizabeth / Penn State University - USA

   "High-Temperature Residual Stress in Textured Oxide Composites".

2. Javier Llorca / Polytechnic University of Madrid - SPAIN

"Processing, Microstructure and Mechanical Behavior of Directionally-Solidified Eutectic Ceramic Oxides".

3. Léo Mazerolles / CNRS - FRANCE

   "Synthesis of Nanostructured Materials Based on Alumina"

4. *Marcelle Gaune-Escard / UISTI* – FRANCE

   "Molten Salts: A Route to Tailored Ceramics"

5. Kenneth Sandhage,/ OSU – USA

   "Bioclastic Processing of Self-Assembled, Three-Dimensional Meso/Nanostructures with Tailored Chemistries".

The main focus of the Oxide ceramics and composites was on the novel processing techniques. Good number of paper of papers on the mechanical characterization and microstructural analysis will be in session entitled Microstructures and Mechanical Behavior. The proposed meeting is expected to create a synergy between the scientist and engineers in the processing and microstructural characterization areas. An concerted effort has been dedicated during the planning time to invite the best processing scientists since their efforts usually have the long lasting impact on the community involved with the oxide ceramics and composites.

In addition to the invited speakers over 26 papers and associated abstracts from diverse backgrounds have participated at the focused topical session *Oxide/Oxide Ceramics and Composites*. In light of the imminent potential for oxide ceramic composites to advanced turbine engines and aircraft, three focused sessions were organized to bring scientists and engineers in the European community and Japan together with US researchers in order to gain an international

perspective on new developments in the high-temperature ceramics field. This provided a state-of-the-art picture of this rapidly evolving field of study. We coordinated this meeting with American ceramic Society and Air Force Office of Scientific Research to achieve productive results.

In addition, oxide material development is a paradigmatic topic in Materials Science, which needs for interdisciplinary research. In this respect, the focused oxide/oxide composite sessions was an attractive meeting point for chemists, physicists, and engineers.

Oxide Ceramics and Composites

Session: **Intrinsic Properties of Oxides (Magnetic, Electrical, Optical, Mechanical)**
10:20:00 AM - 12:00:00 PM 1/29/2003

Lynnette Madsen, "Opportunities in Ceramics".

Elizabeth Dickey, "High-Temperature Residual Stress in Textured Oxide Composites"
Invited

Robert Gall, "Cu-Based Transparent Conducting Oxides of the Delafossite Structure".

Robert Reeber, "Corresponding States Principles for the Thermal Expansion of Oxides of MgO, CaO , SrO and BaO"

Session: **Microstructures and Mechanical Behavior**
1:20:00 PM - 6:00:00 PM 1/29/2003

Javier Llorca, "Processing, Microstructure and Mechanical Behavior of Directionally-Solidified Eutectic Ceramic Oxides".
Invited

Kristin Keller, "Evaluation of Dense Monazite Fiber-Coatings in Oxide-Oxide Minicomposites"

Lee Pengyuan, "The Rare-Earth Phosphate Coated Fiber for Oxide CMCs".

Emmanuel Boakye, "Monazite Coatings on Nextel 720 Fiber Tows: Effect of Precursor Morpholgy Coating".

Richard Goettler, "Properties of CMC with Scheelite and Uncoated Nextel 610 Fibers".

Dong-Kyu Kim, Fibrous Monoliths of Alumina -Mullite In Situ Composite Maxtrix-Aluminum Phosphate Interphase

Pavel Mogilevsky, "Anisotropy in Room Temperature Deformation and Fracture in CaWO4 Sheelite".

Javier Llorca, "Deformation and Fracture Mechanisms of Single Crystal ZrO2(Er2O3)".

Waltraud Kriven, "In Situ High-Temperature Phase Transformation in YNbO4"

Derek Northwood, "The Effect of a High Strength Electric Field on the Low Temperature Degradation of a Y-TZP Ceramic".

Hitomi Yamaguchi, "Magnetic Field-Assisted Machining for Internal Parts of Alumina Ceramic Components".

Paul-Francois Paradis, "Contactless Density Measurement of Liquid Nd-Doped 50%CaO-50%Al2O3"

Session: **Novel Processing Techniques**
8:00:00 AM - 12:00:00 PM 1/30/2003

Jun Akedo, "Aerosol Deposition (ADM) for Nanocomposite Material Synthesis: - A Novel Method of Ceramics Processing Without Firing".

Léo Mazerolles, "Synthesis of Nanostructured Materials Based on Alumina".
Invited

Maxim Lebedev, "Al2O3 - PZT Nanocomposite Mixture Ceramic Layer Fabricated Using Aerosol Deposition Method".

Erik Bartscherer, "Preparation of High Density Translucent PLZT Ceramics by Hot Isostatic Pressing".

Cari August, "Rheology of Fine Alumina Pastes".

Marcelle Gaune-Escard, "Molten Salts: A Route to Tailored Ceramics"
Invited

Rolf Janssen, "Reaction Synthesis of Refractory Metal-Ceramic Composites".

Kenneth Sandhage, "Bioclastic Processing of Self-Assembled, Three-Dimensional Meso/Nanostructures with Tailored Chemistries".
Invited

Victor Orera, "Ni and Co-ZrO2 Composites Produced by Laser Zone Melting".

POSTER SESSION

Magali Pinho, "A Comparative Study of the Microstructure, Electric and Piezoelectric Properties of PZTCeramic Materials".

Hathaikarn Choosuwan, "Dielectric Relaxation and Thermal Expansion Properties of Niobium Based Oxides".

Kazuya Tsujimichi, "Mechanical and Electrical Properties of Al2O3 Thin Films on Metals, Ceramics and Resins Prepared by Aerosol Deposition Method".

Harry Gorter, "Processing and Mechanical Characterization of In Situ Reinforced Alumina Composites".

Antonio De Arellano Lopez, "Room- and High-Temperature Tensile Fracture of Directionally-Solidified Chromia-doped Sapphire Fibers".

Maria Gregori, "Synthesis and Characterization of Z-Type Hexaferrite for Use as Microwave Absorber".

Focused Topical Session: Oxide/Oxide ceramics and Composites Meeting Budget

Invited Speakers Addresses	**Estimated Expenses: Travel, registration and lodging**	
		Expected payment from AFOSR Grant
Prof.Antonia Ramirez / Uni Seville SPAIN		$600.00
Prof. Vcictor Orera / CSIC –SPAIN		$600.00
Marcelle Gaune-Escard / UISTI – FRANCE		$1,600.00
Prof. Léo Mazerolles / CNRS - FRANCE		$1,000.00
Prof. E. Dickey / PSU USA		$500.00
Prof. K. Sandhage / OSU USA		$500.00
Additional Speakers		
Dr. A. Sayir / USA (Session Co-organizer) USA		$2,577.00
Dr. Maria Souto / AUSTRIA		$2,000.00
TOTAL COSTED AMOUNT OF FUNDING		$9,497.00

27TH ANNUAL COCOA BEACH CONFERENCE AND EXPOSITION ON ADVANCED CERAMICS & COMPOSITES

IN CONJUNCTION WITH THE ACERS ELECTRONICS DIVISION FALL MEETING

Doubletree/Hilton Hotels
Cocoa Beach, Fla.
January 26-31, 2003

Ceramics and Electronics for the New Horizon

From its humble beginnings more than a quarter century ago, the "Cocoa Beach Meeting" has grown in scope and stature to become the preeminent international technical meeting on advanced ceramics and composites. The "Cocoa Beach Meeting" is synonymous with leading edge research and development in these challenging technological areas. This year's meeting will continue the proud tradition of innovative R&D technical exchanges with three directed symposia and a series of focused topical sessions. In particular, to embrace the interdisciplinary needs between structural and electronic ceramics, this year's "Cocoa Beach Meeting" will be held in conjunction with the ACerS Electronics Division Fall Meeting, which will lead to exciting new and constructive cross-community interactions and research developments.

The Cocoa Beach Meeting is a completely open scientific forum for exchange of new ideas and findings. This year's meeting will highlight recent advances, developments, and field applications in engineering ceramics, composites, and electronics, and will emphasize a wide variety of ceramic materials and technologies for the new horizon. Authors are encouraged to submit presentation abstracts for consideration on any relevant topic. Anyone with an interest in ceramic-based materials, composites, or electronic materials is invited to participate including: scientists, engineers, technical and program managers, production and sales personnel, educators, and students.

Information regarding attendance arrangements will be available later this summer. Further information will be available on The American Ceramic Society's web site at www.ceramics.org.

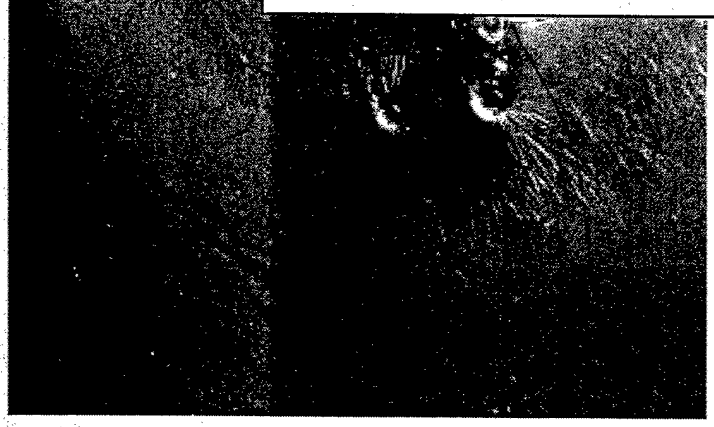

CALL FOR PAPERS

Abstract Deadline: July 12, 2002
Submit online at www.ceramics.org

Focused Topical Sessions

The following list of topics consists of technical sessions concentrated on specific areas of interest. The points of contact (POC) identified may be contacted prior to abstract submission to determine technical content relevance. Publication of the proceedings from the Focused Sessions will be included in the *Ceramic Engineering and Science Proceedings.*

Product Development and Manufacturing of Advanced Ceramics and Composites

Animesh Bose (POC), Materials Processing, Inc., USA
Phone: 817/294-0135 • E-mail: animesbose@aol.com
Elis Carlstrom, Swedish Ceramic Institute, Sweden
Charles Lewinsohn, Ceramatec Inc., USA

Opportunities and issues on product development and manufacturing of advanced ceramics and composites will be emphasized:

- Approaches to technology analysis and manufacturing feasibility studies (including lifecycle analysis)
- Integrated component design and prototyping (design with ceramics, joining/assembly)
- Processing of advanced ceramics and composites (includes all near net shape processing and consolidation techniques)
- Novel applications for engineering ceramics and composites (unconventional components and compositions)

Engineering Porous Materials

Manuel E. Brito (POC), Synergy Materials Research Center, AIST, Japan
Phone: 011-81-52-739-0135 • E-mail: manuel-brito@aist.go.jp
Heino Sieber, University of Erlangen-Nuernberg, Germany
Tatsuki Ohji, Synergy Materials Research Center, AIST, Japan

The Engineering Porous Materials focused session will emphasize, but not be limited to, the following topics:

- Advances in processing of porous materials
- Structural characterization of porous materials
- Structure-mechanical and thermal properties relationships
- Applications and design issues for porous materials
- Industrial case studies

Biomaterials

Mineo Mizuno (POC), Japan Fine Ceramics Center, Japan
Phone: 011-81-52-871-3500 • E-mail: mizuno@jfcc.or.jp
Gary Fischman, University of Illinois at Chicago, USA
Richard P. Rusin, 3M ESPE Dental Products, USA

A coordinated forum for advances in biomaterials and technologies, technical and commercialization issues, and opportunities:

- Implants, coatings, cements and drug delivery
- Biomimetic materials and synthesis

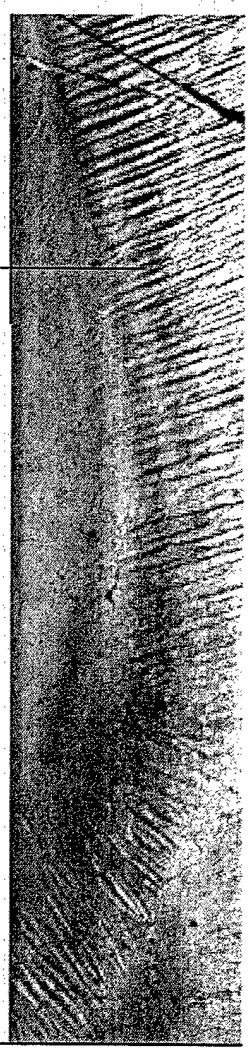

- Dental ceramics
- Bioactive and bioinert ceramics
- Structure/properties of nature ceramic-based materials
- Behavior in biological environment (in vivo, vitro)
- Synthesis, processing, characterization and properties

Synthesis and Processing of Nanomaterials

William Mullins (POC), US Army Research Office, USA
Phone: 919/549-4286 • E-mail: mullinsw@aro-emh1.army.mil
Kazunori Kijima, Kyoto Institute of Technology, Japan
Rolf Clasen, University of Saarland, Germany

A coordinated forum for advances in all aspects on the synthesis and processing of nanomaterials.

- Nanoscale synthesis
- Self-assembly, templated assembly and growth
- Nanopowders, nanostructured films and coatings
- Organic/ceramic structures
- Sintering of nanocrystalline systems
- Nanocomposite processing
- Modeling and simulation of system processing

Topics in Ceramic Armor

Jeffrey J. Swab (POC), US Army Research Laboratory, USA
Phone: 410/306-0753 • E-mail: jswab@arl.army.mil
James McCauley, Andrew Wereszczak, Jerry LaSalvia, Ernest Chin, US Army Research Laboratory, USA
Lisa Prokurat-Franks, US Tank and Automotive Research/Development and Engineering Center, USA
David Stepp, US Army Research Office, USA

This annual topical session will bring together researchers from industry, academia, and government organizations working on opaque and transparent ceramic armor. Focused sessions will emphasize, but will not be limited to, the following areas:

- Processing and manufacturing
- Ultra-lightweight, high density and transparent ceramics
- Novel material concepts
- Penetration modeling
- Testing (impact, shock and high strain rate studies, etc.)
- Damage evolution and micromechanisms

Cocoa Beach Conference Program Chair

Dr. Hua-Tay Lin
Oak Ridge National Laboratory
Metals and Ceramics Division
Building 4515, Mail Stop 6068
One Bethel Valley Road
Oak Ridge, TN 37831-6068, USA
Phone: 865/576-8857
Fax: 865/574-8445
E-mail: linh@ornl.gov

Electronics Division Program Chair

Dr. Dwight Viehland
Virginia Polytechnic Institute
Department of Materials Science and Engineering
201 Holden Hall
Blacksburg, VA 2406, USA
Phone: 540/231-2276
Fax: 540/231-8919
E-mail: viehland@mse.vt.edu

Oxide Ceramics and Composites

Ali Sayir (POC), NASA Glenn Research Center, USA
Phone: 216/433-6254 • E-mail: ali.sayir@nasa.grc.gov
Joan Fuller, Air Force Office of Scientific Research, USA
Marie-Helene Berger, Centre Des Materiaux, Ecole des Mines de Paris, France

A coordinated forum to address various scientific and technical aspects related to multiphase oxide ceramics.

- Novel processing techniques
- Microstructures and mechanical behavior
- Intrinsic properties of oxides (magnetic, electrical, optical, mechanical)
- Polyphase oxide ceramics: processing and properties

Fuel Cells: Materials, Developments and Applications

Co-sponsored by the Society for Automotive Engineering

Harlan Anderson (POC), University of Missouri-Rolla, USA
Phone: 573/341-4886 • E-mail: harlanua@umr.edu
Tim Armstrong, Oak Ridge National Laboratory, USA
Armin Reller, University of Augsburg, Germany

This session will focus on the recent advances in the scientific and technological developments, processing/properties, reliability, system design/applications, and field demonstrations and commercialization of the fuel cell materials. Specifically, contributions in the following topic areas are solicited:

- Materials processing and development of fuel cell materials
- Processing/microstructure/properties relationship
- Designing fuel cells for production/manufacturing
- Thermochemical reactivity and durability of fuel cells
- Modeling of materials transport and stability
- Environmental effects on long-term reliability
- Commercialization/demonstration status

Gas, Chemical and Biological Ceramic Sensors

Girish Kale (POC), University of Leeds, United Kingdom
Phone: 0044-113-2332805 • E-mail: g.m.kale@leeds.ac.uk
Sheikh Akbar, Ohio State University, USA
Henk Verweij, Ohio State University, USA

This session will focus on ceramic materials and related technologies for sensors and use of these sensors in industrial applications and processes.

- Novel materials and designs for sensors
- Novel or improved fabrication techniques for sensors
- Novel types of sensors and/or new sensor applications
- Theory, modeling and simulation
- Sensor data analysis and packaging
- Intrinsic capabilities or limitations of sensors or sensor materials

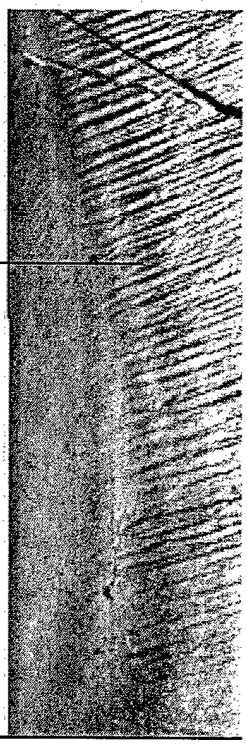

Symposium Topics

Symposium I: Mechanical Behavior and Design of Engineering Ceramics and Composites

Symposium Organizers:

Andrew Wereszczak (POC), US Army Research Laboratory, USA
Phone: 410/306-0858 • E-mail: awereszczak@arl.army.mil
Mark Andrews, Caterpillar, USA
Ramakrishna Bhatt, US Army Research Laboratory, USA
Stephen Duffy, Cleveland State University, USA
Jurgen Heinrich, Technical University Clausthal, Germany
Michael Jenkins, University of Washington, USA
Akira Kohyama, Kyoto University, Japan
Walter Krenkel, DLR German Aerospace Center, Germany
Edgar Lara-Curzio, Oak Ridge National Laboratory, USA

Sponsored by:
Engineering Ceramics Division, US Army Research Laboratory, DOE Office of Distributed Energy Resources

A coordinated forum for the presentation of advances in all aspects of the R&D of the performance evaluation of ceramics and composites and their application to structural component design. Specifically, contributions in the following topic areas are solicited:

- **Performance Evaluation of Ceramics and Composites**
  - Mechanical characterization
  - Thermal response
  - Damage evolution and its effects
  - Residual and internal stresses and their effects
  - Time-dependent properties and environmental effects
  - Statistical variation in properties and performance
  - Wear properties and interaction of ceramics with metallic components
  - Advanced characterization methods (e.g., NDE methods to assess surface-subsurface strength limiting failure modes)
- **Material and Property Modeling**
  - Microstructural and physics-based design
  - Fiber architecture effects on predicted performance
  - Interface mechanics
  - Laminate and multiphase structures
  - Control and engineering of residual stresses
- **Design, Modeling and Testing of Structural Components**
  - Strength-size-scaling issues
  - Flaw populations and data censoring
  - Consideration of creep and fatigue

Conference Papers

All conference papers will be published under one cover in the *Ceramic Engineering and Science Proceedings*.

All papers must be mailed to Society Headquarters by January 10, 2003. Papers submitted at the meeting may not be included in the proceedings.

Submit to:
Sarah Godby
Cocoa Beach Manuscript
The American Ceramic Society
735 Ceramic Place
Westerville, OH 43081-8720, USA

Exhibit Opportunities

Reach 500 research and product development engineers involved in composites, advanced ceramics, electronic materials and structures. Two booth sizes are available in limited quantities: 8'x8' – $800 and10'x10' – $1000.

The evening exhibits take place Monday and Tuesday, January 27 and 28, 2003, from 5:30-8 p.m. at the Hilton Hotel. A cash-bar and horsd'oeuvres reception takes place each night. On Monday, the conference poster session is held adjacent to the exhibit room. On Tuesday night, winners of the poster session are displayed in the Exhibit Hall.

For more information on Cocoa Beach marketing opportunities and to reserve your booth space, contact Peter Scott, sales manager, at 614/794-5844 or pscott@acers.org.

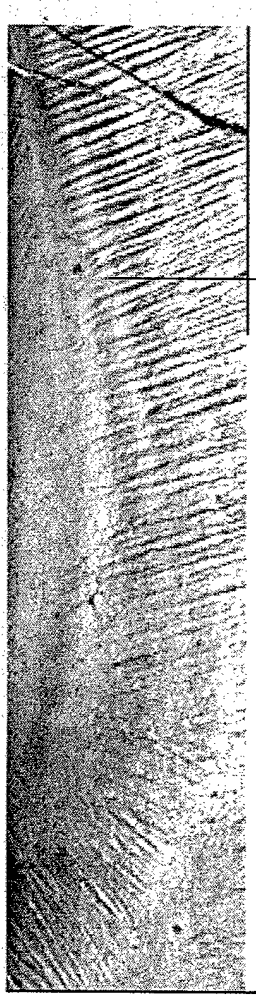

- Proof testing, NDE analysis and quality assurance
- Case studies
  - IC and gas turbine engine applications
  - General structural applications
  - When mechanical performance of a non-structural ceramic subcomponent can be a life limiter of the component's intended functionality (e.g., electronic devices, fuel cells, membranes, nuclear fission and fusion components, etc.)

Publication of the proceedings of this symposium will be included in the *Ceramic Engineering and Science Proceedings.*

Symposium II: Advanced Ceramic Coatings for Structural, Environmental and Functional Applications

Symposium Organizers:

Dongming Zhu (POC), NASA Glenn Research Center, USA
Phone: 216/433-5422 • E-mail: dongming.zhu@grc.nasa.gov
Uwe Schulz, DLR-German Aerospace Center, Germany
Ellen Y. Sun, United Technologies Research Center, USA
Hartmut Schneider, DLR-German Aerospace Center, Germany
Jeffrey I. Eldridge, NASA Glenn Research Center, USA
Yutaka Kagawa, University of Tokyo, Japan
Kazuhisa Miyoshi, NASA Glenn Research Center, USA
Jitendra P. Singh, Argonne National Laboratory, USA
Narottam P. Bansal, NASA Glenn Research Center, USA
William J. Clegg, Cambridge University, UK

Sponsored by:
Engineering Ceramics Division, NASA Glenn Research Center, DOE Office of Distributed Energy Resources.

This symposium will focus on recent advances in coating development, processing, microstructure and property characterization, and life prediction. Integrated structural, environmental properties and functionality through advanced coating processing and structural design are particularly emphasized. Specifically, contributions in the following topic areas are solicited:

- Thermal barrier coatings
- Environmental barrier coatings
- Nanostructured and smart coating systems
- Radiation barrier and thermal control coating systems
- Tribological coatings
- Advanced testing and non-destructive evaluation
- Interface phenomena, adhesion and failure mechanisms
- Micromechanics modeling and coating life prediction

Publication of the proceedings of this symposium will be included in the *Ceramic Engineering and Science Proceedings.*

Hotel Information

A block of rooms has been reserved for meeting attendees at the following hotels. The group rates (per night) are available until January 4, 2003. Rates do not include the 10% sales tax.

DoubleTree Oceanfront Hotel
(Conference hotel)
Phone: 800/552-3224 or
321/783-9222
Single/Double: $99
Triple/Quad: $115

Hilton Hotel
(Exhibition hotel; shuttle to DoubleTree provided)
Phone: 800/526-2609 or
321/799-0003
Single/Double: $105

Howard Johnson Express Inn
(Adjacent to DoubleTree)
Phone: 800/552-3224 or
321/783-8855
Single/Double/Triple/Quad: $75
(Inlcudes continental breakfast)

Be sure to mention The American Ceramic Society when making your reservations.

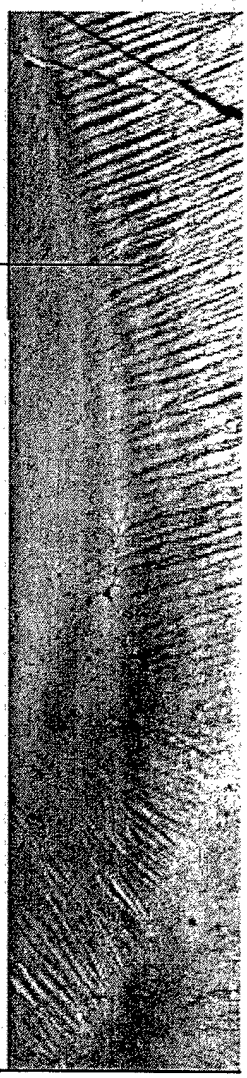

ABSTRACT DEADLINE: JULY 12, 2002

Symposium III: Functional Ceramics

Symposium Organizers:

Clive A. Randall (POC), Pennsylvania State University, USA
Phone: 814/863-1328 • E-mail: car4@psu.edu

Angus Kingon (POC), North Carolina State University, USA
Phone: 919/515-8636 • E-mail: angus_kingon@ncsu.edu

Igor Kosacki, Oak Ridge National Laboratory, USA

Sponsored by:
Electronics Division, Engineering Ceramics Division

The aim of this symposium is to critically review the state-of-the-art issues in functional ceramics. Specifically, proposed sessions will cover powder processing in electroceramics, dielectric materials and applications, piezoelectric transducers and actuators, conducting oxides, interfacial and scaling phenomena in electroceramics, and thin film ferroelectrics.

- Interfacial and scaling phenomena in electroceramics
- Microwave dielectrics and LTCC materials
- Conducting oxides: transparent oxides and ionic conductors
- Thin film ferroelectrics
- Piezoelectric transducers and actuators
- Modern challenges in processing electroceramics

Publication of the proceedings of this symposium will be included in the *Ceramic Engineering and Science Proceedings*.

Abstract Instructions

Visit the ACerS web site at www.ceramics.org to review the symposia descriptions and use the new Online Conference Management System. Follow these simple instructions:

- Click on Meetings & Expositions
- Click on Meetings Schedule and Information
- Click on Cocoa Beach: The 27th International Conference on Advanced Ceramics and Composites
- Click on Submit Abstracts
- Follow the system prompts to complete the online abstract form

Your abstract will be immediately available for review by potential attendees, co-participants and the program organizers. When your abstract has been accepted and scheduled, you will receive a confirmation e-mail.

We encourage authors to use the web site for submission. However, you may submit your abstract by e-mail, mail or fax. Please note that your abstract may not be available to the general public or the program organizers for 30 days after receipt. Follow these instructions to submit your abstract by mail or fax. Modify as necessary for e-mail. Be sure to include all information in your text.

- At the top of an 8-1/2 x 11 inch sheet of white paper, type Cocoa Beach—The 27th International Conference on Advanced Ceramics and Composites.
- Double-space and type the **Session/Symposium Title** for which your abstract is submitted. This information is mandatory.
- Double space and type the **Title of Your Presentation**, using capital and lower case letters, indicating any special characters, subscripts or superscripts as appropriate.
- Double space and type the **Initials and Last Names, Affiliations and Countries of the Authors** in the order in which they are to appear when your abstract is viewed or published. Use an asterisk after the last name of the presenting author.
- Double space and type **Your Abstract**, single-spaced, with 1 inch left and right margins. There is no word limit to your abstract, however, do not exceed one page.
- On a separate sheet of paper, **list All Authors with Complete Mailing and E-mail Addresses**.
- E-mail, mail or fax both the abstract page and the author list to:

  Technical Program Coordinator–CB
  The American Ceramic Society
  P.O. Box 6136
  Westerville, OH 43086-6136, USA
  Fax: 614/794-5882
  E-mail: jdavis@acers.org

CALL

A Novel Bioclastic Route to Self-Assembled, 3-D Nanoparticle Structures with Tailored Chemistries: the BaSIC Process

Ken H. Sandhage
Professor, Dept. Materials Science & Engineering
The Ohio State University, Columbus, OH

Abstract: "Bioclastic" is defined as "of rock or similar material attaining its present form through the action of living organisms" (Websters 3rd New International Dictionary, unabridged). A novel, hybrid (biological + synthetic chemical) fabrication route is introduced that utilizes bioclastic preforms to generate chemically-tailored nanoparticle structures with complex, three-dimensional (3-D) shapes: the **BaSIC** (**Bioclastic and Shape-preserving Inorganic Conversion**) Process. This process is illustrated by converting diatom (biosilica) microshells into other compositions while retaining the starting microshell shapes and meso-to-nanoscale features.

Diatoms are single-celled planktonic algae that are ubiquitous to marine and freshwater environments (e.g., from arctic to equatorial conditions). Diatoms form intricate microshells (frustules) comprised of self-assembled nanospheres of amorphous silica. The number of extant diatom species is $\approx 10^5$, with each species forming a 3-D frustule possessing a unique shape and a distinct pattern of fine features (e.g., meso-to-nanoscale pores, ridges, channels, protuberances). Enormous numbers of identical frustules can be generated by the continued reproduction of a single diatom species (e.g., 80 replications = 2^{80} = 1.2 trillion trillion > Avogadro's number!). Such massively parallel and precise self-assembly of 3-D nanoparticle structures is highly attractive for nanotechnological applications. However, the range of potential applications is severely limited by the silica-based chemistry of diatom frustules.

The compositional limitation of diatom frustules is overcome in the **BaSIC** process by using fluid/solid conversion reactions to alter the chemistry, but not the shape or fine features, of the frustules. To demonstrate this process, capsule-shaped *Aulacoseira* diatom frustules have been converted into MgO, CaO, TiO_2, ZrO_2, and SiC with a retention of the capsule shape and features. Biosculpted silica structures with non-natural shapes, obtained by patterning with silaffins (peptides extracted from diatoms), have also been converted. Reactions leading to a variety of other ceramics have been identified. Such shape-preserving chemical conversion, coupled with genetic tailoring of diatom frustule shapes, would allow for the low-cost mass production of **G**enetically-**E**ngineered **M**icro/nanodevices (**GEMs**) for numerous applications.

Biosketch: Ken H. Sandhage received a B.S. in Metallurgical Engineering with Highest Distinction from Purdue University and a Ph.D. in Ceramics from the Massachusetts Institute of Technology. Prior to joining OSU in 1991, Sandhage worked as a Senior Scientist on process R&D at Corning, Inc. and at American Superconductor Corporation. Sandhage's research at OSU has focused on novel reaction processing of a variety of ceramics and ceramic composites for biomedical, sensor, refractory, electromagnetic, and structural applications. He has received the Purdy (best paper) Award from the American Ceramic Society (1996), the Lumley Research Award from OSU (2002, 1997), and an Outstanding Materials Engineer Award from Purdue (1997). In 1999-2000, Sandhage was a Humboldt Fellow in the Advanced Ceramics·Group at the Technical University of Hamburg-Harburg. He is a Fellow of the American Ceramic Society.

Using Microorganisms to Manufacture 3-D Ceramic Microdevices

A novel, biologically-based approach for mass producing chemically-tailored, three-dimensional (3-D) ceramic microdevices with fine (meso-to-nanoscale) features is being examined in a collaborative research effort between the groups of Dr. Ken Sandhage (Ohio State University, Columbus, OH) and Dr. Morley Stone (Air Force Research Laboratory, Wright-Patterson Air Force Base, OH) through support provided by the Air Force Office of Scientific Research. This revolutionary process could open the door to low-cost microdevices for a host of DoD and commercial applications (e.g., optical, biomedical, sensor, microfluidic, catalytic).

The conventional production of microdevices has been focused on two-dimensional, layer-by-layer processes (e.g., micromachining by photolithography/chemical etching). Such processing is not well-suited for the fabrication of microdevices with complex, 3-D shapes. Nature, on the other hand, provides numerous examples of microorganisms that directly generate 3-D ceramic microstructures with complex shapes. The shapes of such "bioclastic" structures are a result of self-assembly that is directed by the microorganisms. Among the most dramatic examples of bioclastic structures are the microshells (frustules) of diatoms (*Bacillariophyta*). Diatoms are single-celled algae that populate a wide variety of aquatic environments (marine and freshwater; equatorial to arctic climates). Indeed, it is estimated that more than 20% of the carbon used to generate new primary organic matter on earth each year is tied up in diatoms. Each diatom cell contains a frustule comprised of a nanoporous assembly of amorphous silica nanoparticles (typically tens of nanometers in diameter). Each species of diatom assembles such nanoparticles into a frustule with a unique 3-D shape. Because the number of extant diatom species is estimated to be on the order of 10^5, nature provides a tremendous variety of frustule shapes for potential microdevice applications (Figure 1). The maximum dimensions of diatom frustules can range from less than 1 micron (e.g., for *Chaetoceros galvestonensis*) to several millimeters (e.g., for *Ethmodiscus rex*). The frustules are decorated with fine, meso-to-nanoscale ($<10^2$ nm) features, such as pores, ridges, channels, and protuberances, arranged in well-defined, species-specific patterns. Continued replication of a single parent diatom can yield enormous numbers of descendant diatoms, each of which would possess a frustule of the same shape. For example, 80 replications of a single parent diatom would yield 2^{80} or $1.2X10^{24}$ (twice Avogadro's number!) similarly-shaped frustules. Such massively-parallel, precise, and direct fabrication of 3-D micro-structures with fine (meso-to-nanoscale)

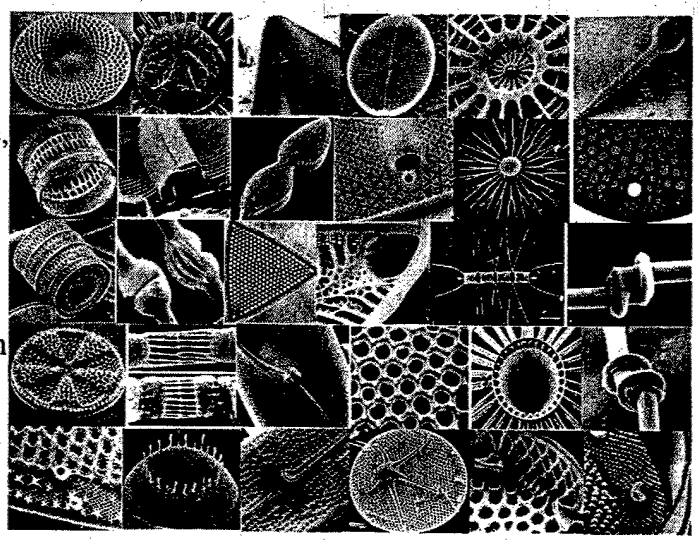

Figure 1. Secondary electron images of diatom frustules (reprinted with permission from F. E. Round, R. M. Crawford, D. G. Mann, The Diatoms: Biology and Morphology of the Genera, Cambridge University Press, 1990).

features under environmentally benign conditions is highly attractive for micro/nano-technological applications. However, the range of potential applications is severely limited by the silica-based composition of all diatom frustules.

The chemical limitation of diatom frustules has been overcome via a new process invented by Ken Sandhage, a professor in the Department of Materials Science and Engineering at Ohio State University, and his team of students. This new method, termed the **BaSIC** process (for **B**ioclastic and **S**hape-preserving **I**norganic **C**onversion), utilizes certain chemical reactions to *convert diatom frustules into new compositions while retaining the original frustule shape and fine features*. One class of such reactions are oxidation-reduction displacement reactions of the following type:

$$2Mg(g) + SiO_2(s) => 2MgO(s) + \{Si\} \qquad (1)$$

where {Si} refers to silicon dissolved within a Mg-Si liquid (note: this Mg-Si liquid is a result of the continued reaction of the silicon, generated upon reduction of silica, with excess gaseous magnesium). This displacement reaction has been used to convert capsule-shaped frustules of the diatom *Aulacoseira* into magnesium oxide, as shown in Figure 2. The images in Figures 2a and 2b reveal that the overall shapes and fine features (nodules, protuberances, pores) of the frustules were well preserved after conversion into magnesium oxide. Image analyses of the fine pores running in rows along the *Aulacoseira* wall (Figs. 2a and b) revealed little change in the pore size distribution upon conversion. Indeed, the average pore size before and after conversion agreed to within 30 nm! Solidified Mg-Si liquid (the {Si} product of reaction (1)) can also be seen under a reacted frustule in Figure 2b. Because this liquid preferred to wet the metallic substrate more than the MgO, the liquid sweated away during reaction at 750-900°C, so as to yield monolithic MgO frustules. A higher magnification secondary electron image, revealing the crystalline nature and fine grain size (a few hundred nm) of the converted frustule, is shown in Figure 2c. An energy-dispersive x-ray (EDX) spectrum, revealing the presence of Mg and O in the converted frustule, is shown in Figure 2d (note: the small gold peak in this EDX pattern is due to a gold coating applied to the frustule to avoid charging). Transmission electron microscopy of ion-milled cross-sections confirmed the fine-grained nature of the MgO frustule, and the absence of residual silica or Mg-Si liquid within the converted frustule wall, after 1 hour of reaction at 900°C.

Work over the past year has demonstrated that the BaSIC process can be used to convert diatom silica into a variety of other ceramic compositions, including ZrO_2, TiO_2, CaO, and SiC, while preserving the starting frustule shape and features. Examples of *Aulacoseira* frustules converted into zirconia and silicon carbide are shown below in Figures 3a and b, respectively. Thermodynamically-favored reactions leading to a number of other ceramics have also been identified and are under active study.

The BaSIC process has also been applied to biosilica structures with tailored (non-natural) shapes generated by Dr. Rajesh Naik and Dr. Morley Stone (Biotechnology Group, Air Force Research Laboratory, Wright-Patterson Air Force Base). A 19 amino acid peptide segment of a silaffin polypeptide, derived from the diatom *Cylindrotheca fusiformis*, has been found to dramatically enhance the rate of precipitation of silica from silicic acid solutions. By applying external forces (e.g., from flow fields, electric fields) during such precipitation, Naik and Stone

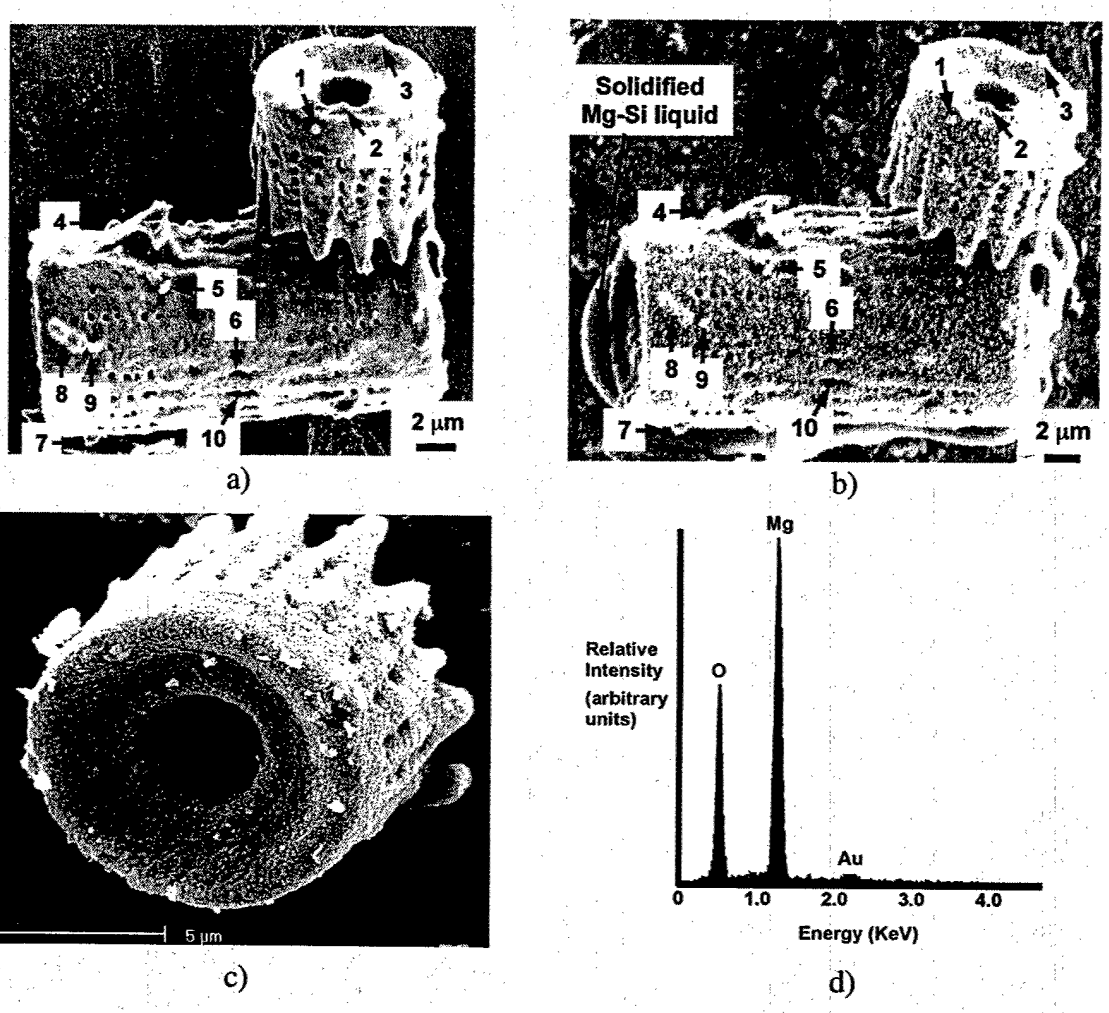

Figure 2. Secondary electron images of the same *Aulacoseira* diatom frustules: a) before and b) after conversion into MgO via reaction (1) at 900°C. Ten specific features are identified in the starting and converted frustules. A higher magnification image of a converted MgO frustule is shown in c). An EDX pattern obtained from the converted frustule is shown in d).

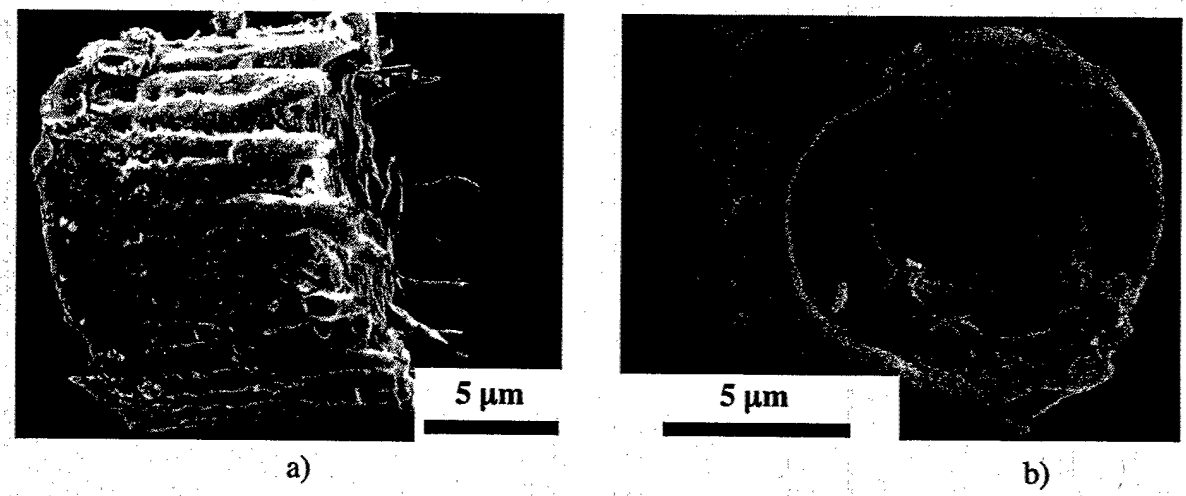

Figure 3. Secondary electron images of capsule-shaped *Aulacoseira* diatom frustules converted into: a) ZrO_2 (side view of converted frustule) and b) SiC (end view of converted frustule).

have succeeded in sculpting the resulting biosilica into tailored shapes. For example, a multifilamentary biosilica structure, generated by forcing a solution of the peptide segment and silicic acid to flow in a pattern involving laminar shear, is shown in Figure 4a. This biosilica structure was then exposed to Mg(g) at 900°C. The resulting multifilamentary MgO is shown in Figure 4b. The general shape and multifilamentary nature were retained upon conversion into

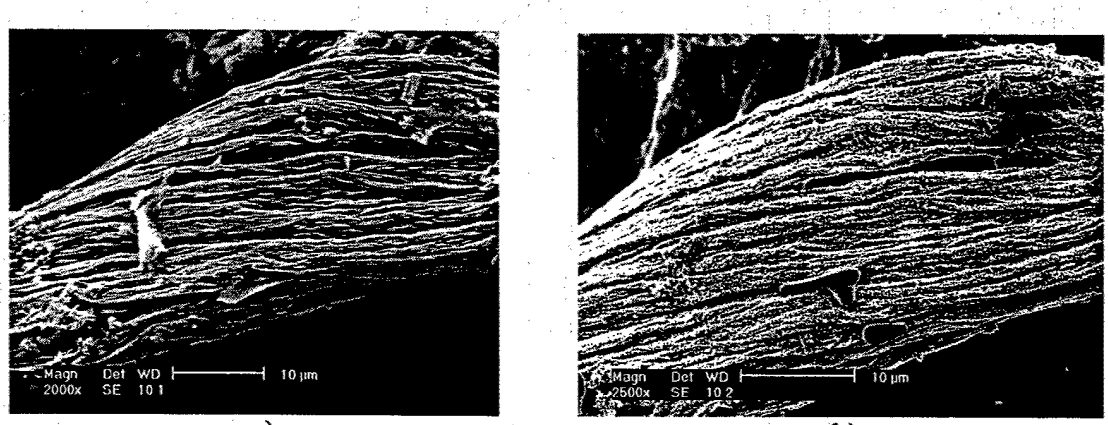

a) b)

Figure 4. Secondary electron images of a biocatalyzed, multifilamentary silica structure: a) before, and b) after reaction with Mg(g) for 4 h at 900°C.

MgO. These images demonstrate that biosilica structures with tailored (non-natural) shapes may also be converted into other ceramics with a retention of the starting shapes and fine features. That is, peptides derived from diatoms may be used to "biosculpt" silica structures with tailored shapes that, in turn, may be converted into desired compositions through shape-preserving reactions. *This novel biosculpting and reactive conversion approach opens the door to a wider variety of ceramic shapes and compositions than are available in nature*, so that a broader range of potential microdevices may be produced that are of interest to the U.S. Air Force (e.g., sensors, biodegradable microcapsules, etc.).

The BaSIC process merges the attractive characteristics of biology (i.e., rapid, directed self assembly of precise 3-D nanoparticle structures under ambient conditions) with those of synthetic reaction processing (i.e., low-temperature, near net-shape conversion of ceramic preforms into new compositions) to yield complex-shaped 3-D nanoparticle structures with tailored chemistries. A schematic illustration of a BaSIC manufacturing process is shown in Figure 5. Microorganisms, like diatoms, may be used as biofactories to generate large numbers of bioclastic microstructures with identical shapes and fine features (i.e., through sustained reproduction). Subsequent conversion reactions may then be used to simultaneously convert all of the microstructures into the desired ceramic composition while preserving the starting shapes and fine features (such conversion is illustrated with a color change in Figure 5).

While the feasibility of the BaSIC process has been demonstrated, further research is required to obtain better fundamental understanding and control of shape-dictating mechanisms during diatom biosilicification, and of the mechanisms of shape-preserving chemical conversion. Such research is the subject of a recently-awarded MURI proposal ("Genetically-Engineered Microdevices with Tailored 3-D Shapes, Nanoscale Features, and Chemistries," K. H. Sandhage,

M. M. Hildebrand, B. P. Palenik, R. R. Naik, M. O. Stone, R. A. Rapp, A. T. Conlisk, Jr., D. J. Hansford) involving a multidisciplinary team with expertise in diatom microbiology, diatom genetics, biochemistry, and shape-preserving reaction processes.

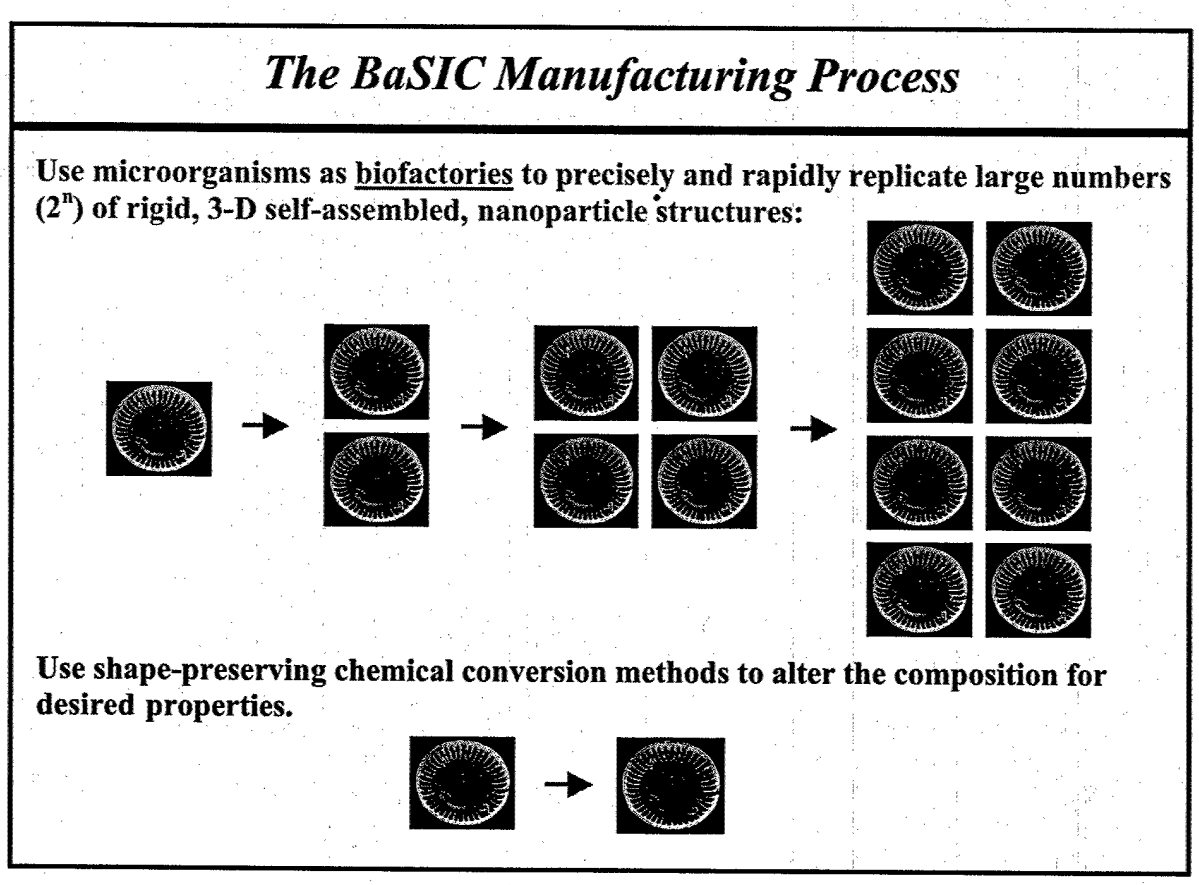

Figure 5. Schematic of the BaSIC process for mass producing 3-D ceramic microcomponents with tailored shapes, fine (meso-to-nanoscale) features, and chemistries.

Given the precision with which frustule shapes are replicated upon reproduction of a particular diatom species, it is apparent that such fidelity is under genetic control. Furthermore, given the wide variety of shapes exhibited by extant diatom species, it also appears that extensive alteration of the genes controlling the frustule shape is possible in viable diatoms. Hence, it is likely that genetic engineering of viable diatoms will lead to frustules with tailored (non-natural) shapes and nanoscale features. Genetically-Engineered Microlnanodevices (GEMs) with tailored structures and compositions could then be mass produced by sustained reproduction of genetically-altered, viable diatoms followed by chemical conversion via the BaSIC process. Such BaSIC-derived micro/nanostructures with tailored shapes, features, and compositions could find widespread use in medicine (e.g., for targeted radiation or drug delivery), telecommunications (e.g., microoptical devices), transportation (e.g., microfluidic devices), manufacturing (e.g., microelectromechanical devices), energy production and storage (e.g., microfuel cells, microbatteries), and defense-based applications (e.g., microsensors, microtags).

High-Temperature Residual Stresses in Textured Oxide Composites

Elizabeth C. Dickey and Colleen Frazer
Department of Materials Science and Engineering
Materials Research Institute
Pennsylvania State University

AFOSR Grant F49620-02-1-0211

January 28, 2003

Motivation

- Many ceramic composites are textured
- Thermal residual stresses arising from mismatches in thermal expansion properties affects mechanical behavior and degradation

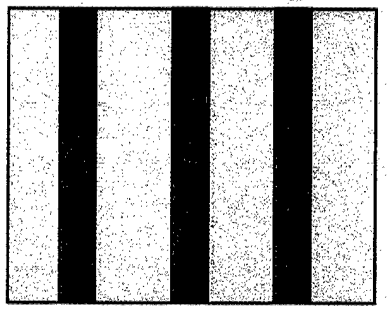

Ceramic Matrix Composites

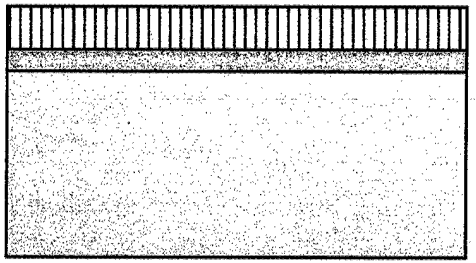

Environmental Coatings

Objectives

To understand the residual stress state of ceramic composites as a function of temperature and implications for mechanical behavior and degradation.

Approach

Develop experimental techniques based on x-ray diffraction that facilitate residual stress measurement as a function of temperature.

Outline

I. Material Systems Studied: Directionally Solidified Oxide Eutectics (DSEs)

- Al_2O_3-YAG
- Al_2O_3-$ZrO_2(Y_2O_3)$ DSEs
- -microstructure and crystallography

II. Measuring Residual Stresses in Highly-Textured Materials

- Measurement of strain tensor
- Conversion to stress tensor

III. Room Temperature Residual Stresses in DSEs

IV. High Temperature Residual Stresses

V. Conclusions

Eutectic Systems

Al_2O_3-YAG
Al_2O_3-$ZrO_2(Y_2O_3)$

Material	α_{11} ($*10^{-6}$ C^{-1})	α_{33} ($*10^{-6}$ C^{-1})
Al_2O_3	9.1	9.9
ZrO_2	14	
YAG	8.9	

Directionally solidified oxide eutectics have excellent high-temperature strength and creep resistance

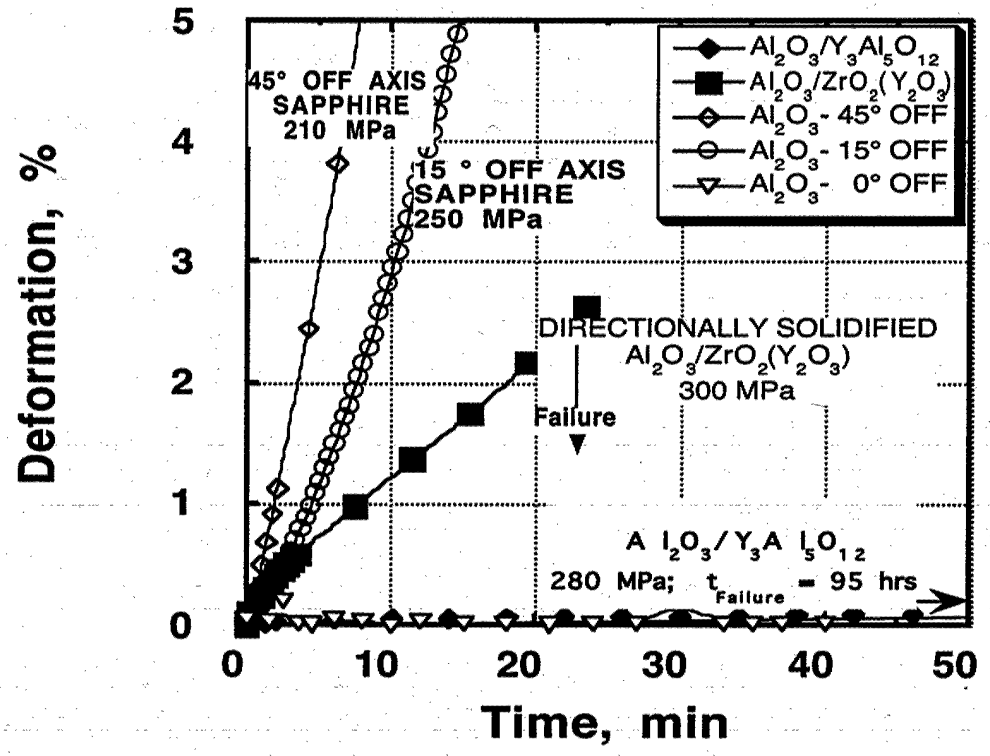

Summary of Mechanical Behavior (DSE) Composites

» Better mechanical properties than either single phase

»Tensile strength ~1 GPa for 3.2-7.6 m/o Y_2O_3

» Strength maintained at elevated temperatures

» Creep resistance

»~1.8×10^{-5}/s at 1400 C -Al_2O_3-ZrO_2

» Inherent oxidation resistance

Al_2O_3-YAG DSEs

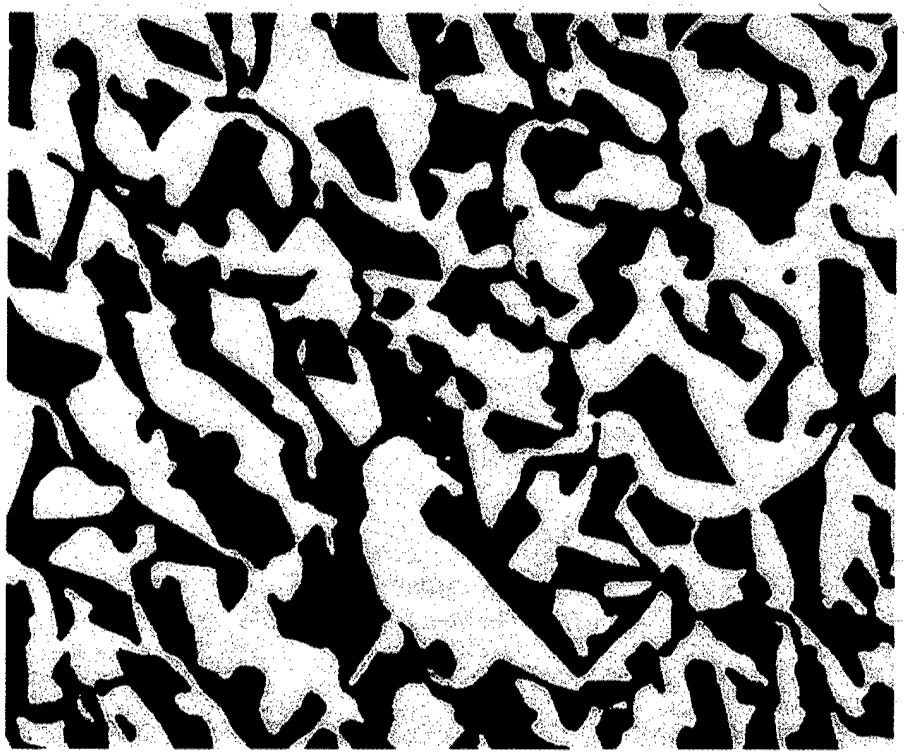

X-ray Diffraction Pole Figures Show the Al_2O_3-YAG DSEs to be Highly Textured

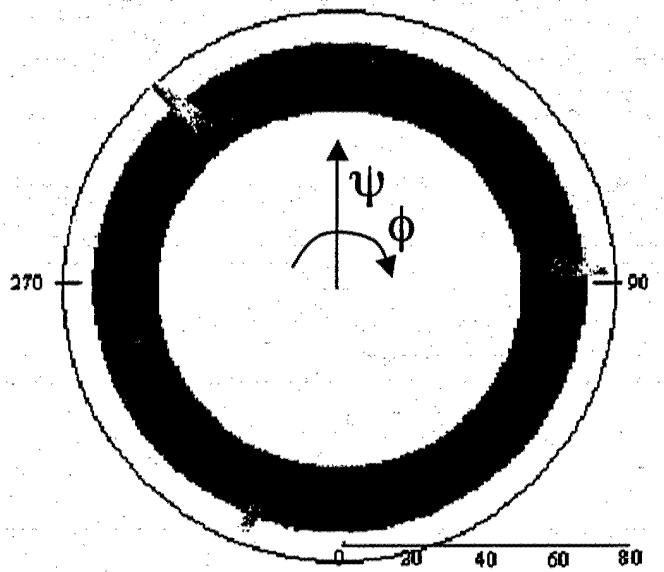

{111}
YAG

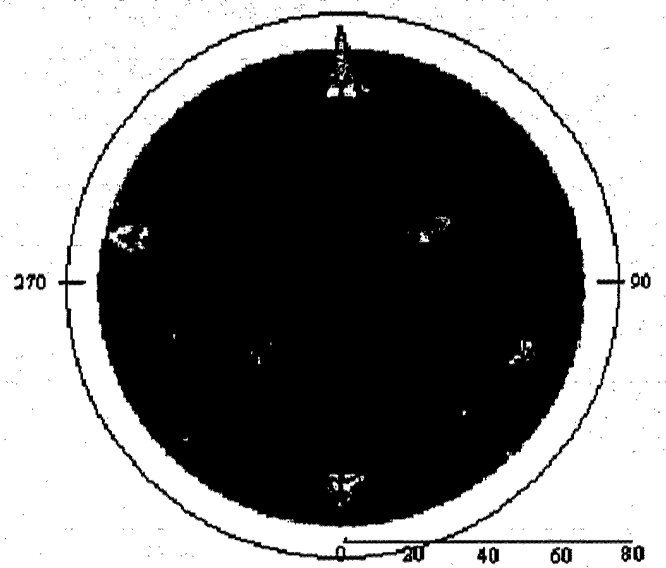

{012}
Al_2O_3

$[\bar{1}\,\bar{1}\,1]_{YAG}$ // $[\bar{1}\,2\,\bar{1}]_{Al_2O_3}$ // growth direction

$(2\bar{1}\,1)_{YAG}$ // $(111)_{Al_2O_3}$

Eutectic Microstructure

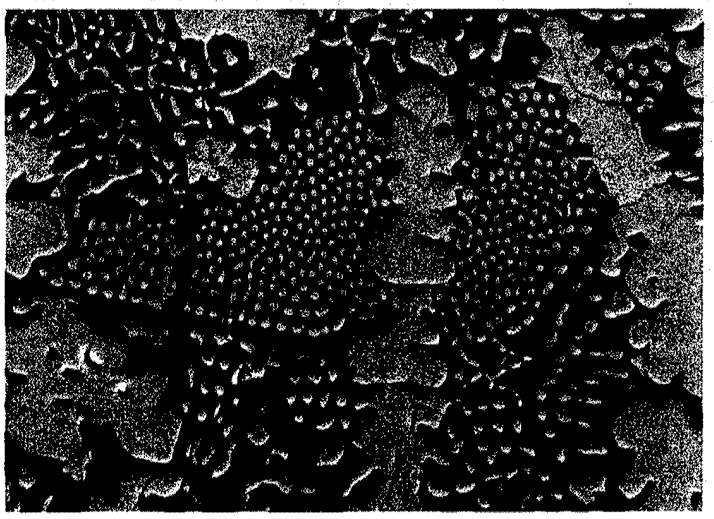

10 μm

Al_2O_3-ZrO_2 (6.7%Y_2O_3)

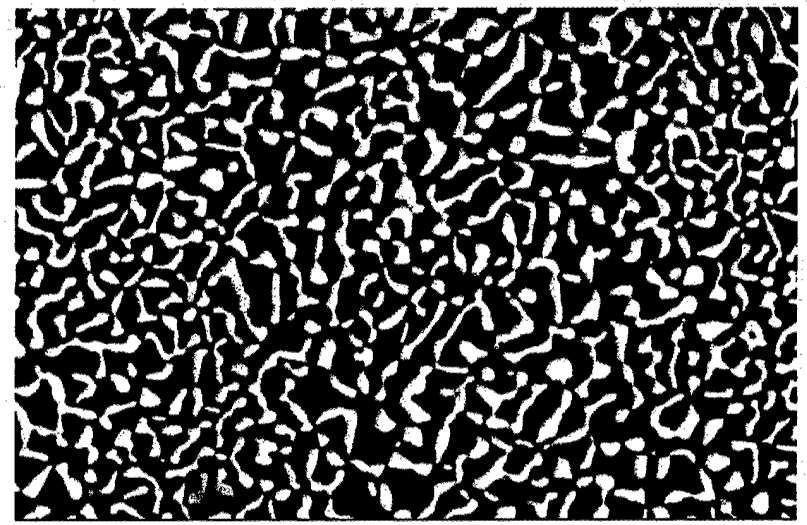

5 μm

Al_2O_3-ZrO_2 (3.6% Y_2O_3)

X-Ray Diffraction Pattern of Al_2O_3-cubic ZrO_2 Eutectic

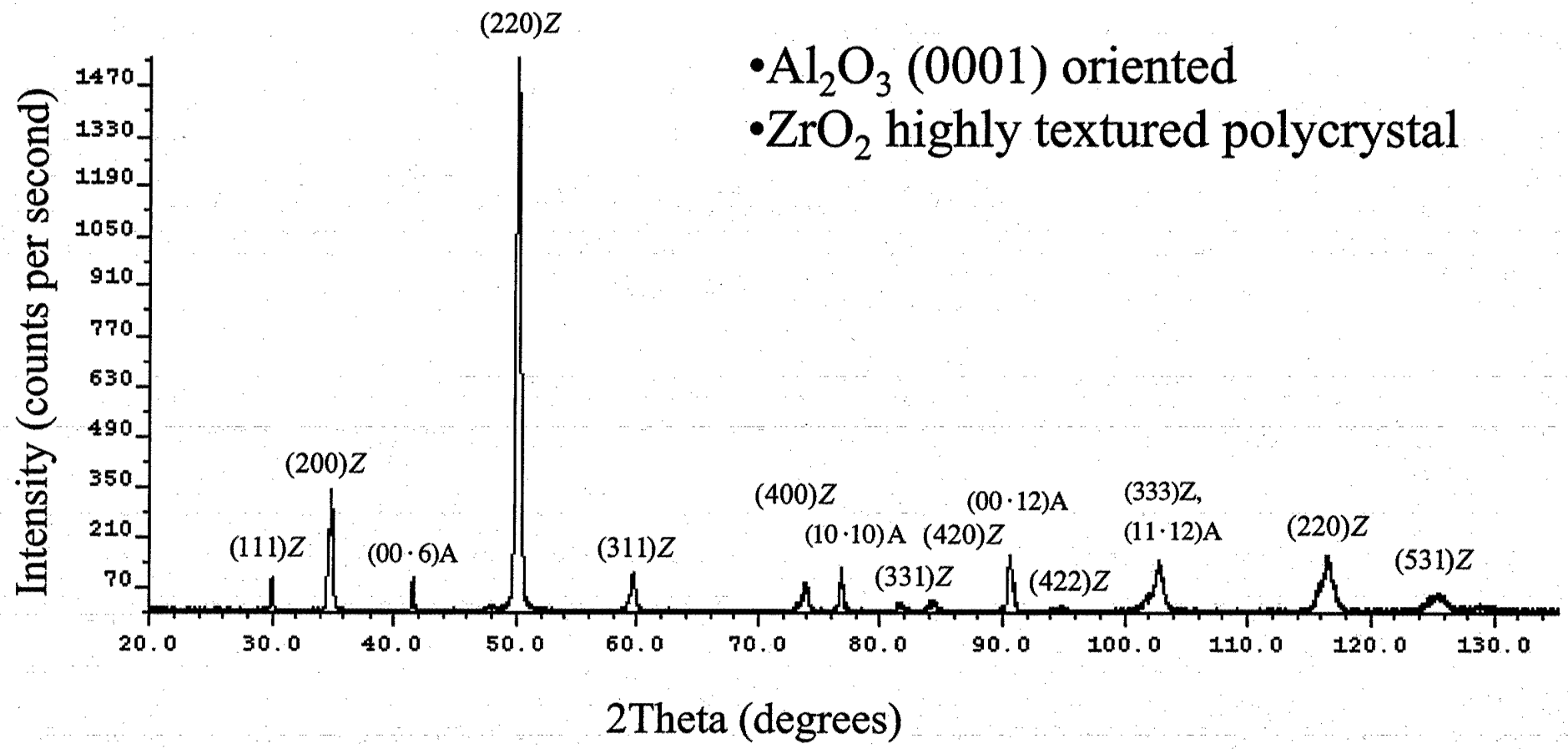

Crystallographic Texture Quantified from Pole Figure Analysis

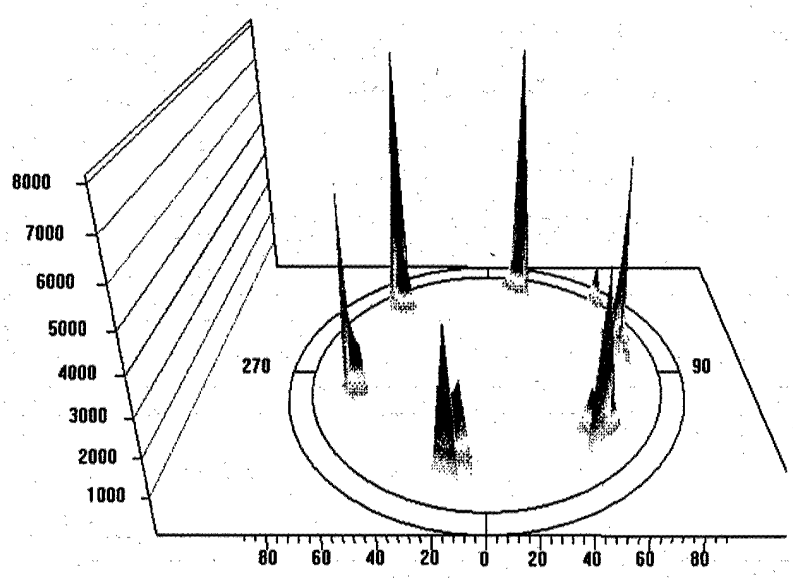

$(11\bar{2}3)$ Al_2O_3 pole figure

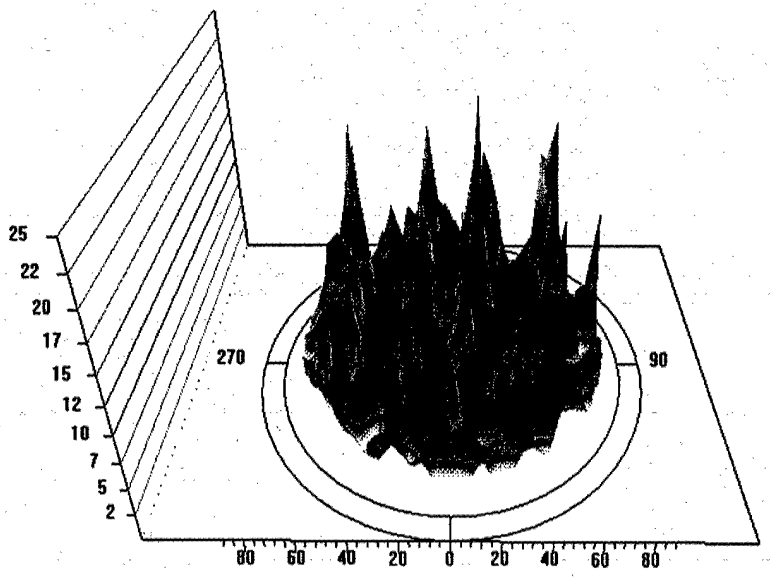

(311) ZrO_2 pole figure

Predominant Orientation $[0001]Al_2O_3//[110]ZrO_2$//growth axis

Outline

I. Material Systems Studied

Al_2O_3-YAG

Al_2O_3-$ZrO_2(Y_2O_3)$ DSEs

-microstructure and crystallography

II. Measuring Residual Stresses in Highly-Textured Materials

III. Room Temperature Residual Stresses in DSEs

IV. High Temperature Residual Stresses

V. Conclusions

Residual Stress Analysis

- Sample rotated to several different orientations (ψ,ϕ)
- d values measured from θ-2θ scans
- d_0 values measured from unstressed powders
- ε values calculated for all sample orientations ($\varepsilon_{\phi\psi}$)
- ε and error values fit to x-ray strain equation using SVD least squares regression

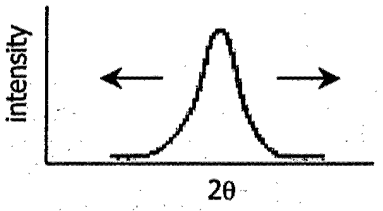

Fundamental Equation of X-ray Strain Determination

$$\varepsilon_{\phi\psi} = \frac{d_{\phi\psi} - d_0}{d_0} = \varepsilon_{11}\cos^2\phi\sin^2\psi + \varepsilon_{12}\sin 2\phi\sin^2\psi + \varepsilon_{22}\sin^2\phi\sin^2\psi + \varepsilon_{33}\cos\psi + \varepsilon_{13}\cos\phi\sin 2\psi + \varepsilon_{23}\sin\phi\sin 2\psi$$

Parallel-Beam Optics on a Four-Circle Goiniometer XRD Required for Stress Measurements

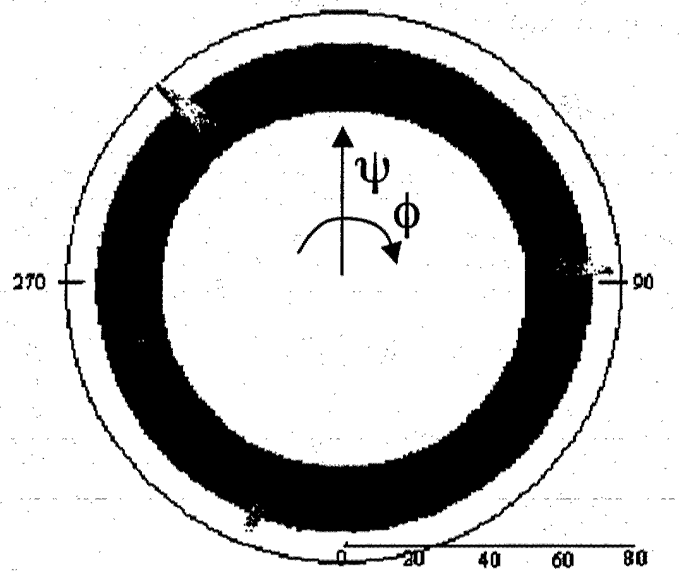

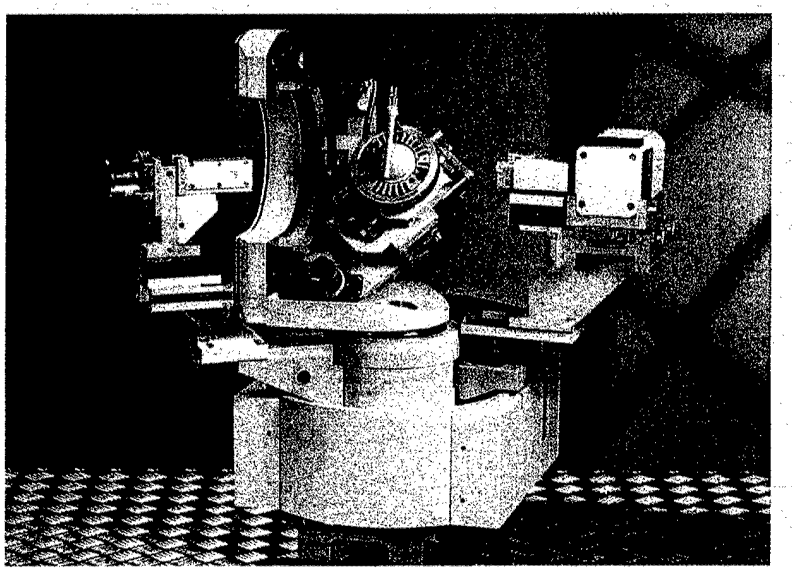

Choice of Reflections Used for Strain Analysis
e.g. YAG

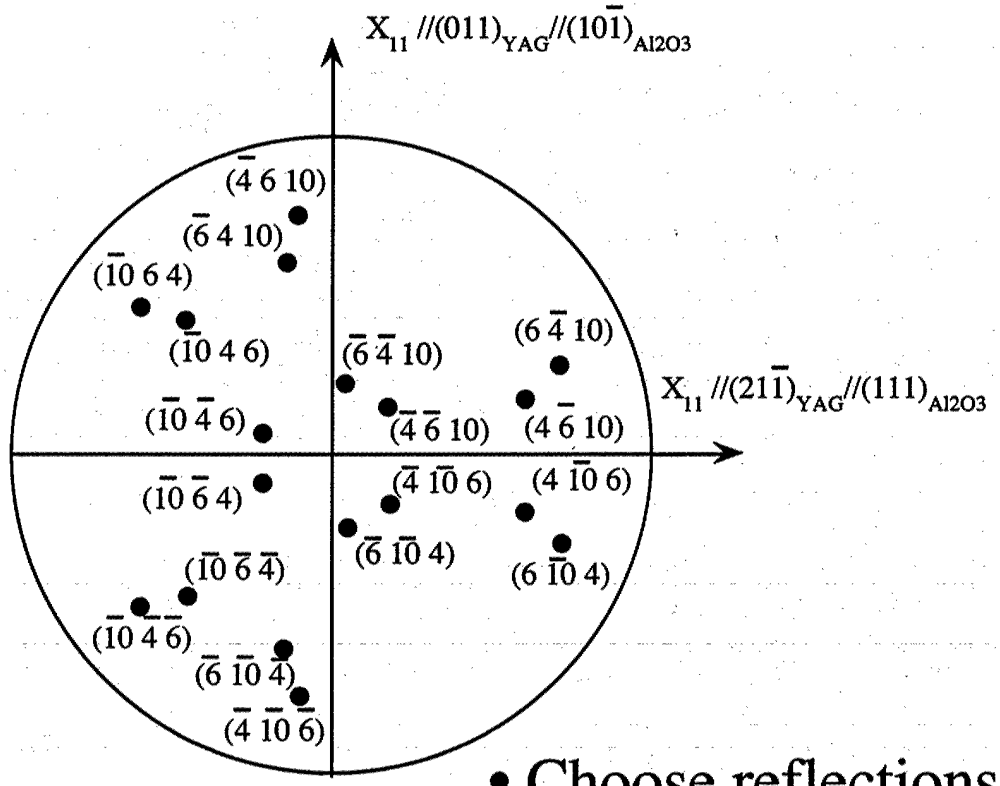

- Choose reflections that have high scattering angles (better angular resolution)
- Choose reflections that have a high multiplicity

Choice of Reflections Used for Strain Analysis
e.g. Al_2O_3

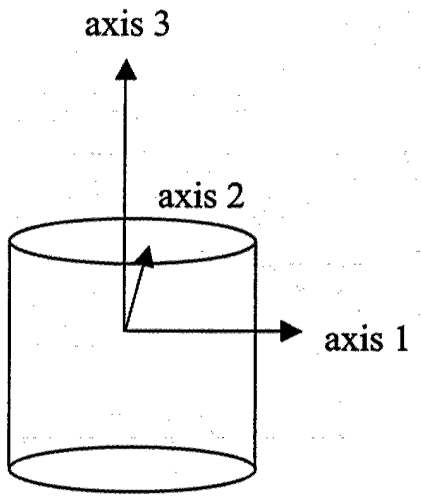

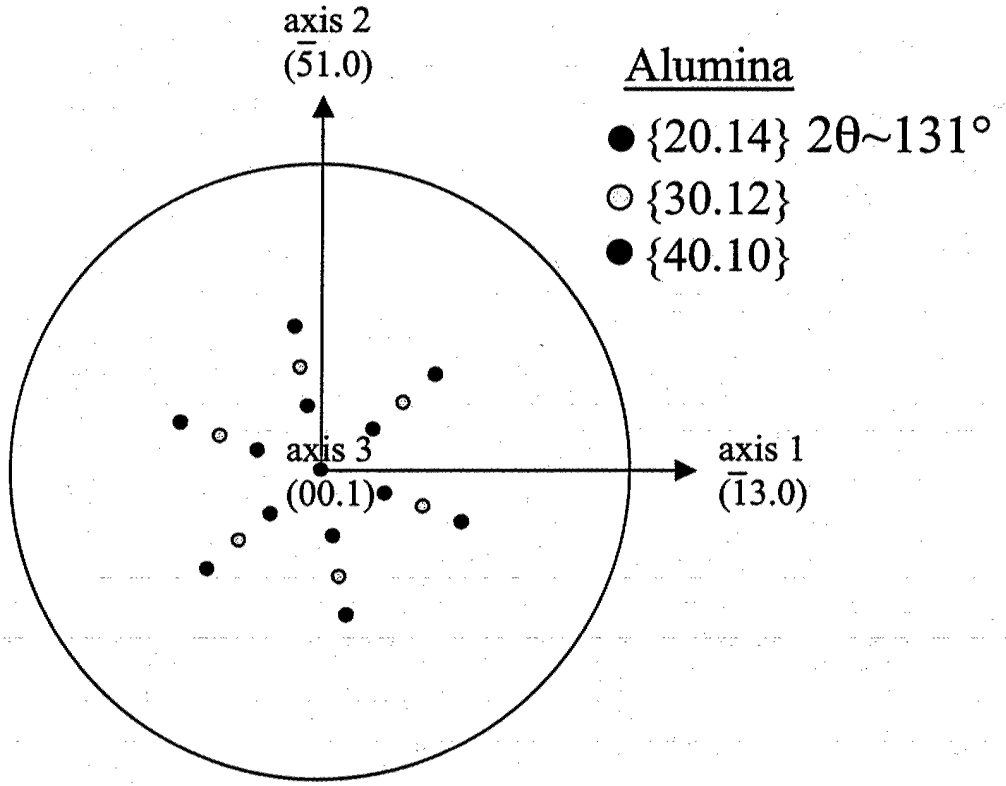

Alumina

- ● {20.14} 2θ~131°
- ○ {30.12}
- ● {40.10}

Conversion to Stress Tensor

$$\sigma_{ij} = C'_{ijkl}\varepsilon_{kl}$$

For single crystal:

rotate stiffness tensor to correct reference frame

For highly textured:

weight stiffness tensor with orientation distribution function

Weighting Stiffness Matrix with Orientation Distribution Function

- Weighted stiffness tensor found
  - 3 pole figures measured: (311), (111), (220)
  - ODF calculated using Harmonic Coefficients (popLA)
  - Produced weighted file of Euler angle orientations
  - Used single crystal stiffness tensor as input file

$[C]_{ij}$ (MPa)

406	105	105	0	0	0
105	406	105	0	0	0
105	105	406	0	0	0
0	0	0	55	0	0
0	0	0	0	55	0
0	0	0	0	0	55

+ weights

336	140	140	-2	-1	2
140	334	141	1	0	-1
140	141	334	0	1	-1
-2	1	0	91	-1	0
-1	0	1	-1	90	-2
2	-1	-1	0	-2	90

Outline

I. Material Systems Studied

Al_2O_3-YAG

Al_2O_3-$ZrO_2(Y_2O_3)$ DSEs

-microstructure and crystallography

II. Measuring Residual Stresses in Highly-Textured Materials

III. Room Temperature Residual Stresses in DSEs

IV. High Temperature Residual Stresses

V. Conclusions

Room Temperature Stresses in Al_2O_3-YAG

YAG

43	-26	-71		89	36	32
-26	18	-111	+/-	36	78	40
-71	-111	119		32	40	58

Alumina

296	-70	29		137	34	54
-70	276	65	+/-	34	136	33
29	65	238		54	33	118

Stress (MPa) Error

18 YAG measurements on {10 6 4}

11 Alumina measurements on {420}{532}{22-2}

Finite Element Modeling

- Microstructure
- Crystallography

→ Finite Element Modeling

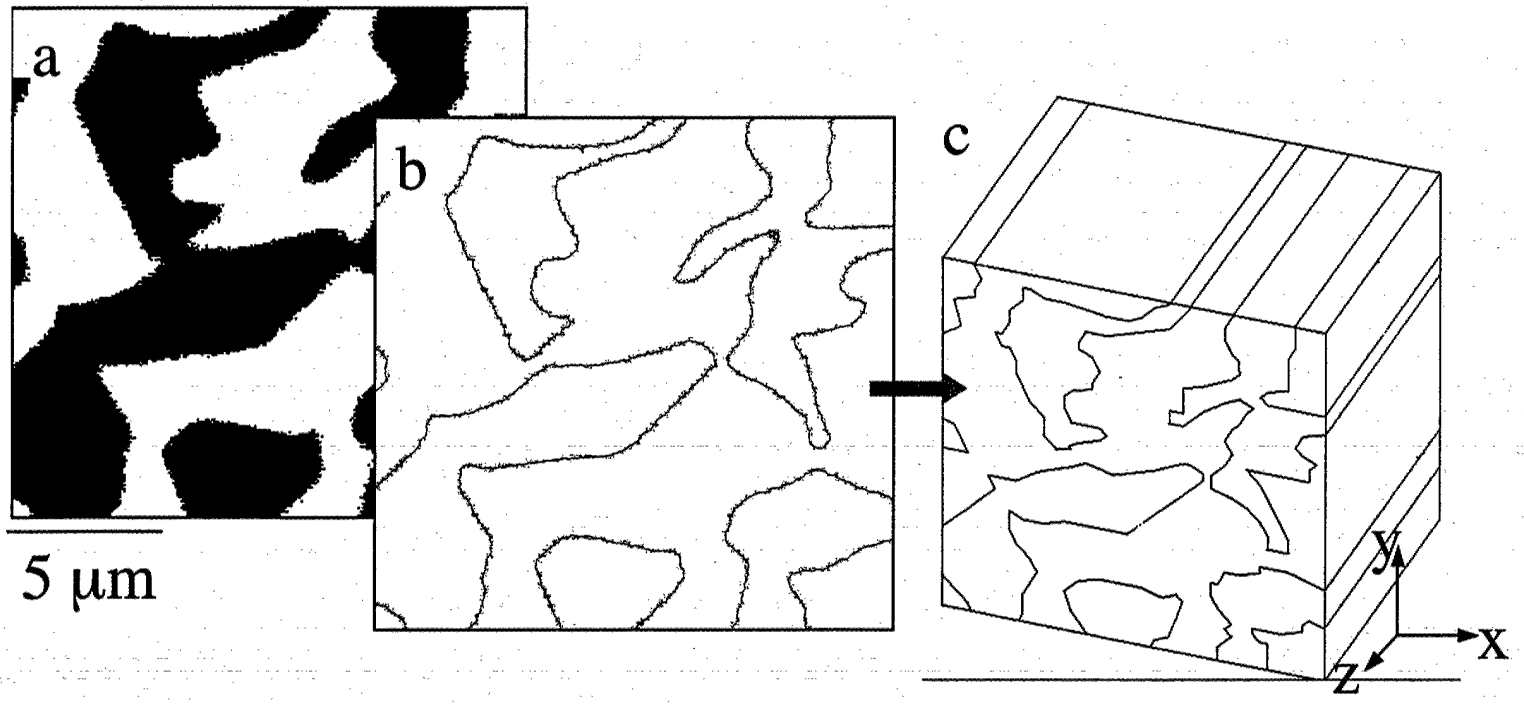

Stress Concentrations Observed in FEM of YAG-Al_2O_3

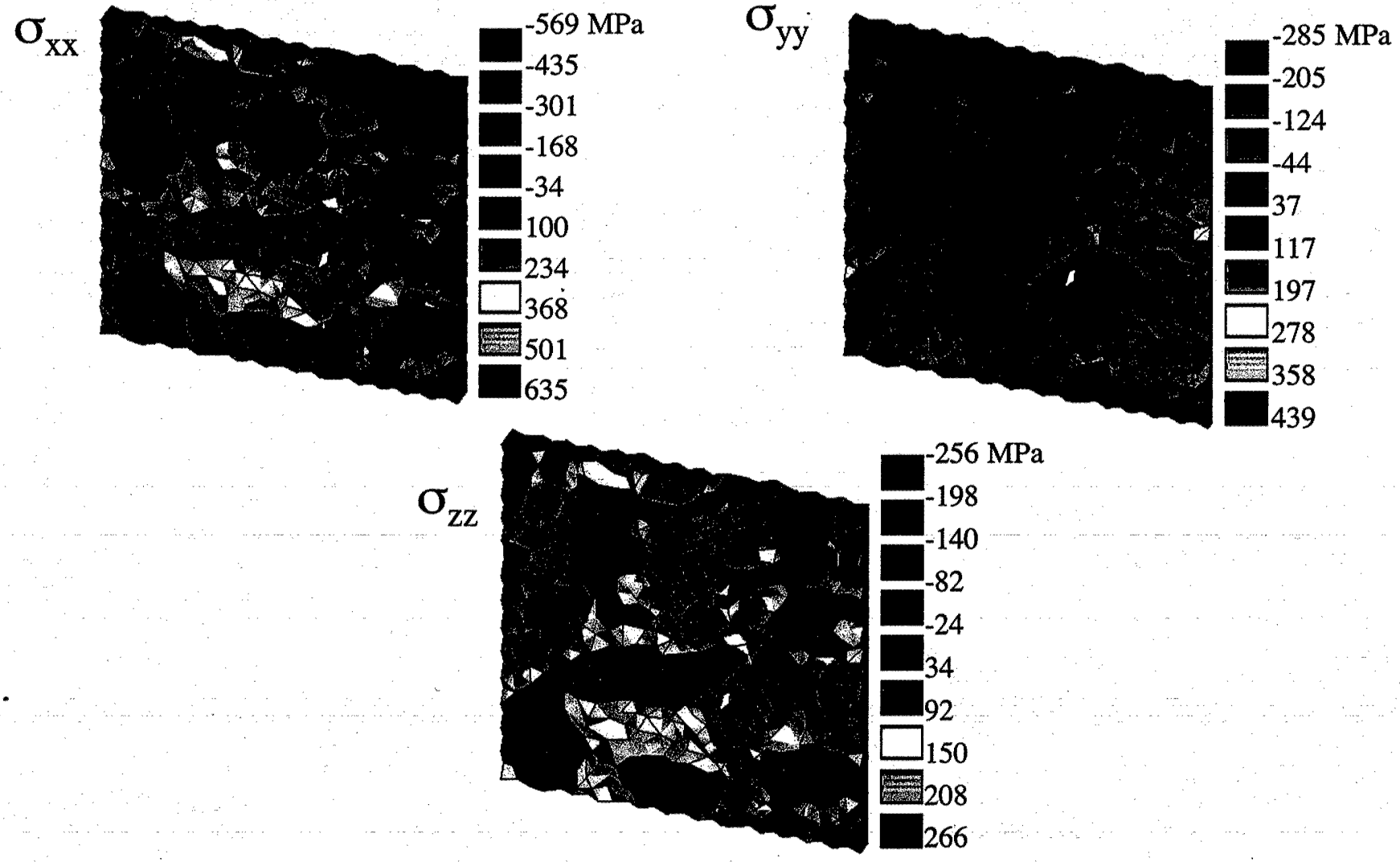

Alumina-ZrO_2 Room Temp. Residual Stresses

Al_2O_3-ZrO_2 (3.6% Y_2O_3)

Al_2O_3:

-211	-4	-17		29	5	2	(MPa)
	-247	12	+/-		30	12	
		-455				16	

Comparison of Residual Stresses in Different Material Systems

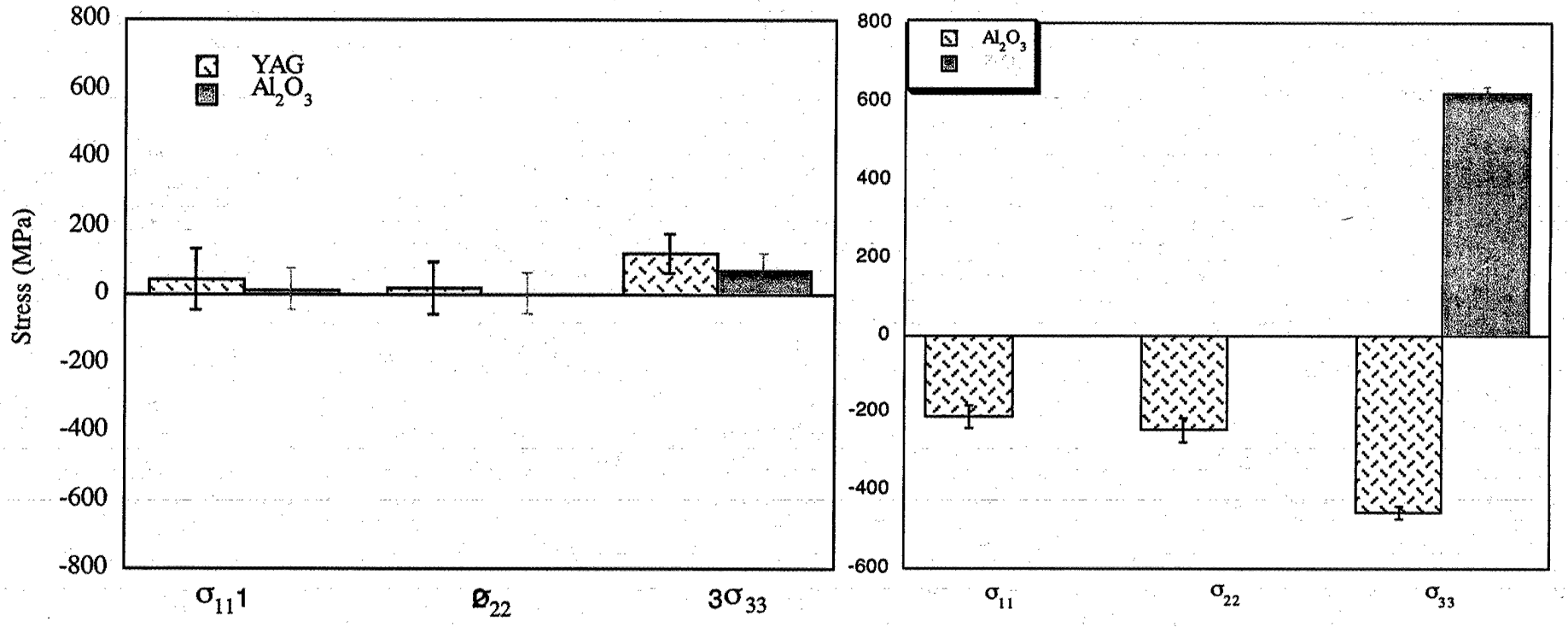

Outline

I. Material Systems Studied

Al_2O_3-YAG

Al_2O_3-$ZrO_2(Y_2O_3)$ DSEs

-microstructure and crystallography

II. Measuring Residual Stresses in Highly-Textured Materials

III. Room Temperature Residual Stresses in DSEs

IV. High Temperature Residual Stresses

V. Conclusions

High-temperature X-ray Diffraction

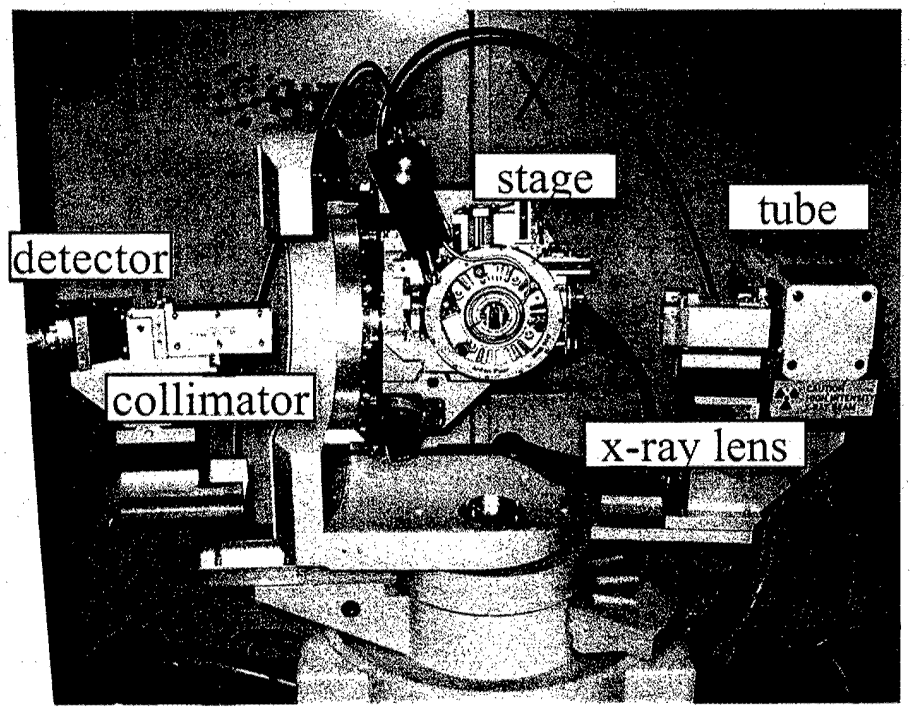

4-Circle Goniometer

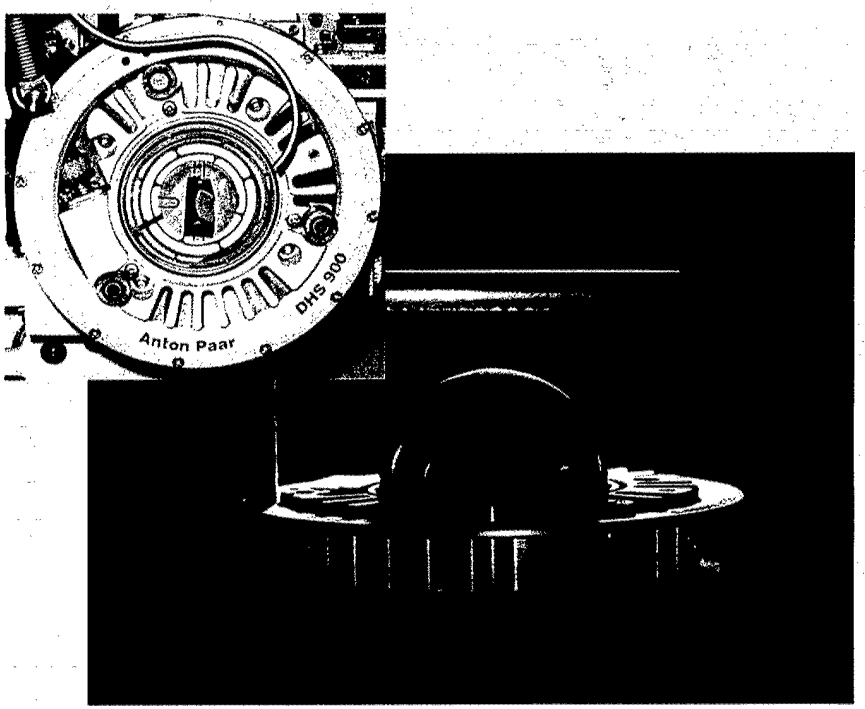

Anton Paar DHS 900 Domed Hot Stage

-Domed furnace capable of 900°C
-air, vacuum, inert gas

Temperature Effects on Residual Strain and Stress

Temperature effects:

- thermal expansion
- stress-relieving mechanisms

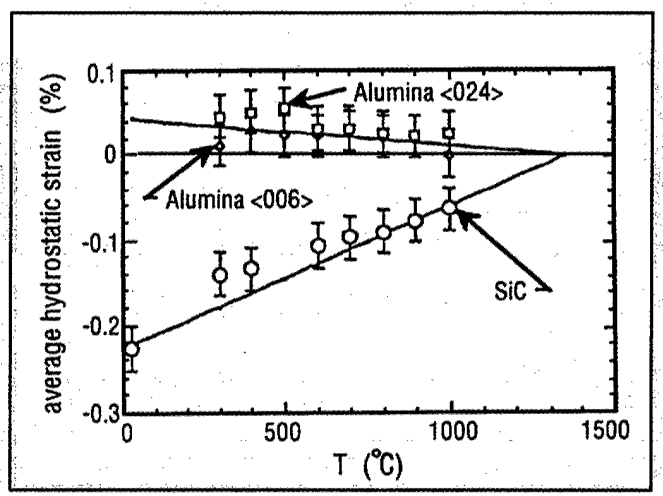

stress relief due to elevated temperature

$$\varepsilon_{\phi\psi}'(T) = \frac{d_{\phi\psi}(T) - d_0(T)}{d_0(T)}$$

$$\downarrow$$

$$\varepsilon_{kl}(T)$$

$$\downarrow$$

$$\sigma_{ij}(T) = C'_{ijkl}(T)\varepsilon_{kl}(T)$$

Thermal Expansion Calibrated from Powder Samples

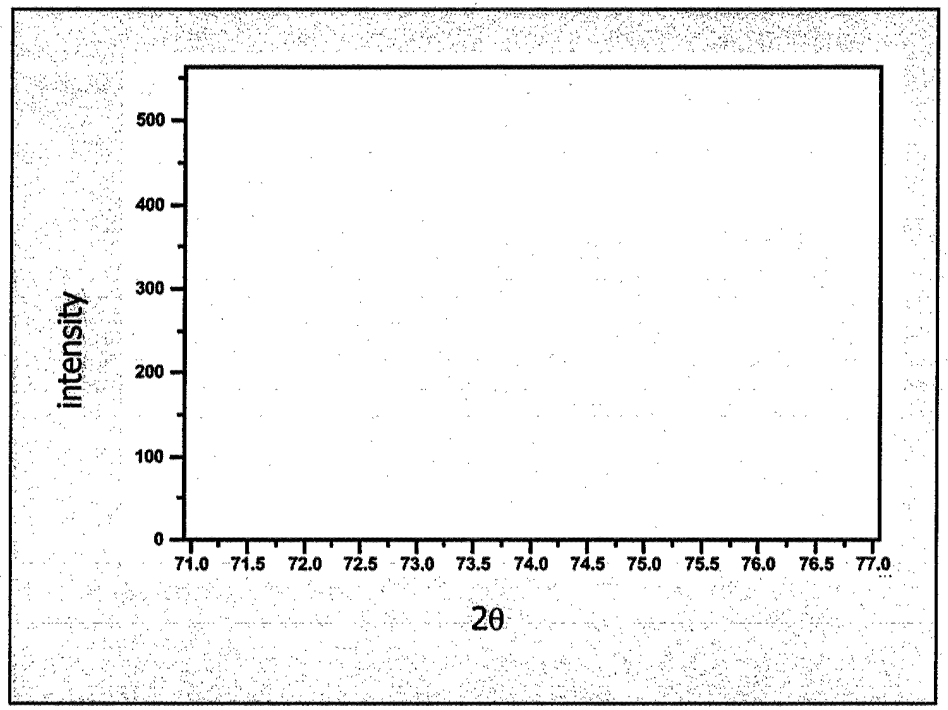

peak shift due to thermal expansion

Variation in Alumina Stiffness Tensor with Temperature

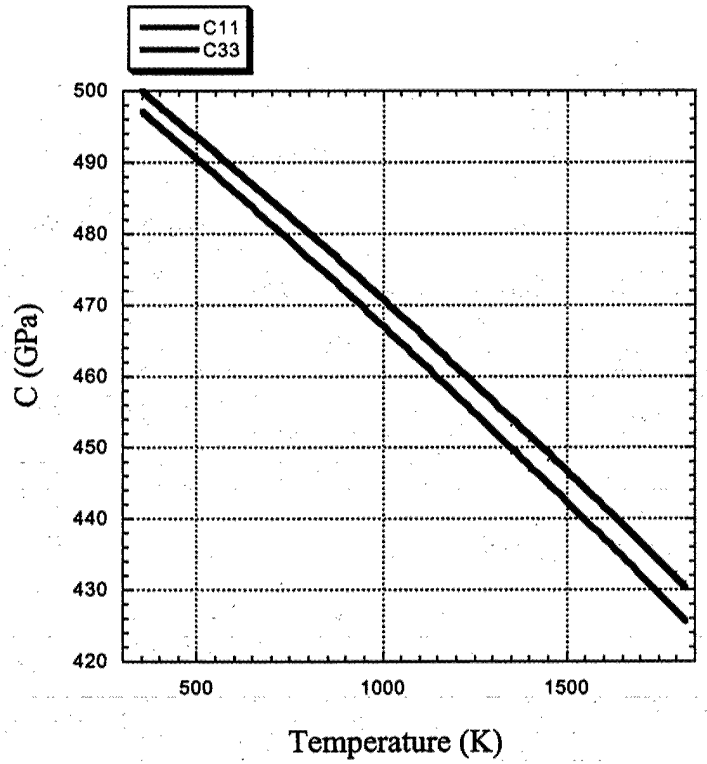

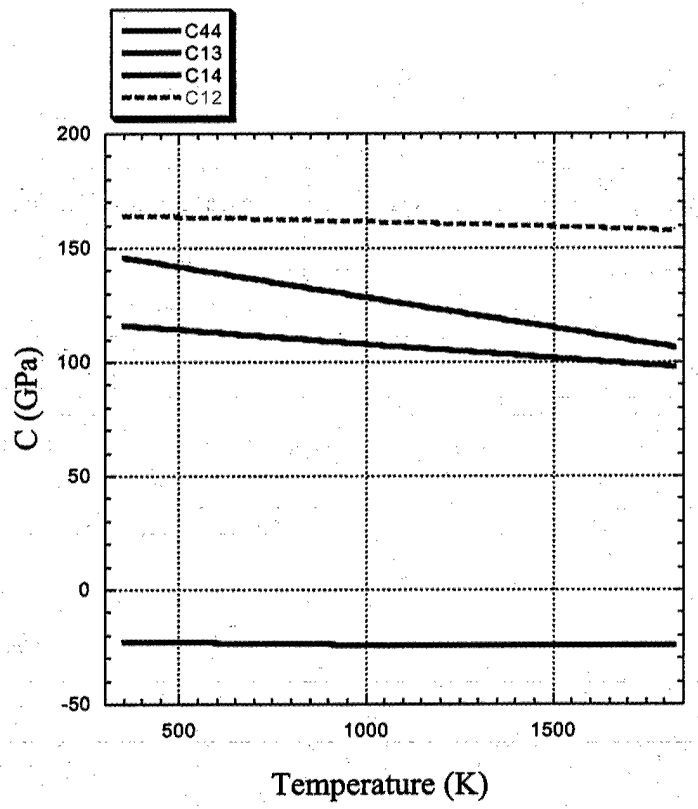

*Goto, T. and O. L. Anderson, "Elastic Constants of Corundum Up To 1825 K", Journal of Geophysical Research, [94] 7588-7602 (1989)

$[C_{ij}]$ 25°C

495	160	115	-19	12	0
160	495	115	19	-12	0
115	115	497	0	0	0
-19	19	0	146	0	-12
12	-12	0	0	146	-19
0	0	0	-12	-19	167

(GPa)

a)

$[C_{ij}]$ 450°C

480	163	111	-20	13	0
163	480	111	20	-13	0
111	111	484	0	0	0
-20	20	0	136	0	-13
13	-13	0	0	136	-20
0	0	0	-13	-20	158

(GPa)

b)

$[C_{ij}]$ 900°C

459	161	106	-20	13	0
161	459	106	20	-13	0
106	106	463	0	0	0
-20	20	0	124	0	-13
13	-13	0	0	124	-20
0	0	0	-13	-20	149

(GPa)

c)

High-Temperature Stresses in Al_2O_3-ZrO_2 (3.6% Y_2O_3)

a) $[\sigma_{ij}]$ 25°C

$$\begin{vmatrix} -211 & -4 & -17 \\ & -247 & 12 \\ & & -455 \end{vmatrix} \pm \begin{vmatrix} 29 & 5 & 2 \\ & 30 & 12 \\ & & 16 \end{vmatrix} \text{ (MPa)}$$

b) $[\sigma_{ij}]$ 450°C

$$\begin{vmatrix} -89 & 3 & -12 \\ & -107 & 9 \\ & & -253 \end{vmatrix} \pm \begin{vmatrix} 40 & 6 & 3 \\ & 41 & 15 \\ & & 22 \end{vmatrix} \text{ (MPa)}$$

c) $[\sigma_{ij}]$ 900°C

$$\begin{vmatrix} 236 & 2 & -8 \\ & 224 & 7 \\ & & 120 \end{vmatrix} \pm \begin{vmatrix} 39 & 6 & 3 \\ & 39 & 14 \\ & & 21 \end{vmatrix} \text{ (MPa)}$$

Stress-Free Temperature Determined

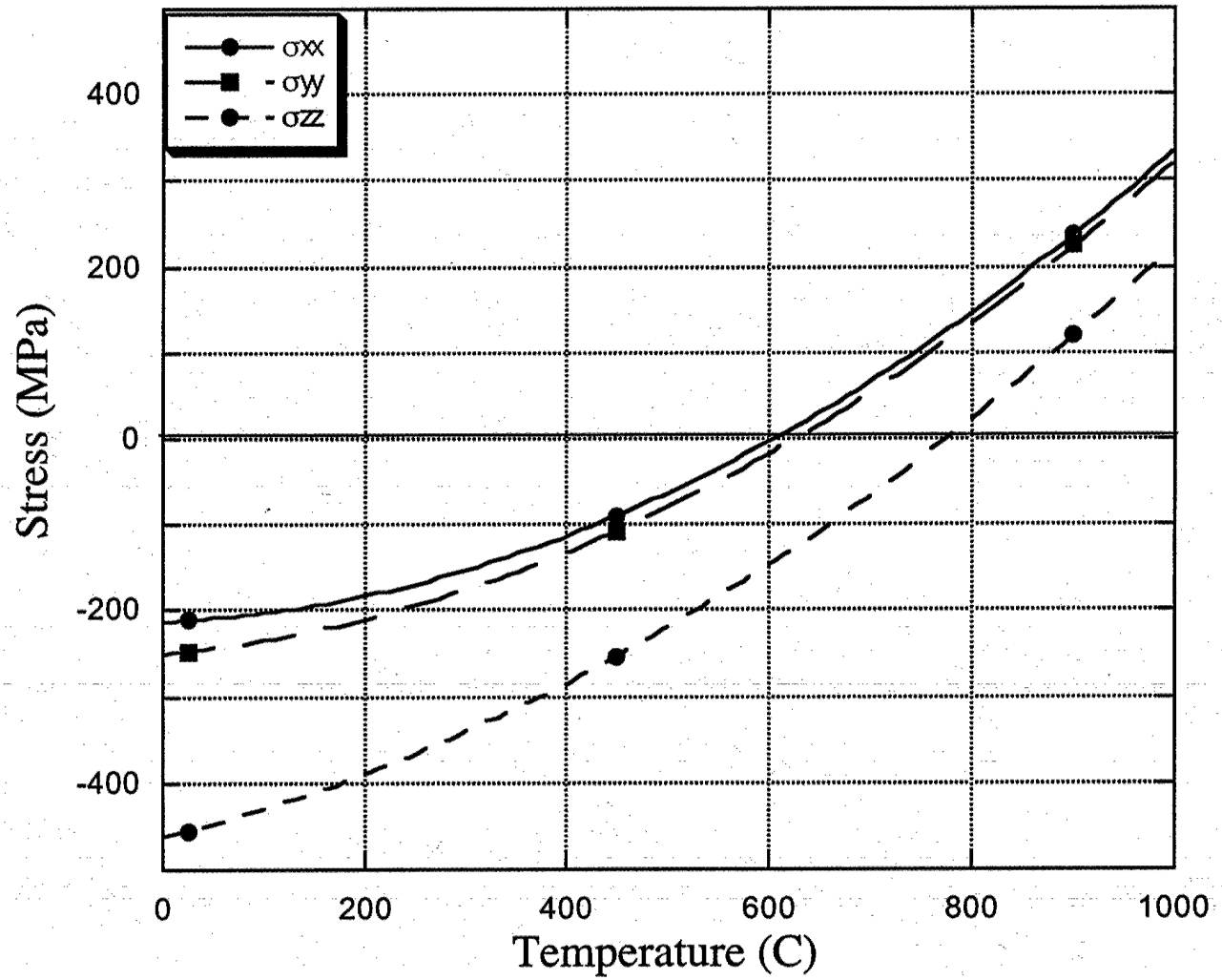

Summary

- Developed a protocol for measuring residual stresses in highly textured composites
- Achieved successful operation of high-temperature 4-circle goniometer XRD
- Residual stresses are relatively insignificant in the Al_2O_3-YAG DSE
- Residual Stresses in Al_2O_3-$ZrO_2(Y_2O_3)$ DSE measured from RT-900°C
- Stress-free temperature determined to be 600-800°C
- Using finite element modeling to help interpret x-ray diffraction data and to understand stress distributions in the microstructure

MOLTEN SALTS :
A ROUTE TO TAILORED CERAMICS

Marcelle Gaune-Escard

Ecole Polytechnique, Mecanique & Energétique
CNRS UMR 6595,Technopole de Chateau-Gombert
5 rue Enrico Fermi
13453 Marseille cedex 13, FRANCE

Marcelle.Gaune-Escard@polytech.univ-mrs.fr

Formation of ceramics in molten salts

Molten salt synthesis is a well established process of forming a desirable compound in a flux of low melting point .

- **✓It offers a significant reduction in the formation temperature when compared to that required in a conventional solid state reaction, since the diffusivities of the reactants are accelerated .**
- **✓It also provides great control on the particle size and morphology of the resulting copowders .**

The formation process of ceramic phase in a molten salt is complicated;

- **✓in some cases, the molten salt reacts with the reactant to form an intermediate compound, which then decomposes to the required ceramic phase. For example, in the preparation of $Bi_4Ti_3O_{12}$ powders, the component oxides firstly react with LiCl flux to form an intermediate compound, which subsequently decomposes into $Bi_4Ti_3O_{12}$ and LiCl [4].**
- **✓In other cases, the molten salt is acting as a mere reaction and diffusing medium accelerating the rate of formation of the desirable ceramic phase.**

T. Kirnura, T. Kanazawa, T. Yamaguchi
J. Am. Ceram. Soc. 66(8) (1983) 597

•The method consists of adding precursors in the required ratio to a molten salt mixture often close to an eutectic stoichiometry, which accelerates the kinetics of formation of the desired compounds. Molten salt mixtures either serve the role of a solvent with no direct participation in the reaction or may actually enter into reaction with the oxide additives.

✓In cases where the molten salt serves merely as a solvent medium, its sole purpose is to accelerate the kinetics by enhancing diffusion, since coefficients in the liquid state are lower than those in the solid state.

✓Reactions are presumed to occur by the dissolution of constituents, reaction of the constituents in solution, and precipitation of the required compounds upon exceeding the solubility limit.

❑**Molten salts as reaction media provide an alternative to aqueous chemistry by offering the possibility to change the solubility and/or the reactivity of the reactants, and to increase the reaction temperature**

✓**used for the preparation of solids, recrystallization and growth.**

✓**So far, attention in this field has been largely focused on the alkali and alkaline-earth halides and polychalcogenides . To grow anisotropic crystals, KCl–NaCl and K_2SO4–Na_2SO_4 fluxes have been used, as well as molybdates and tungstates.**

✓**Alkali carbonate and alkali hydroxide fluxes have also been used for the preparation of various oxides.**

✓**These oxosalts offer a wide range of reaction temperatures (see next Table) and a great variety of possible chemical reactions, including those of complexation, oxidation–reduction, and acid–base type reactions.**

Melting points of some oxosalt mixtures (m.p.: melting point)

Molten salt	$NaNO_3$–KNO_3	Li_2CO_3–Na_2CO_3	Li_2SO_4–K_2SO_4	$LiBO_2$–KBO_2	Na_2SiO_3–K_2SiO_3
Composition (mole%)	50–50	50–50	71.6–28.4	56–44	18–82
M.p. (K)	501	773	808	855	1026

Acid–base type reactions occurring in molten oxosalts are classified as Lux–Flood (L–F) acid–base reactions , oxide donors and acceptors being defined as L–F bases and acids, respectively, and the reaction is understood as follows:

$$\text{Oxoacid} + O^{2-} \Rightarrow \text{Oxobase} \qquad (1)$$

The basicity of the melt is usually expressed by

$$pO^2 = -\log m(O^{2-})$$

where $\log m(O^{2-})$ corresponds to the concentration of O^{2-} ions. Depending on the reactant and basicity of the oxosalt, precipitation of an oxide or formation of an oxoanion can occur in the molten bath.

For example, the reaction of silicon tetrachloride with an oxosalt melt at moderate pO^{2-} leads to precipitation of silica:

$$SiCl_4 + 2O^{2-} \Rightarrow SiO_2 + 4Cl^-, \quad (2)$$

whereas if the melt basicity is further increased (low pO^{2-}), redissolution of SiO_2 may occur, caused by formation of metasilicate:

$$SiO_2 + O^{2-} \Rightarrow SiO^{2-}_3. \quad (3)$$

Then, depending on the nature of the molten salt, different species can be obtained and the nature of the products can be controlled.

The chemistry of molten nitrates

$$NO_3^- + Acid \Rightarrow NO_2^+ + Acid.O_2^-, \quad (4)$$

$$NO_2^+ + NO_3^- \Rightarrow 2\,NO_2 + 1/2\,O_2. \quad (5)$$

- zirconium oxide is obtained from zirconium(IV) salts according to the following equation:

$$ZrOCl_2.8H_2O + 2NO^-_3 \Rightarrow ZrO_2 + 2NO_2 + 2Cl^- + 1/2O_2 + 8H_2O. \quad (6)$$

- Soluble oxoanions can be produced from molybdenum oxide which undergoes stepwise transformations (Eqs. (3)–(6)), leading to alkali metal molybdates A_2MoO_4 (A=K, Na) :

$$3MoO_3 + 2NO^-_3 \Rightarrow Mo_3O^{2-}_{10} + 2NO_2 + 1/2O_2, \quad (7)$$

$$2\,Mo_3O^{2-}_{10} + 2NO^-_3 \Rightarrow 3\,Mo_2O^{2-}_7 + 2NO_2 + 1/2O_2, \quad (8)$$

$$Mo_2O^{2-}_7 + 2NO^-_3 \Rightarrow 2\,MoO^{2-}_4 + 2NO_2 + 1/2O_2. \quad (9)$$

Synthesis of solids in molten nitrates:

Usually performed in a Pyrex glass reactor in air or under an inert atmosphere

✓ Precursor salt(s) mixed with a large excess of the nitrate salt

✓ The most often used melts : equimolar $NaNO_3$–KNO_3 mixture (mp=501 K),or individual alkali metal nitrates.

✓ Mixture pretreated at 423 K to eliminate water from the precursor salt(s) up to above T_{fus}.

✓ After cooling down, the solidified melt is thoroughly washed with distilled water to separate the (necessarily water-insoluble) solid product from the soluble salts.

✓ Then the product is dried in air at 393 K..

✓ For catalytic applications, the dried product is usually calcined in air at 683–773 K.

P. Afanasiev, C. Geantet
Coordination Chemistry Reviews, 178–180 (1998) 1725–1752

Zirconium oxide

Several studies were devoted to the influence of the MS reaction conditions on the properties of zirconia obtained.

❑ The nature of the cation of the alkali metal nitrate has a strong influence on the properties of the oxide, affecting the specific surface areas, as well as pore size distributions.

❑ It has been shown by transmission and scanning electron microscopies that the oxide obtained from molten nitrates has nearly spherical morphology, very different from that of aqueous precipitates, which are rough and irregular. It may be one of the reasons for its higher stability toward calcination. This parameter is important for catalytic applications.

❑ The influence of acidity/basicity of nitrate melt as also

❑ the effects of the starting materials of α-$Zr(SO4_2$ and β-$Zr(SO4)_2$, on the phase composition and the crystallite size of zirconia powders prepared were investigated

Aluminum oxide

$$Al_2(SO4)_3+6NO_2^- \Rightarrow Al_2O_3 +3NO_2+3NO+3SO^{2-}_4 \text{ , (10)}$$
$$Al_2(SO4)_3 +6NO^-_3 \Rightarrow Al_2O_3+6NO_2+3/2O_2+ 3SO^{2-}_4. \text{ (11)}$$

- The nature of the starting compounds is of primary importance in the case of aluminium.
- With highly reactive anhydrous salts : reaction at very low T (to some extent already upon mixing), and α-alumina formed.
- With hydrated Al(III) salts : much lower reactivity and quite different properties of the product, e.g. solid obtained hydrated Al(III) chloride or nitrate at 450–550 °C in molten NaNO3, KNO3 or their mixture, was virtually amorphous. On contact with washing water it could easily be hydrated, forming crystalline $Al(OH)_3$ as Bayerite. Since the washing step leads to the chemical transformation of the product, the MS preparation for alumina from hydrated precursors seems rather useless.
- Moreover, though well-dispersed aluminium oxide could be prepared from molten nitrates, more simple precipitation routes give at least as good textural parameters as the MS technique.

Lanthanum oxide

❑Since La (III) is a weak L–F acid, the reaction of $LaCl_3$ occurs at high temperatures (above 450 °C). It is diffcult to accomplish because the intermediate product LaOCl is poorly reactive and insoluble. Washing of the reaction product with water always leads to crystalline $La(OH)_3$ as in the case of alumina.

❑However, the reaction of LaCl3 seems to be of some interest since **pure LaOCl can be obtained** at 450–500 °C (Fig.).
Using the MS preparation, this compound possesses highly oriented sheet-like morphology, as can be seen from the scanning electron microscopy images . The oxychloride obtained by this method can be used as an **intercalation host** , or as a **reactive precursor** for further solid preparations.

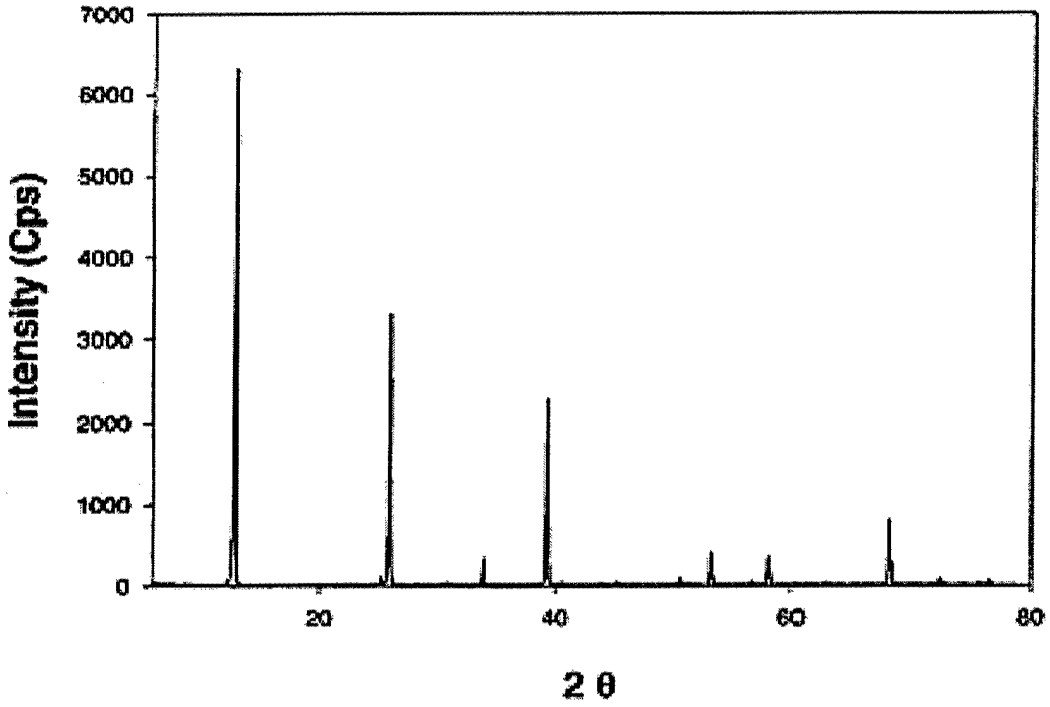

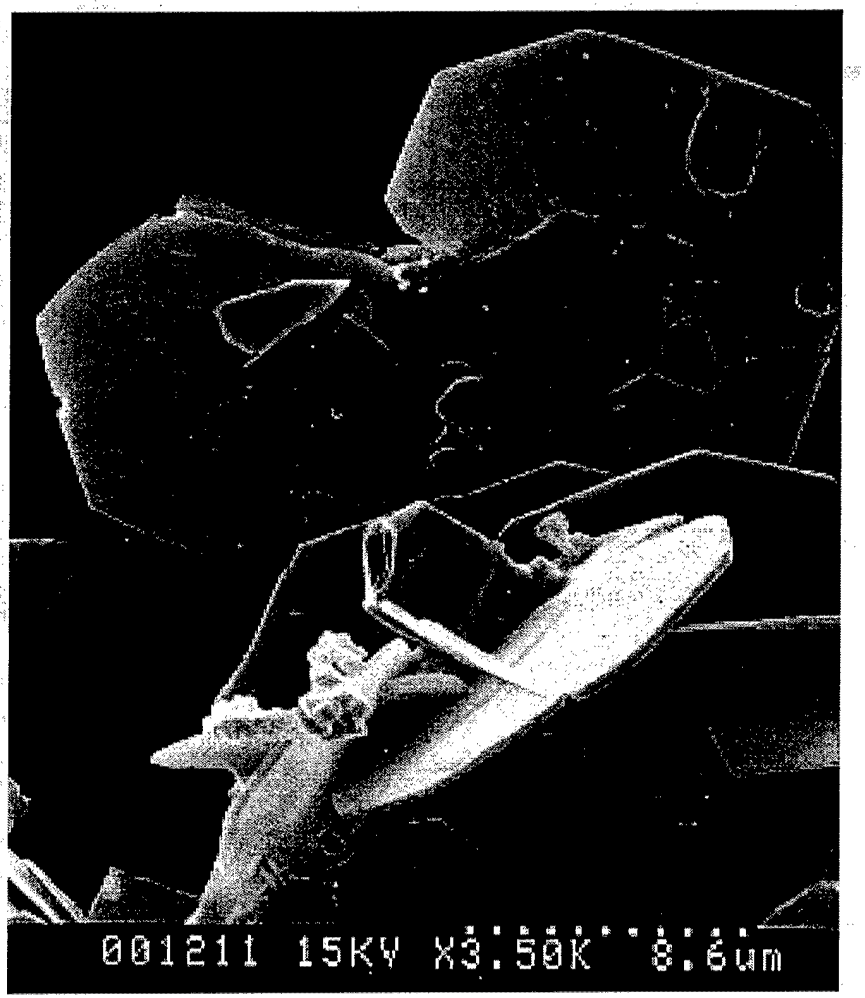

XRD pattern and SEM picture of LaOCl prepared in molten $LiNO_3$ at 773 K.

P. Afanasiev, C. Geantet
Coordination Chemistry Reviews, 178–180 (1998) 1725–1752

Synthesis of multicomponent oxide systems

Most advanced materials for ceramics and catalysis are complex multicomponent systems, containing, for instance, solid solutions such as yttria-stabilised zirconia ceramics or fine dispersions i.e. mixed oxide catalytic supports on the base of alumina, doped with La, B, Ti etc.

▪Various methods developed to achieve the desired chemical composition and morphology of the multicomponent inorganic materials.

▪ Used for tailor-made preparations of solids with given properties, not available by classical solid preparation methods involving heating and grinding.

▪ The common feature of these methods is that the solid products keep some memory about the precursors and additives used during the preparation. Being carried out at relatively low temperatures, they often lead to metastable solids: homogeneous or heterogeneous nanodispersions; double hydroxides; or organic–inorganic hybrid materials.

ZrO_2–Y_2O_3

- **Solid solutions ZrO_2–$Y2O_3$ prepared in Ref. [a] by simultaneous reaction of zirconium oxychloride and yttrium chloride in $NaNO_3$–KNO_3 melt at 450 °C.**
- **A tetragonal or cubic phase was obtained according to the yttrium content.**
- **The large specific area of the powders was observed (up to 120 m2 g-1), suggesting their possible application for ceramics or catalysis.**

ZrO_2–Al_2O_3

- **by simultaneous reaction of hydrated $ZrOCl_2$ and $AlCl_3$ at 450 °C, using different nitrate melts [b, c].**
- **The presence of alumina delays the growth of the zirconia particles, stabilising its tetragonal modification.**

[a] M. Jebrouni, B. Durand, M. Roubin, Ann. Chim. Fr. 17 (1992) 143.
[b] M. Jebrouni, B. Durand, M. Roubin, Y. Saikali, Ann. Chim. Fr. 19 (1994) 55.
[c] D. Hamon, M. Vrinat, M. Breysse, B. Durand, L. Mosoni, M. Roubin, T. des Courières, Eur. J. Solid State Inorg. Chem. 30 (1993) 713.

Ternary oxides and oxosalts

If one of the precursors precipitates an oxide and another provides an oxoanion soluble in the melt, the formation of ternary or more complex stoichiometric compounds is possible.

•Molybdenum-based unsupported catalysts represent an important class of industrial oxidation catalysts and several transition-metal-doped molybdates were prepared including $NiMoO_4$, $K_3FeMo_4O_{15}$; $NaFe(MoO_4)_2$; $Fe_2(MoO_4)_2$; $NaCO_{2..31}(MoO_4)_3$; and $CoMoO_4$.

•Bismuth molybdate is used as a catalyst for the production of acrylonitrile via ammoxidation of propene (SOHIO process). A bismuth molybdate has been prepared in molten nitrates at 773 K from the simultaneous reactions of hydrated $Bi(NO_3)_3$ and $(NH_4)_6Mo_7O_{24}$.

The product corresponds to the Bi_2MoO_6 phase,

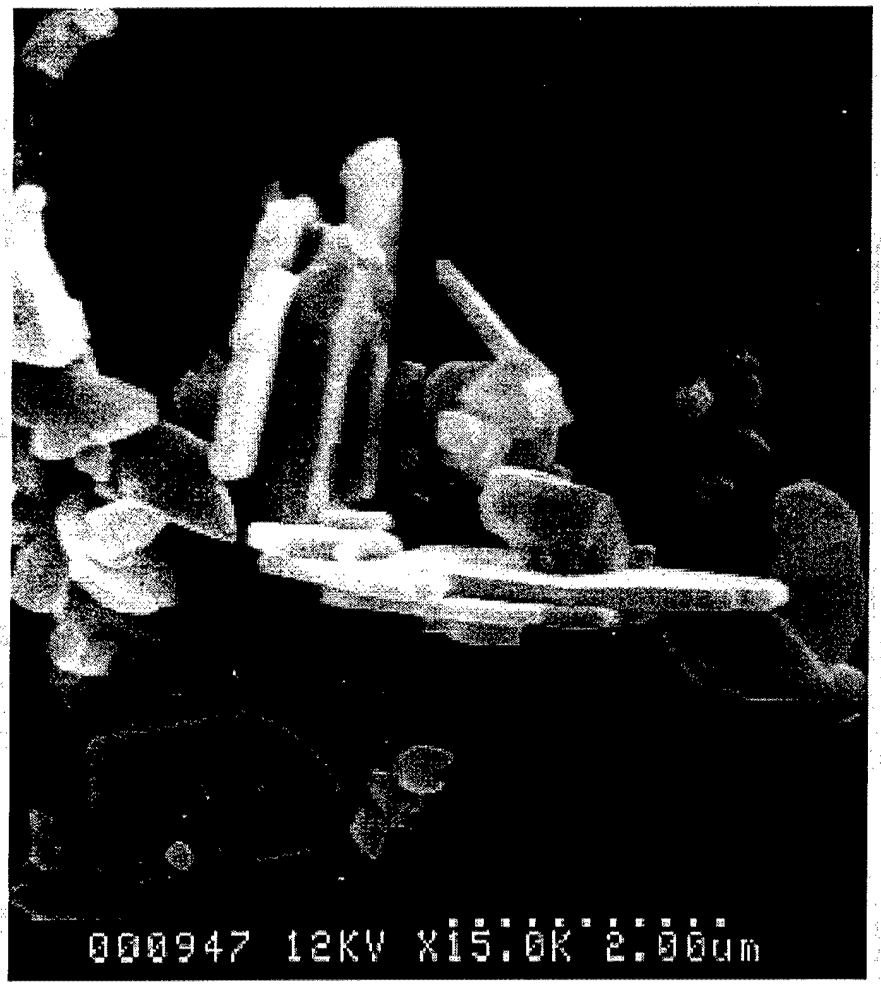

P. Afanasiev, C. Geantet
Coordination Chemistry Reviews,
178–180 (1998) 1725–1752

Lamellar Zr_Na sulphate

- It was reported earlier that the reaction of $Zr(SO_4)_2$ in molten nitrate gives ZrO_2 at 500 °C, but, due to the complexing properties of sulphate, the reaction is difficult to accomplish.

- It appears that an intermediate product of this reaction,which can be isolated at lower temperatures, presents independent interest as a new lamellar compound with ion-exchanging properties and the possibility to be intercalated with organic amines.

- The product (called NaZ) was obtained by reacting $ZrOCl_2$ in molten $NaNO_3$–Na_2SO_4 (molar ratio=4/1) melt at 673 K. The chemical composition of the product corresponds with the composition $ZrS_{0.33}Na_{0\cdot21}O_x$.

Synthesis of lamellar Zr–Na sulphate: new ion exchanger and intercalation host

SEM picture of $K_2Ni_4(P_2O_7)_2(PO_4)$

prepared in molten KNO_3 at 773 K.

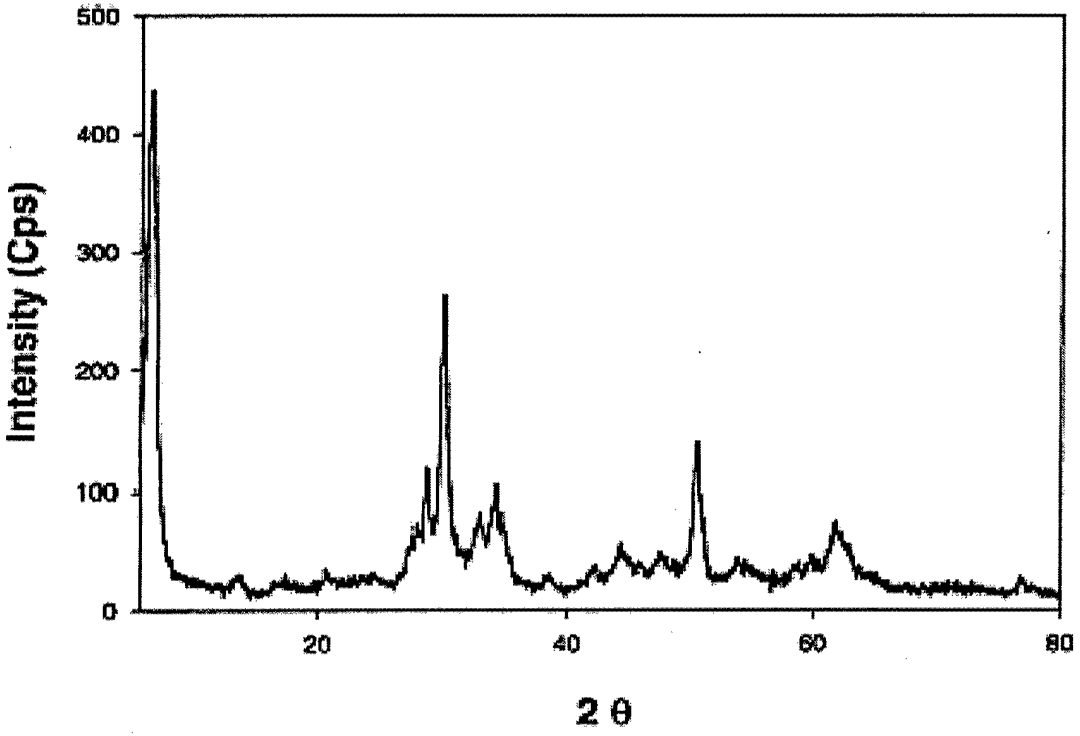

XRD pattern and SEM picture of NaZ compound.

One step preparation of supported catalysts

Numerous possibilities offered for the simultaneous synthesis, just by combining the precursors. From this variety of cases, several combinations have been tried, presenting potential interest for catalysis.

Phase composition of products issued from the simultaneous reactions of precursor alts in molten $NaNO_3$–KNO_3 at 500 °C

Oxoanion(s) oxide	SO_4^{2-}	MoO_4^{2-}	VO_4^{3-}	PO_4^{3-}
Al	Al_2O_3	Al_2O_3	Al_2O_3.	Al_2O_3
Zr	ZrO_2	ZrO_2	ZrO_2	$Na_2Zr(PO_4)_2$
Ti	TiO_2	TiO_2	TiO_2	$Na_2Ti(PO_4)_2$
Zn	ZnO	ZnO	$NaZnVO_4$	$NaZnPO_4$
Mg	MgO	$MgMoO_4$	$Na_4Mg(VO_4)_2$	$Na_4Mg(PO_4)_2$
Ni	NiO	$NiMoO_4$	$NaNiVO_4$	$NaNiPO_4$
Ca	$CaSO_4$	$CaMoO_4$	$NaCa_4(VO_4)_3$	$NaCaPO_4$

Preparation and characterization of lanthanum nickel oxides by combined coprecipitation and molten salt reactions

- Coprecipitation combined with high temperature melting was used to form lanthanum nickel oxides.

- The advantage of this method is that salts, such as NaCl, LiCl or KCl that are formed as by products during co-precipitation were not washed out.

- They act as a flux in which the precipitates dissolve and react to give oxides

Chen-Feng Kao, Charng-Lih Jeng - Ceramics International 25 (1999) 375-382

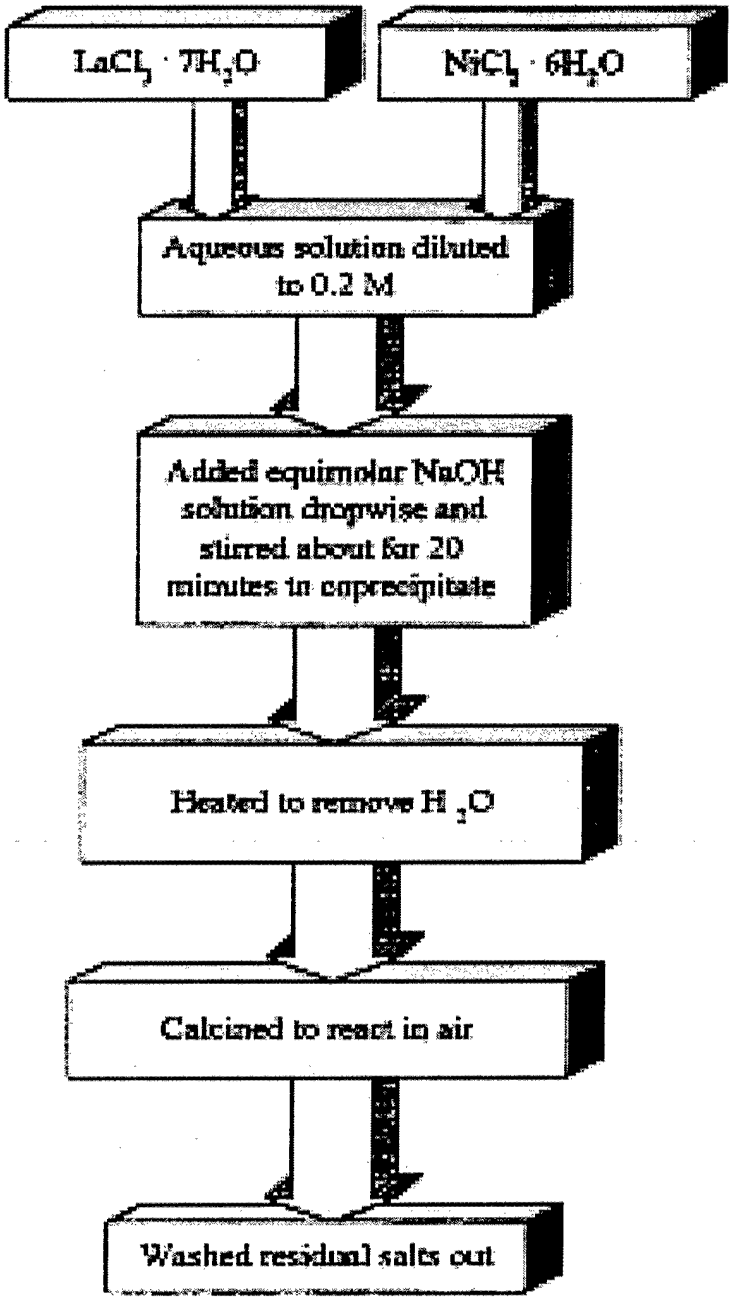

(a)

(a) La:Ni=1:1

(b)

(b) La:Ni=2:1

SEM images in 5 K magnification of the coprecipitated samples in NaOH.

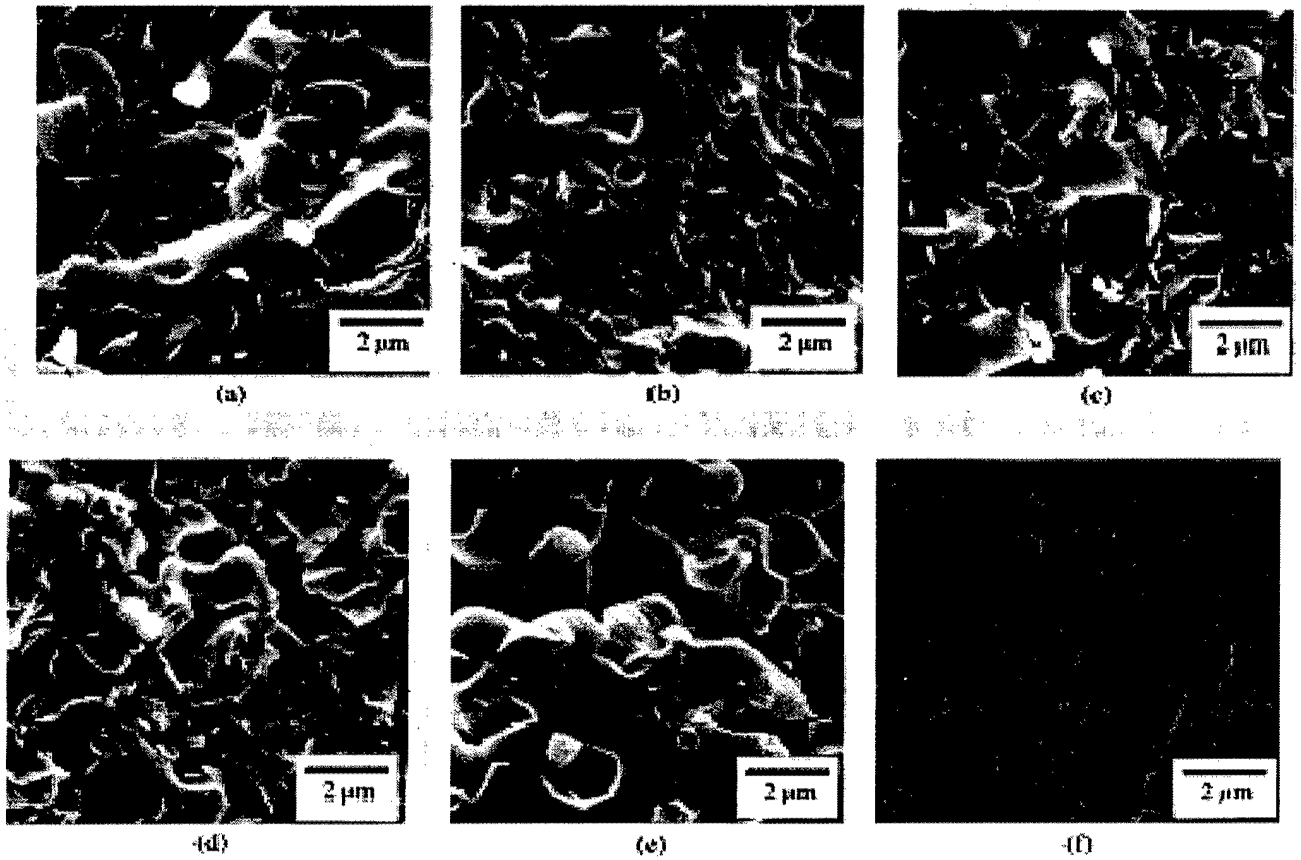

SEM images in 15 K magnification of the sintering samples:(a) La:Ni=1:1 at 1673 K with NaCl; (b) La:Ni=2:1 at 1573 K with NaCl; (c) La:Ni=1:1 at 1673 K with KCl; (d) La:Ni=2:1 at 1573 K with KCl; (e) La:Ni=1:1 at 1673 K with LiCl; (f) La:Ni=2:1 at 1573 K with LiCl.

1. The $LaNiO_3$ and La_2NiO_4 could be obtained from coprecipiting with NaOH or KOH in about 0.2-0.4 M aqueous solution, but not with LiOH

2. According to the experimental results, the $LaNiO_3$ and La_2NiO_4 could be synthesized by calcining its precursor at 1073 K for 8 h with NaCl and at 1173 K for 8 h with KCl, respectively.

3. Using NaCl as a flux, the formation of $LaNiO_3$ is best at 1073 K and some is converted to La_2NiO_4 at 1173 K.

4. The reaction temperature is lower for LiCl as auxiliary melting.

(In the course of this study a clear crystalline phase Li_2NiO_2 was discovered at 973 K).

Synthesis of superconducting $Ba_{1-x}K_xBiO_3$ by a modified molten salt process

A modified molten salt process has been developed to directly synthesise the superconducting $Ba_{1-x}K_xBiO_3$. Advantages over other known synthetic procedures in which either multiple steps are necessary (ceramic method) or the chemical composition and the superconducting properties may depend on various factors (electrolytic method):

- low temperature synthesis,
- single-step reaction
- easy control of stoichiometry.

Further, this process may, potentially, be extended to other related systems.

S.F. Liu, W.T. Fu - Materials Research Bulletin 36 (2001) 1505–1512

By using KOH as flux, a low temperature synthetic method has been used to prepare the K-doped $BaBiO_3$ in the past years [a–c]. For example, small sized crystals of $Ba0.87K0.13BiO_3$ [a] or a powdered form of $Ba_{1-x}K_xBiO_3$ consisting of at least two phases [b] have been obtained from the molten KOH-$Ba(HO)_2$-Bi_2O_3 system in air. By adding strong oxidizing agents, such as $LiNO_3$, $LiClO_4$, superconducting $Ba_{0.6}K_{0.4}BiO_3$ could also been prepared in a similar way [c]. However, the existing processes required either relatively high temperature (e.g.360°C) or prolonged synthetic time, since the oxidation of the active elements by air or other oxidizing agents in the presence of strong base is not expected to be high.

[a] J.P. Wignacourt, J.S. Swinnea, H. Steinfink, J.B. Goodenough, Appl. Phys. Lett. 53 (1988) 1753.
[b] N.L. Jones, J.B. Parise, R.B. Flippen, A.W. Sleight, J. Solid State Chemistry 78 (1989) 319.
[c] L.Z. Zhao, B. Yin, J.B. Zhang, J.W. Li, C.Y. Xu, M. Xie, S.H. Liu, Physica C 723 (1997) 282–287.

✓ 20–30g in the form of pellets KOH into a Teflon crucible and melted at t= 200 - 260°C.

✓ After 30 min., a pre-ground mixture of $Ba(OH)_2.8H_2O$, $NaBiO_3$ and Bi_2O_3 slowly added (continuously stirring with a Pt bar), with mole ratio NaBiO3: $Bi_2O_3 = 2(11x)/(1-x)$ (i.e. ratio Bi^{5+}:Bi^{3+} ions in $Ba_{1-2x}K_xBiO_3$,) but with $Ba(OH)_2.8H_2O$ slightly in excess vs. stoichiometry

✓ As soon as the mixture was added into melted KOH, a black precipitate was formed immediately. The melt was maintained for several hours at the above-mentioned temperatures to improve the homogeneity of the samples.

✓ Finally the liquid in the crucible was poured out, while the precipitate was kept and cooled to room temperature.

✓ The precipitates were thoroughly washed with distilled water to remove the residual KOH and, then, rinsed with ethanol and dried in air for a few hours at about 75°C.

✓ The final products were fine powders.

$$(1-x)\cdot Ba^{2+} + x\cdot K^{+} + (1-2x)/2\cdot BiO_3^{3-}$$

$$+ (1+2x)/2\cdot BiO_3^{-} \rightarrow Ba_{1-x}K_xBiO_3$$

The actual reaction might be more complicated or involves chemical equilibrium since the oxidation (or reduction) of bismuth in air cannot be avoided and the KOH is much more abundant. This can be seen from the fact that using the stoichiometrically calculated amount of $Ba(OH)_2.8H_2O$, Bi_2O_3 and $NaBiO_3$ results in a composition of slightly higher K content.

SEM of the $Ba_{1-x}K_xBiO_3$ powders :

The particle sizes are of a few micrometers, and are quit uniform.

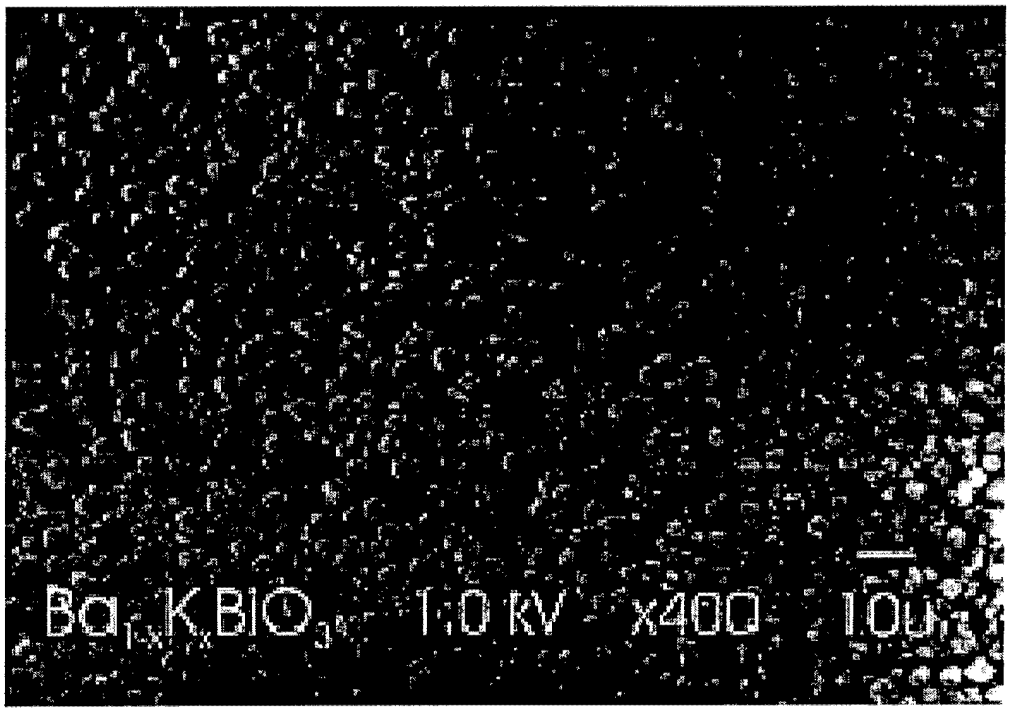

AC susceptibility data of $Ba_{0.6}K_{0.4}BiO_3$.

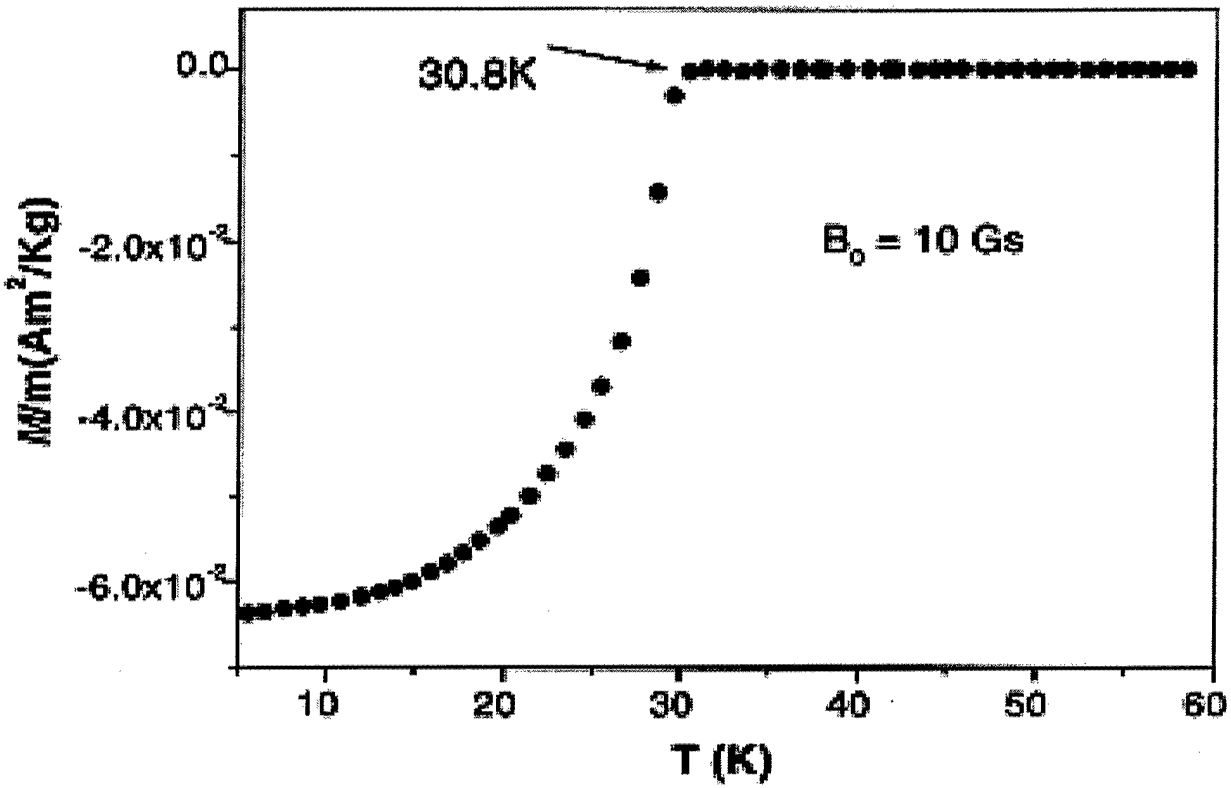

The superconducting T_{tr} is about 30.8 K (i.e slightly > than the reported T_{tr} of ceramically prepared $Ba_{1-x}K_xBiO_3$ powders .

The transition is apparently very sharp, indicating a good homogeneity of the sample.

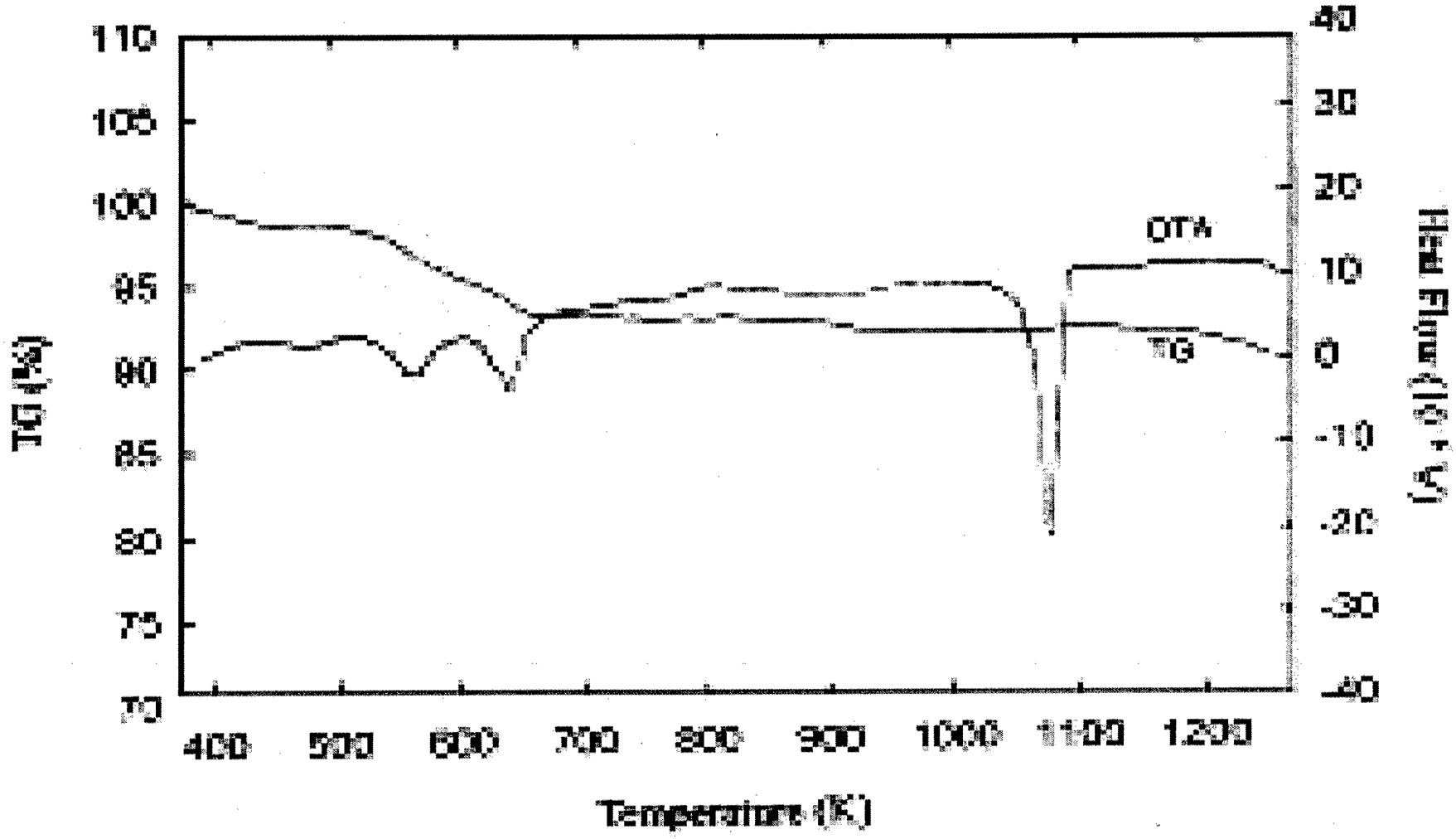

Thermogravimetric analysis and differential thermal analysis of the precursor.

Fabrication of CoO nanorods via thermal decomposition of CoC_2O_4 precursor

- CoO nanorods with diameters of 10–80 nm and lengths of several micrometers have been successfully prepared by a simple and novel method.
- These CoO nanorods are structurally uniform, single crystalline.
- The growth mechanism of the CoO nanorods is similar to the molten salt synthesis.
- Particularly, surfactant NP-9/5 and NaCl flux are of critically importance for the formation of CoO nanorods.

Congkang Xu, Yingkai Liu, Guoding Xu, Guanghou Wang - Chemical Physics Letters 366 (2002) 567–571

Nanorods : great potential to provide an opportunity to test fundamental quantum mechanics concepts and to play a vital role in various applications such as photonics , nanoelectronics and data storage.

Cobalt oxide CoO: cubic rock-salt structure ; technologically important applications based on its magnetic or catalytic properties .

Synthesis of cobalt oxides nanocrystals up to now, many routes such as sol–gel , spray pyrolysis , chemical vapor deposition , chemical precursor routes, electro-chemical and sonochemical synthesis

---

fabrication of CoO nanorods: a simple and novel method
by calcining the precursor of CoC_2O_4 obtained via chemical reaction between $Co(CH_3COO)_2 . 4H_2O$ and $H_2C_2O4. 2H_2O$ in the presence of NP-9/5 and NaCl flux.

Starting materials: cobalt acetate $Co(CH_3COO)_2 .4H_2O$, oxalic acid $H_2C_2O4. 2H_2O$, nonyl phenyl ether (9)/(5)(NP-9/5) and NaCl.

- **$Co(CH_3COO)_2.2H_2O$ (4.98 g) and $H_2C_2O4 . 2H_2O$ (2.53 g) according to 1:1 molar rate were mixed with 5 ml of NP9/5 in a mortar, ground for several minutes and kept in a thermostat oven at 50–60 °C for 6h to prepare the precursor, the product was washed several times with distilled water and acetone to remove remaining reactants, NP9/5 and by-product,**
- **and then dried in an oven at 70–80 °C for 12 h.**

- **The obtained product was collected for the fabrication of CoO nanorods. CoC_2O4 (2 g) was simultaneously mixed with 8 g of NaCl powder and then ground for several minutes. The ground mixture was annealed at 900 °C for 2 h. Following heat treatment, it was gradually cooled to room temperature (5°C/min), the as-prepared product was washed with distilled water, ethanol and then ethyl ether by an ultrasonic bath and a centrifuge.**

General TEM morphologies of
the synthesized product.
mostly composed of solid rod-like structures.
(a), smooth nanorods, 10–80 nm diameter , length ranging 1- 3 um.
(b) typical nanorod with conical tips at both ends, about 50 nm.

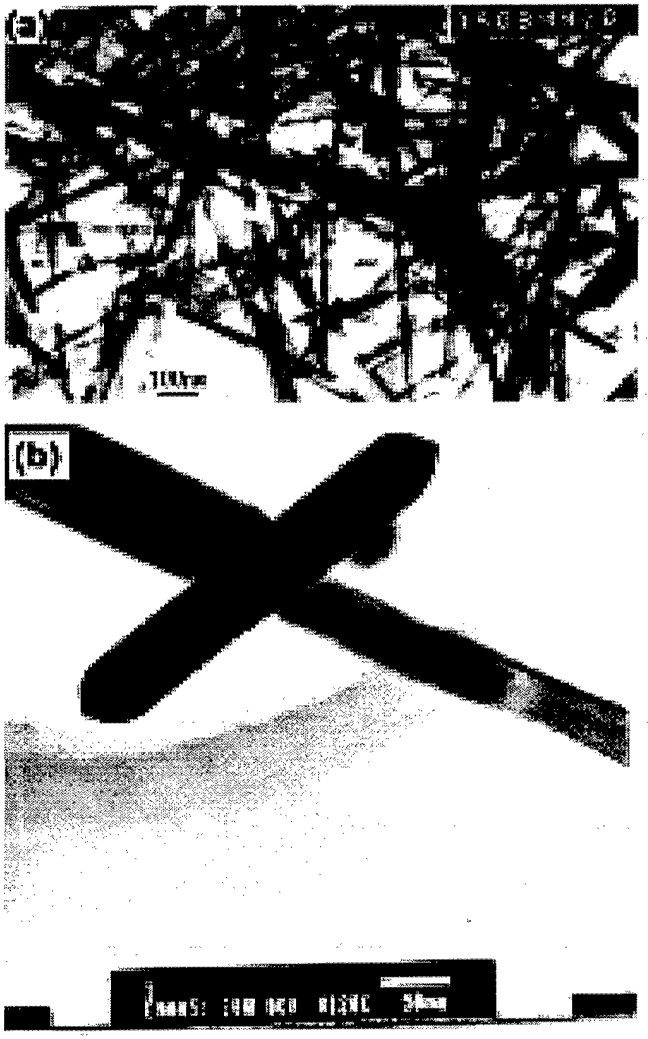

Preparation of lanthanum nickel strontium oxides

- **$LaNiO_3$ has attracted much attention in the past few years, because of technolo gically important applications (conducting layer for application in ferroelectric memories, electrode for high temperature fuel cells , catalyst and as a sensor for ethanol.**

- **$LaNiO_3$ is a cubic or rhombohedrally distorted perovskite-type structure. Its thermal stability is not so high (1170K) because of a partial reduction of Ni^{3+} to Ni^{2+} induced by oxygen partial pressure during heating. Therefore, $LaNiO_3$ is converted to La_2NiO_4, as a two-dimensional structure of K_2NiF_4**

- **The substitution of La_{3+} in $LaNiO_3$ by Sr_{2+} would reduce the Ni_{3+} change to Ni_{2+} for assuring the cubic perovskite structure .**

Chen-Feng Kao, Charng-Lih Jeng - Ceramics International 26 (2000) 237-243

Method: combined coprecipitation and molten salt reactions

1. $La_{1-x}NiSr_xO_3$ and $La_{2(1-x)}NiSr_2xO_4$ obtained from coprecipiting with NaOH in about 0.2-0.4 M of corresponding metal chlorides in ethyl alcohol solution ; particle size : 0.1 mm.

2. limiting amount of Sr^{2+} dopant for $La_{1-x}NiSr_xO_3$ and $La_{2(1x)}NiSr_2xO_4$: x= 0.15 and 0.30, respectively. Further doping with Sr^{2+} would induce appearance of other compounds, such as $La_{1.5}NiSr_{0.5}O_4$.

3. LaNiO3 , doped with Sr^{2+} , would maintain its perovskite phase at higher temperature (no reduction of Ni^{3+} convert to Ni^{2+}).

This process control is much easier

The oxides have more uniform and much better particle size distribution than that of solid-state reaction or general chemical coprecipitation *(the general chemical coprecipitation process needs to wash the precursors with distilled water and to filltrate repeatedly that would make serious deviations from stoichiometry).*

The reactions can be written as follows:

$$2(1-x)LaCl_3 + NiCl_2 + 2xSrCl_2 + (8-2x)NaOH$$

$$\rightarrow 2(1-x)La(OH)_3 + Ni(OH)_2 + 2xSr(OH)_2 +$$

$$(8-2x)NaCl + x/2O_2$$

$$\rightarrow La_{2(1-x)}NiSr_{2x}O_4 + (8-2x)NaCl + (4-x)H_2O\uparrow$$

- Chloride mixture dissolved in absolute ethyl alcohol and diluted to 0.2 M.

- Saturated NaOH aqu. solution used to mix with the above solution to form a lanthanum nickel strontium hydroxide precursor.

- The rotary evaporator was used to obtain the dry precursors and to recovery the alcohol for reuse.

- Solid-phase precursors calcined at 700, 800 and 900°C for 8 h, respectively.

The salt was acted as a flux to improve the reactivity of precursor.

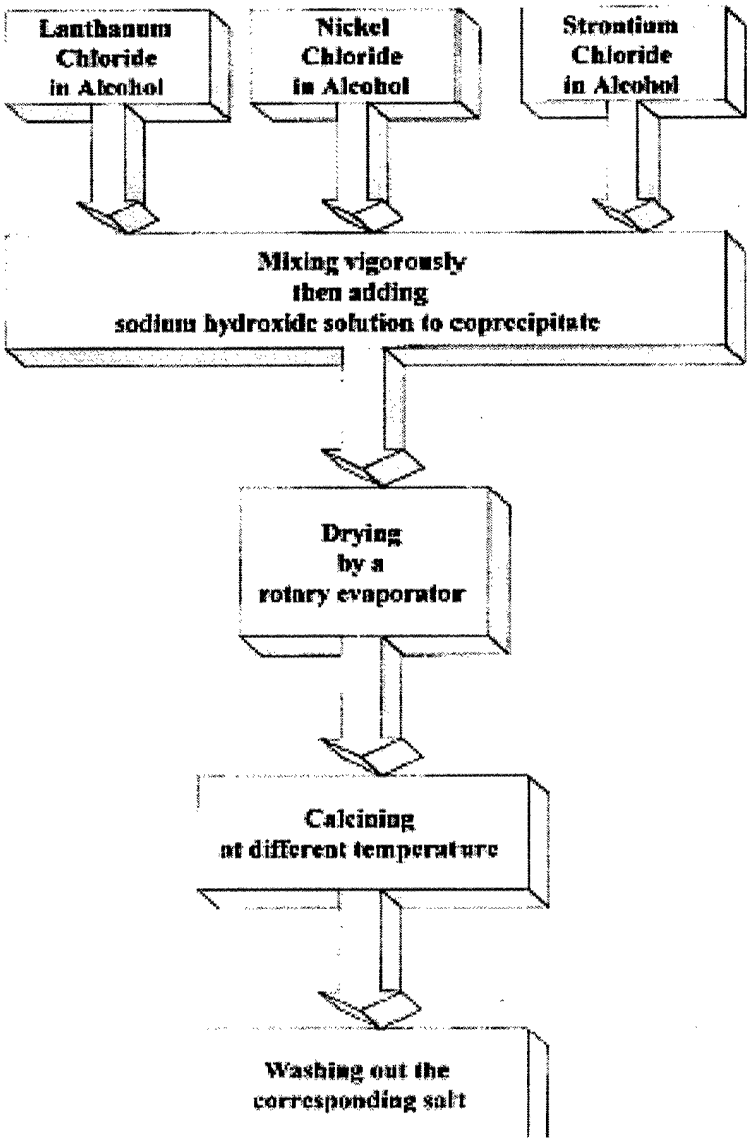

NANOSIZED CeO_2 POWDERS OBTAINED BY FLUX METHOD

- **Nanosized and well-crystallized Ce(IV) oxide powder was prepared by the flux method at relatively low temperature (600°C), utilizing cerium(IV) salt and different eutectic molten salt mixtures**

- **Very simple ; lead to powders with desirable characteristics, including very fine size, narrow size distribution, single-crystal particles, high purity, and good chemical homogeneity.**

- **Same advantages as the hydrothermal technique (low cost, elimination of the calcination process) but does not require elevated temperature and pressure.**

F. Bondioli, A. Bonamartini Corradi, C. Leonelli, and T. Manfredini - Materials Research Bulletin, Vol. 34, Nos. 14/15, pp. 2159–2166, 1999*

Sample Preparation.

- **molten salt reactions in alumina crucibles at 600°C.**

- **Solvents: KOH/NaOH, $NaNO_3/KNO_3$, and LiCl/KCl eutectic mixtures chosen, due to their low melting temperatures (170, 225, and 355°C, respectively)**

- **The Ce(IV) precursor cerium ammonium nitrate $(NH_4)_2Ce(NO_3)_6$ was added in a 1:1 ratio to the molten salt at the reaction temperature.**

- **The melt was maintained at maximum temperature for 120 min. After being quenched to room temperature, the reaction products were separated from the soluble alkali salts by washing with distilled water and then were dried in air at 100°C.**

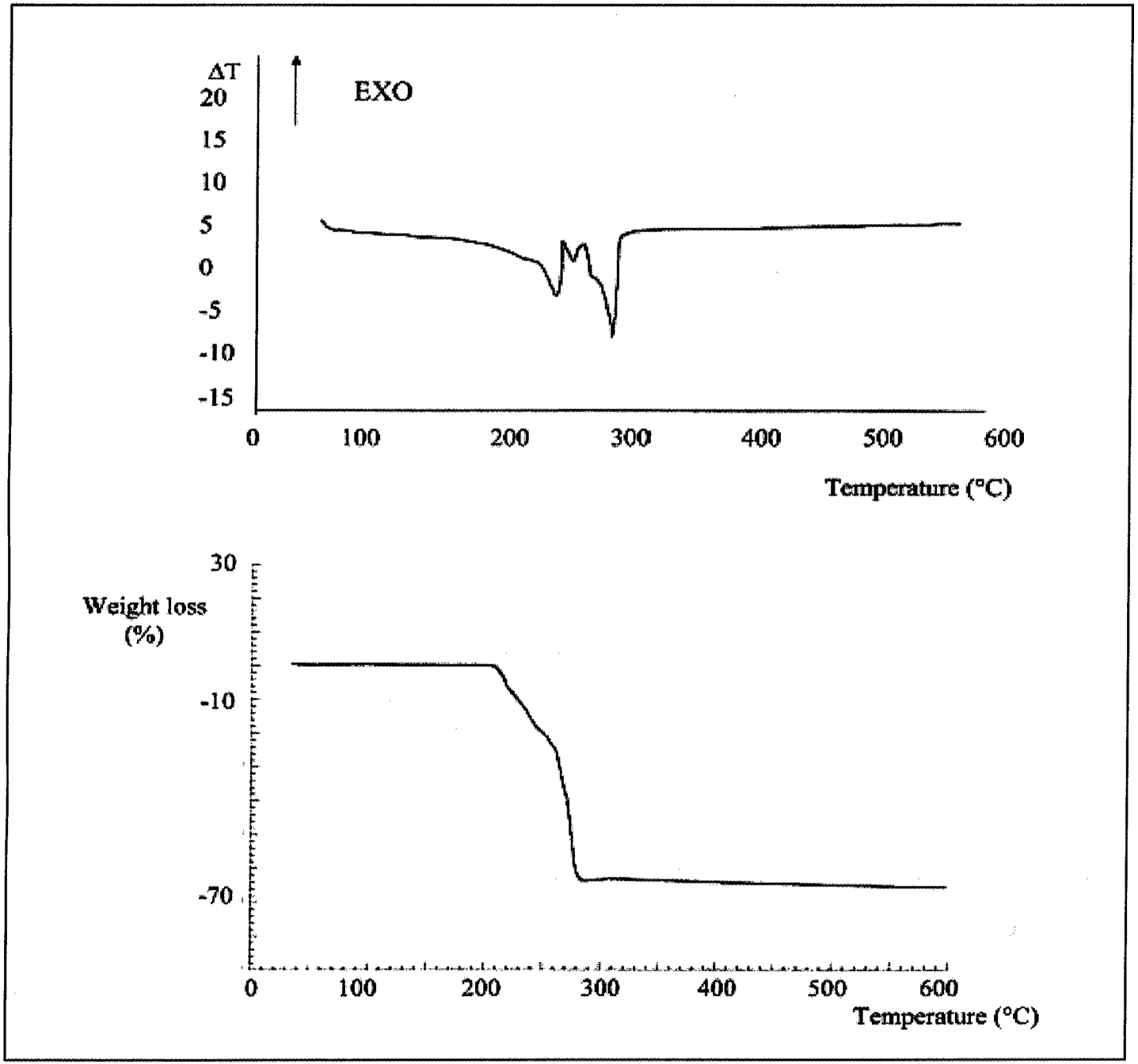

DTA &TGA curves of $(NH_4)_2Ce(NO_3)_6$.

A four-endothermic-step transformation according to the following equations:

$$(NH_4)_2Ce(NO_3)_4 \rightarrow 2NH_3 + H_2O + 2NO_3^- + Ce(NO_3)_4$$

$$Ce(NO_3)_4 + 2NO_3^- \rightarrow Ce(NO_3)_4 + NO_3^- + NO_2 + 1/2O_2$$

$$Ce(NO_3)_4 + NO_3^- \rightarrow Ce(NO_3)_4 + NO_2 + 1/2O_2$$

$$Ce(NO_3)_4 \rightarrow CeO_2 + 4NO_2 + O_2$$

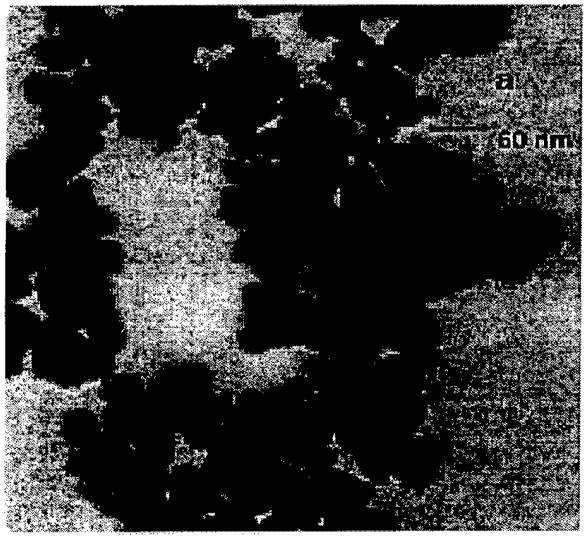

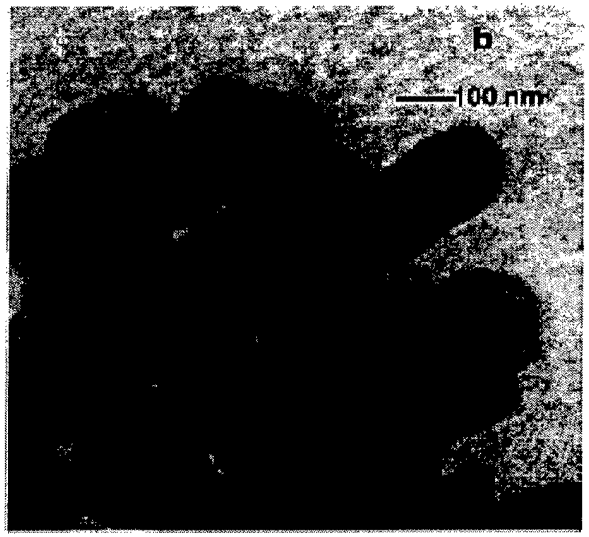

TEM micrographs of the ceria powders obtained by fluxes of

(a) hydroxides,
(b) nitrates, and
(c) chlorides.

The XRD analysis of the as-prepared powders showed the same crystalline structure for all the fluxes used. Peaks were attributed to crystalline cerium oxide, CeO_2, with a cubic fluorite structure

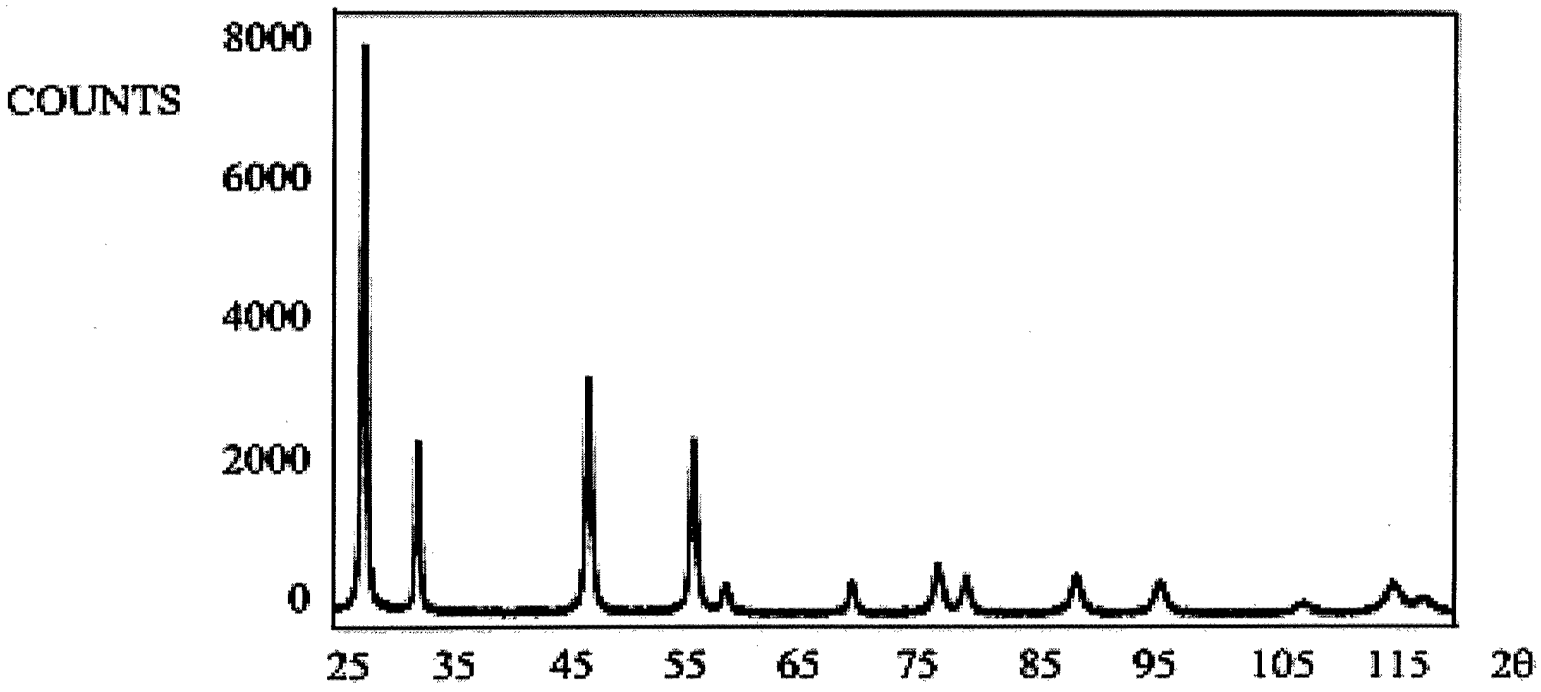

Average Powders Particle Size Calculated by Various Methods

Methods	Flux used		
	Hydroxides	Nitrates	Chlorides
XRD (nm)	18	25	16
TEM (±3 nm)	20	20.5	14
BET (nm)	23	28	20

TEXTURED MICROSTRUCTURES IN BARIUM HEXAFERRITE

- **Seeded reactive matrix and templated grain growth used to produce highly textured materials in the barium hexaferrite system.**

- **This technique, in which seeds are obtained by molten salt synthesis (MSS), provides more flexibility for producing textured microstructures than tape casting or uniaxial pressing.**

- **Since the texture direction is coupled only to the direction of the applied magnetic field, a wide variety of sizes and shapes of textured components are afforded.**

- **It is anticipated that this technique can be employed for a variety of magnetically anisotropic materials.**

David B. Hovis and K.T. Faber - Scripta mater. 44 (2001) 2525–2529

Two components are needed in order to make textured barium hexaferrite by combined magnetic field assisted gelcasting and TGG techniques.

•First, a non-magnetic precursor to barium hexaferrite must be developed that can meet the suspension requirements of gelcasting

(starting materials) Fe_2O_3.$BaCO_3$. ***(molar ratio 5.6:1) with 1.5% by mole of B2O3 and (gel) HMAM initiated with approximately 0.5mL/g slurry of APS TMED)***
The solids loading was 40% by volume. Surfynol CT-131 (was used as the surfactant. The slurries were ball milled

•Second, seed particles must be produced that are sufficiently anisotropic to serve as templates for texturing.

At high temperatures, the iron oxide and barium carbonate react to form a fine-grained barium ferrite matrix surrounding the previously aligned barium ferrite seeds.

Anisotropic "seed" particles were produced **using** a two-stage **molten salt synthesis (MSS).**

• First, Fe_2O_3 and $BaCO_3$ were mixed with KCl as the fluxing agent at a 1:1 reactants:salt weight ratio. Heating to 900°C for hours in an Al_2O_3 crucible produced plate-shaped BaFe12O19 particles approximately 1mm in diameter.

• To coarsen the particles, the $BaFe_{12}O_{19}$ plates from the KCl melt were mixed with $BaCl_2$ and Fe_2O_3.
The $BaCl_2$:Fe_2O_3 ratio was 2:1 by weight and the Fe_2O_3: $BaFe_{12}O_{19}$ ratio was 500:1 by mole. Heating to 1150°C for 8 hours produced particles ranging from 5–25mm and approximately 1–2mm thick. These were deemed adequate for templated grain growth and are shown in Figure 1.

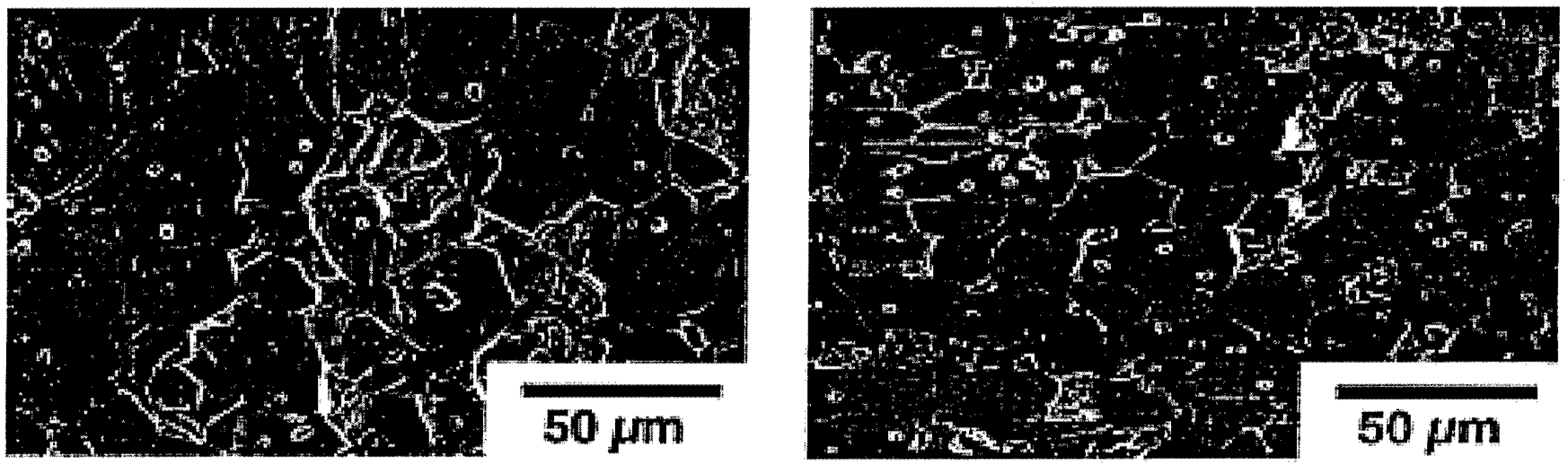

SEM micrographs of the control (a) and magnetically-aligned (b) samples.

The control samples possess a large grain size (20–30mm), but not the plate-like shape indicative of textured barium hexaferrite. The magnetically-aligned samples possess a large grain size (;25–50mm), plate-like shape, and a definitive preferred orientation.

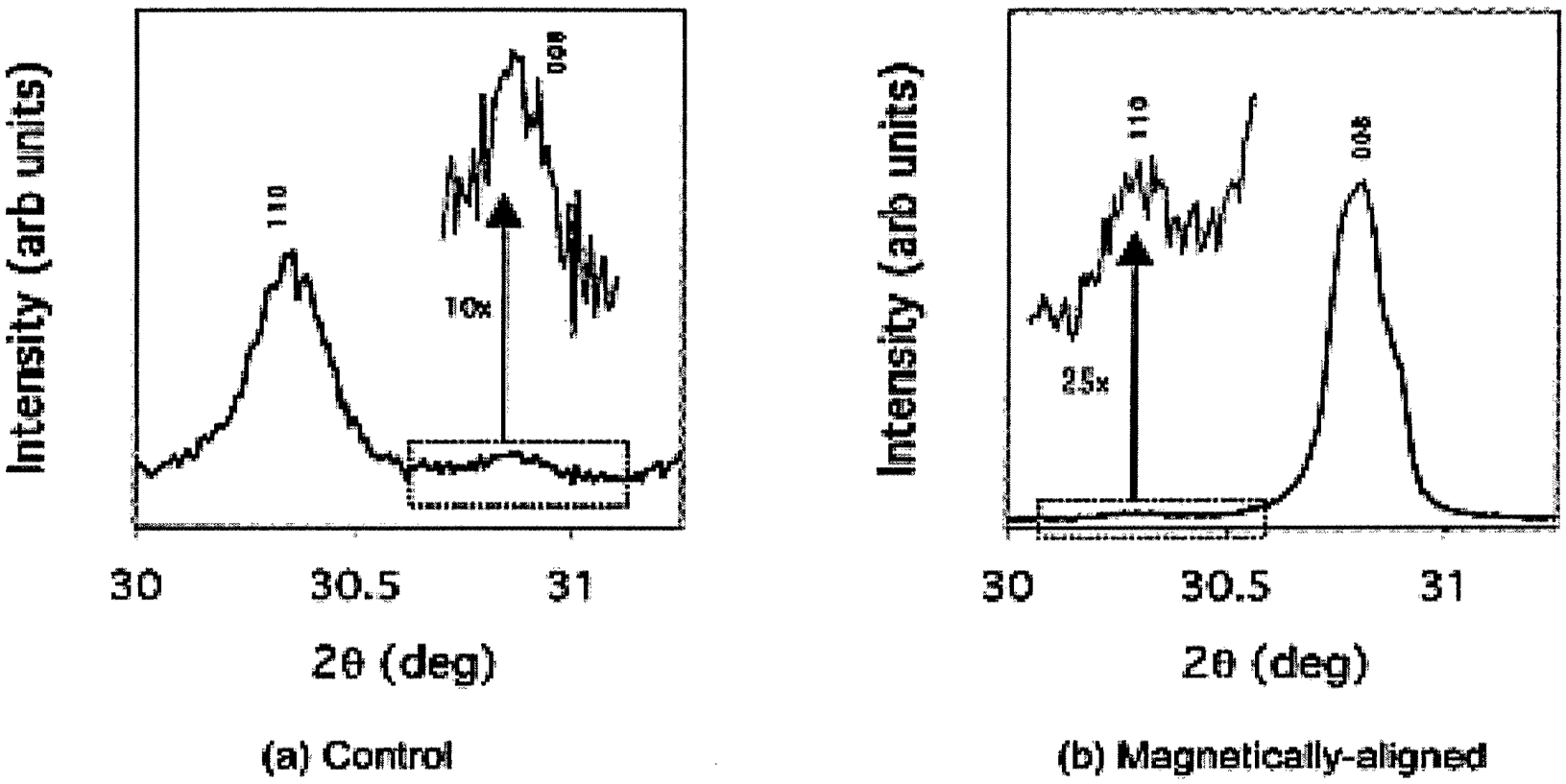

Relative intensities of the (110) and (008) peaks in the control and magnetically aligned samples (Note difference in amplification of smaller peak).

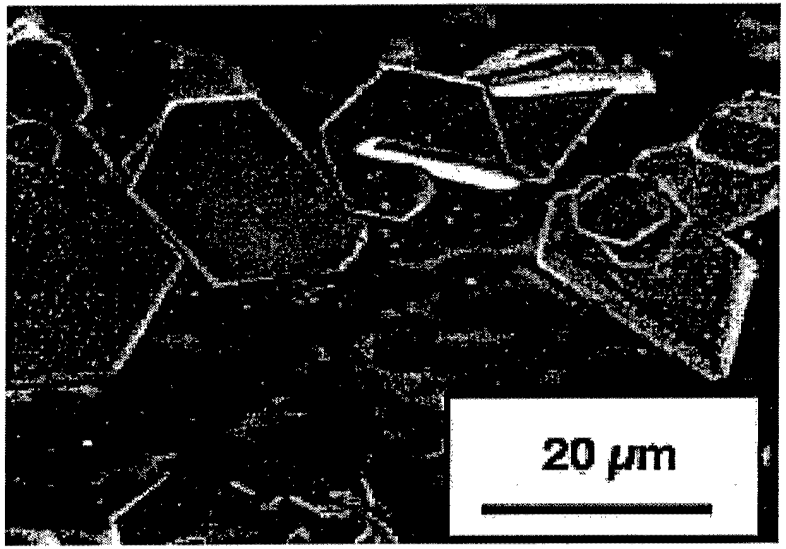

Molten salt synthesized “seed” particles of barium hexaferrite.

- The flux method is a well-known method used for single-crystal growth , but it has seldom been applied to the synthesis of nanocrystalline particles.

- This method is very simple and can lead to powders with desirable characteristics, including very fine size, narrow size distribution, single-crystal particles, high purity, and good chemical homogeneity. As with the hydrothermal technique, the main advantages of this method are not only low cost, but also the elimination of the calcination process.

- In addition, the flux method does not involve the elevated temperature and pressure (4 h at 300°C, 10 MPa) characteristic of the hydrothermal technique.

NbSi coating on niobium using molten salt

•For obtaining better oxidation resistance of niobium in air, a niobium silicide was non-electrolytically deposited onto Nb from a molten salt, where a disproportional reaction occurs between Na_2SiF_6 , SiO_2 , and Si. A single phase of $NbSi_2$ was formed with a homogeneous thickness of about 10 mm above 1073 K.

•The oxidation resistance of pure niobium with this coating layer was improved.

•During the oxidation at the high temperatures, Nb_5Si_3 was formed at the interface between the Nb substrate and the NbSi2 layer. Due to this intermediate layer formation, the oxidation resistance became better than for pure $NbSi_2$

Ryosuke O. Suzuki , Masayori Ishikawa , Katsutoshi Ono - Journal of Alloys and Compounds 336 (2002) 280–285

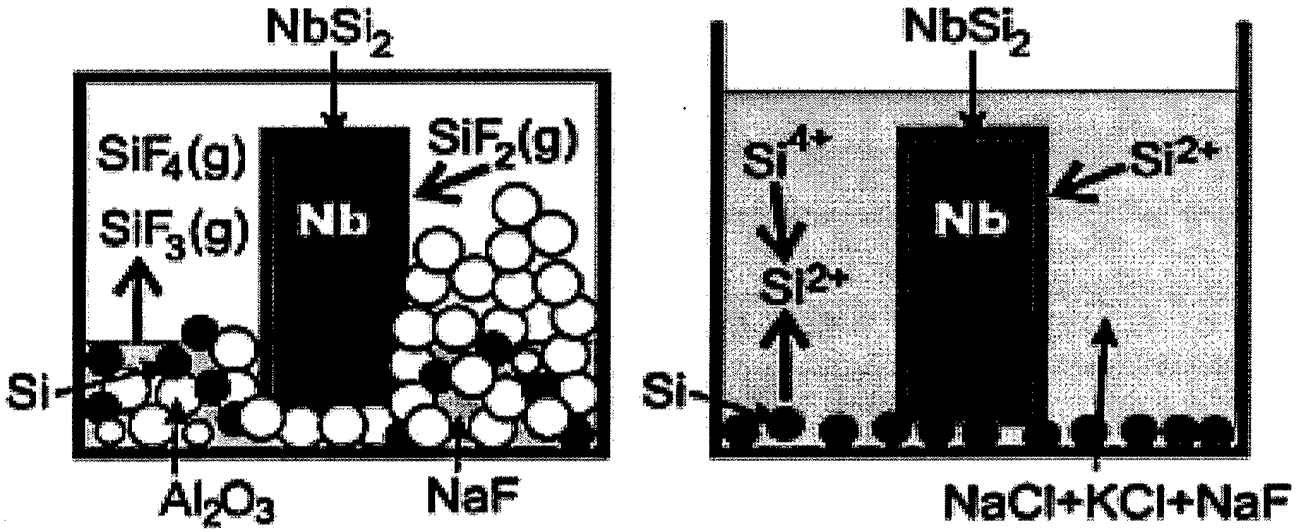

(a) Pack-cementation method : low cost, good adhesion coating but requires encapsulation and a high vapor pressure at temperatures as high as 1273–1473 K.

(b) Electroless plating: operable in open air at 973–1173 K

When Na_2SiF_6 and Si powder are added in the supporting salt of NaCl–KCl, a disproportional reaction between Si and Si^{4+} ions deposits a siliconized layer on the metallic substrates, M, as,

Si (source particles in the molten salt) + 6 F^- + SiF_6^{2-} => 2 SiF_6^{4-}

2 SiF_6^{4-} +M(substrate =>M-Si (siliconized layer) + 6 F^- + SiF_6^{2-}

The deposited Si from Si^{2+} penetrates into the metal surface, and forms an alloy (M–Si) with the metal substrate. The total reaction,

Si (particle in the molten salt) + M(substrate) => M–Si (siliconized layer),

shows that the reaction is driven by the difference between the thermodynamic activity of pure silicon and that of the siliconized layer.

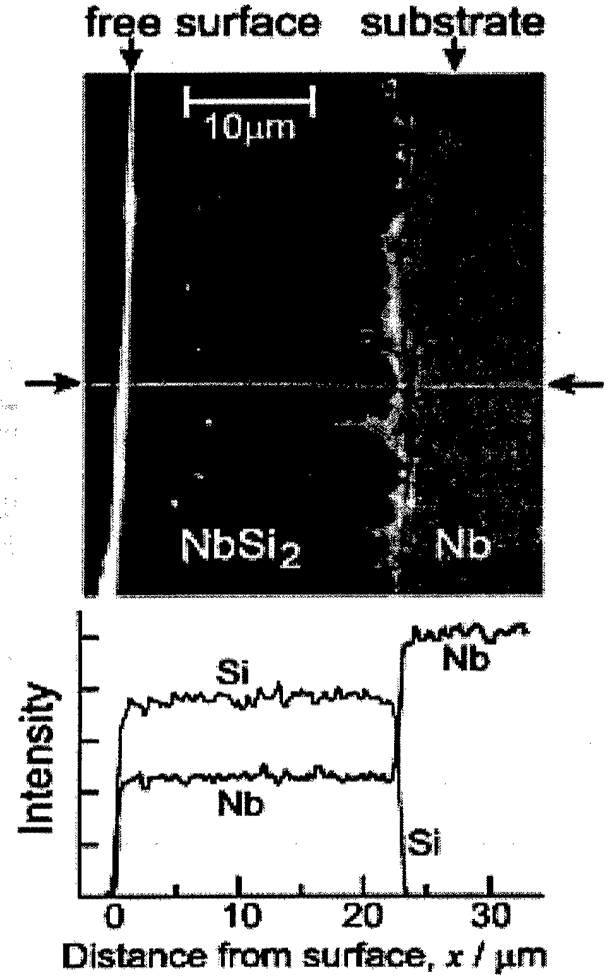

SEM image of the cross-section for the Nb sample siliconized at 1173 K for 7.2 ks. Nb and Si concentration were analyzed along the white line in the SEM image.

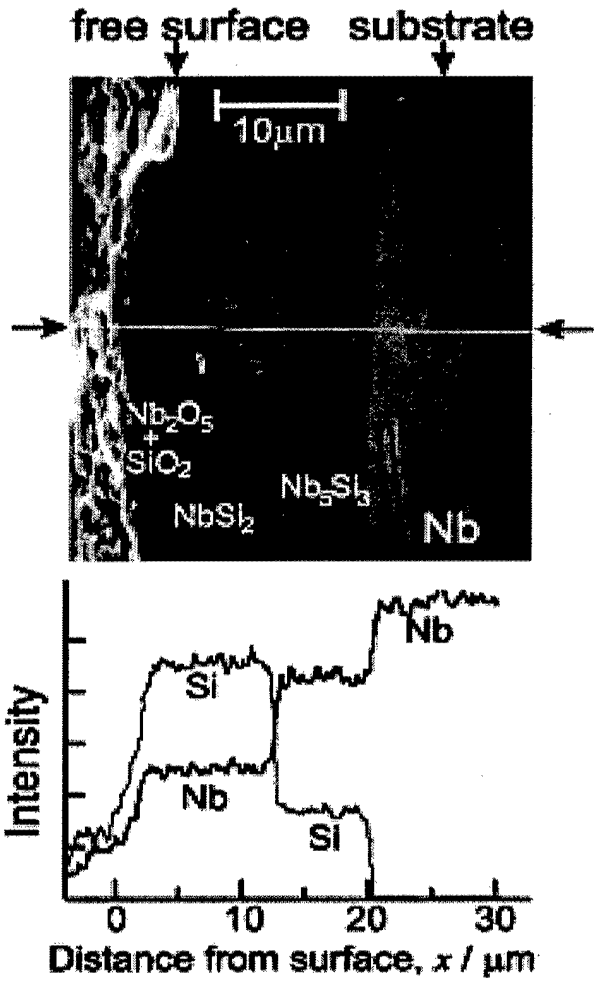

SEM image of the cross-section for the Nb sample siliconized at 1173 K for 7.2 ks. The sample was heated up to 1523 K in air. Nb and Si concentration were analyzed along the white line in SEM image.

A wide range of ceramic powders, including both single and complex perovskite ceramic system, have been synthesized in various molten salts.

- **Alumina and zirconia powders by decomposing aluminum sulfate or aluminum chloride and zirconium sulfate in molten nitrates or nitrites salts, respectively.**

- **Binary oxides of perovskite structure,** such as **BaTiO3–SrTiO3** and **BaZrO3–SrZrO3** : in the **NaOH–KOH** molten salt eutectic @573 K.

- **Lead niobate** : in molten **KCl-NaCl**

- $Pb(Fe_{1/2}Nb_{1/2})O_3$ (PFN) in **NaCl and KCl** @ 800°C,

- **lead magnesium niobate** in **KCl and $(Li,Na)SO_4$** Both the reaction temperature and excess lead in the starting composition were shown to strongly affect the amount of perovskite phase formed in the molten salts.

- **$(1-x)Pb(Mg_{1/3}Nb_{2/3})O_3 - xPb(Fe_{1/2}Nb_{1/2})O_3$** : in KCl flux

Molten salt synthesis of complex perovskite-related dielectric oxides

Several important dielectric materials ($Ba(Zn_{1/3}Nb_{2/3})O_3$, $Ba(Mg_{1/3}Nb_{2/3})O_3$ and $Ba(Zn_{1/3}Ta_{2/3})O_3$) , crystallizing in the cubic perovskite structure, at low T (900°C) with short time of heating using NaCl–KCl mixtures as flux.

- **Sintering at 1000°C retains the disordered cubic structure.**
- **After the 1300°C sintering there is a slight decomposition to $Ba_5Nb_4O_{15}$ in the niobates and nearly complete decomposition to $Ba_{0:5}TaO_3$ in the case of $Ba(Zn_{1/3}Ta_{2/3})O_3$.**
- **The reactivity of the oxide is much higher due to the initial flux treatment. Large faceted grains of size 7–10 microns, were observed in these samples after sintering at 1300°C. The grain size appears to depend on the initial time period of treatment with the flux.**

M. Thirumal, P. Jain, A.K. Ganguli
Materials Chemistry and Physics 70 (2001) 7–11

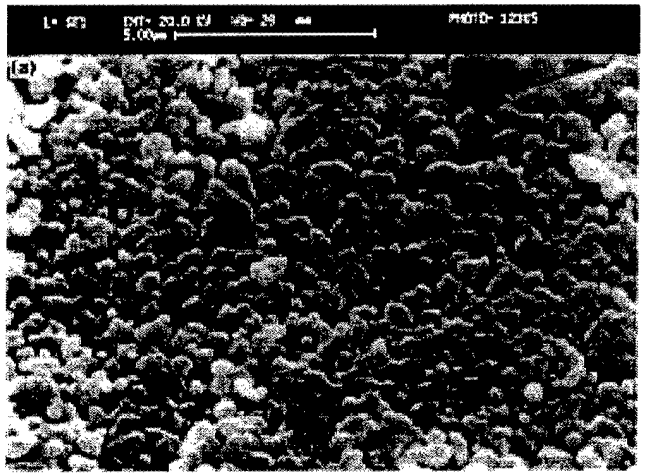

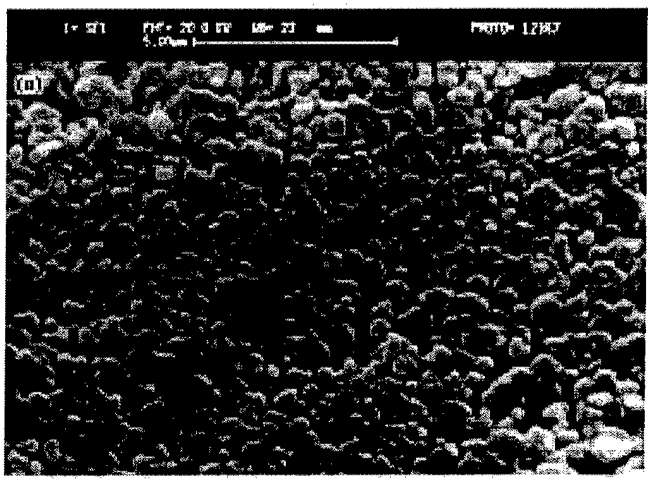

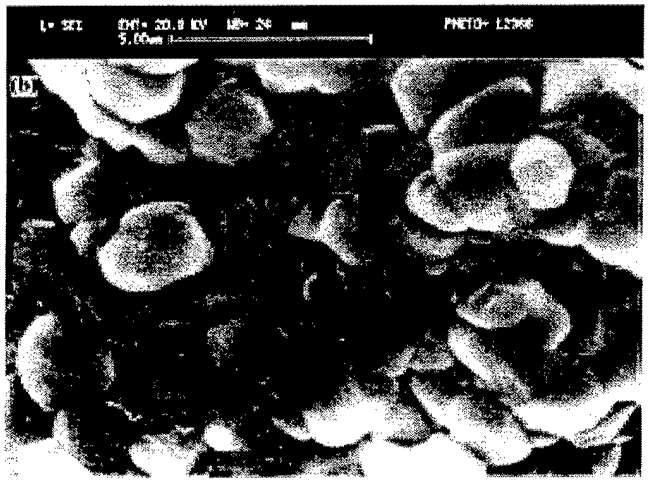

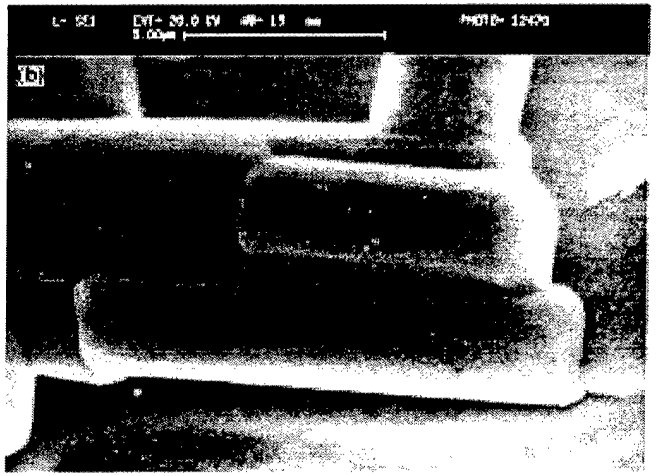

SEM of $Ba(Zn_{1/3}Nb_{2/3})O_3$ (a) sintered at 1000°C (b) sintered at 1300°C (initial flux treatment 900°C/3 h).

SEM of $Ba(Zn_{1/3}Nb_{2/3})O_3$ (a) sintered at 1000°C (b) sintered at 1300°C (initial flux treatment 900°C/6 h).

Formation of lead magnesium niobate synthesized from molten potassium chlorate

•Lead magnesium niobate powders were prepared by reacting PbO, MgO and NbO in molten potassium chlorate. The formation of a single phase perovskite PMN requires a combination of 100 mol % excess lead oxide and a reaction temperature of 900°C.

•The choice of potassium chlorate as a flux is on the consideration that it is is a powerful oxidizing agent, which may be useful in forming the perovskite phase of PMN. As reported, an oxidizing atmosphere is beneficial to prevent the formation of pyrochlore phase in the conventional solid state reactions

D.M. Wan , J. Wang , S.C. Ng , L.M. Gan - Journal of Alloys and Compounds 274 (1998) 110–117

•The average particle size of resulting PMN powders increases with increasing reaction temperature and the amount of excess lead oxide added, while the particles undergo a change from a round to a cubical morphology. Too much excess PbO (.100 mol %) in the starting composition promoted grain growth in the molten salt-derived PMN ceramics, although the sintered density is not much affected at 1200°C and above. It also degrades the dielectric properties of sintered PMN, as a result of the occurrence of PbO-rich precipitates at the grain boundaries and grain junctions.

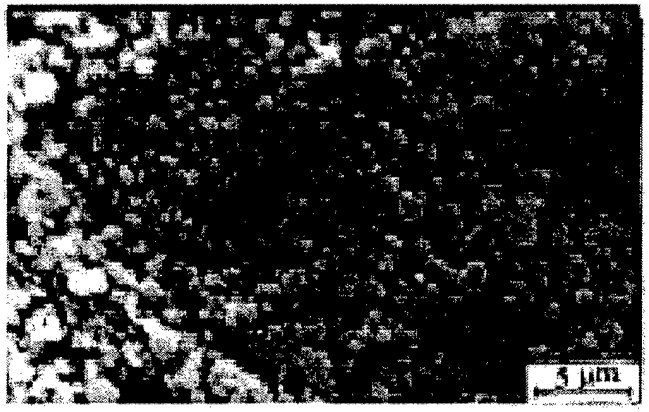

(A)

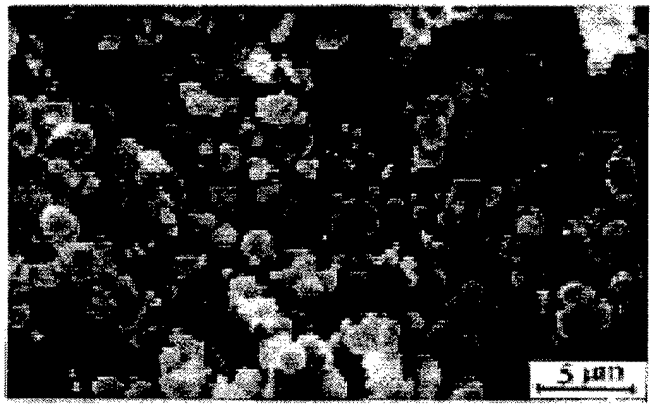

(B)

(C)

(D)

SEM Micrographs of the PMN powders formed in the compositions containing 0, 50, 100 and 200 mol % excess lead oxide, respectively, at 900°C for 2 h.

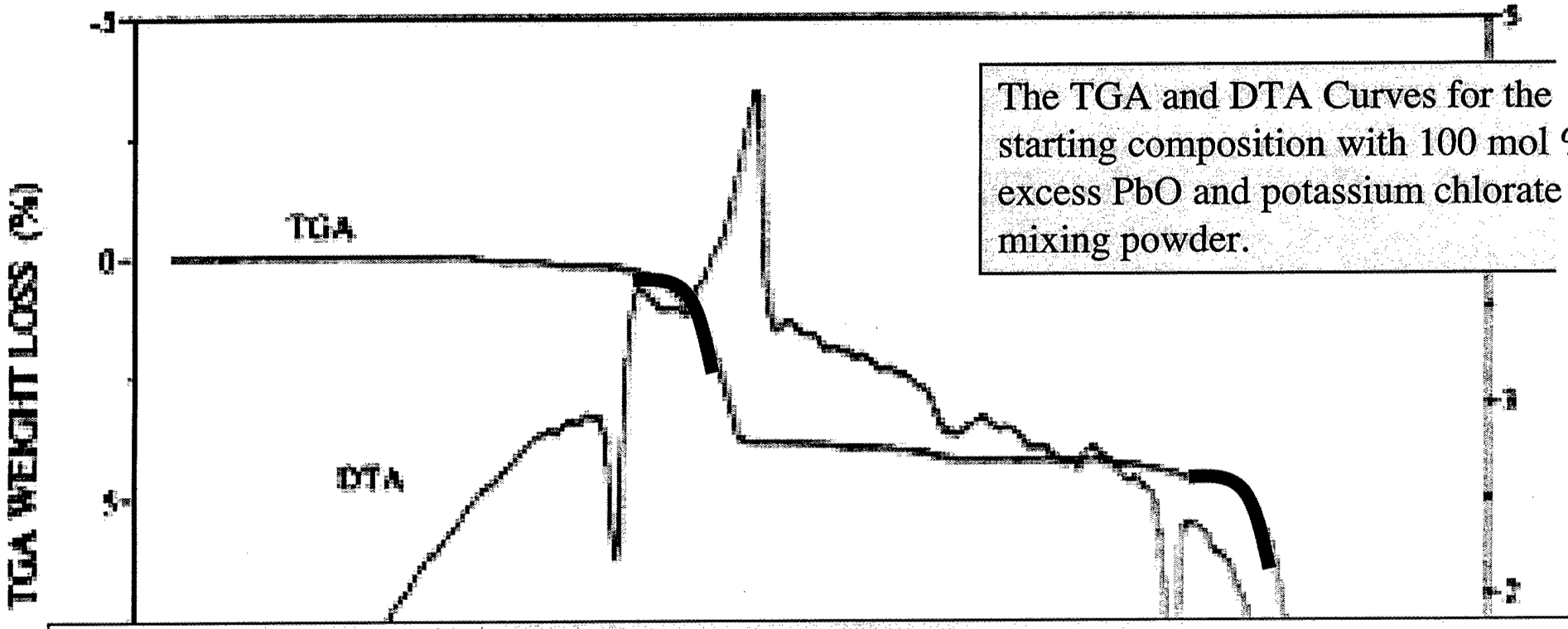

The TGA and DTA Curves for the starting composition with 100 mol % excess PbO and potassium chlorate mixing powder.

TGA curve :

350–500°C, **flux decomposition**, where potassium chlorate melts at 356°C and then resolidifies to form potassium perchlorate. The potassium perchlorate is further decomposed into KCl and O2 with increasing temperature [15].

750–900°C, **loss of lead oxide**

DTA

Endo peaks: @ 356°C **melting of potassium chlorate**,@772°C **melting of KCl**, @ 832°C **eutectic formation** between PbO-$Pb_3Nb_2O_8$ pyrochlore phase.

Exo peaks `@ 373°C **formation of potassium perchlorate**,@ 462°C **formation of KCl**, (= resolidification of potassium chlorate & decomposition of potassium perchlorate.)

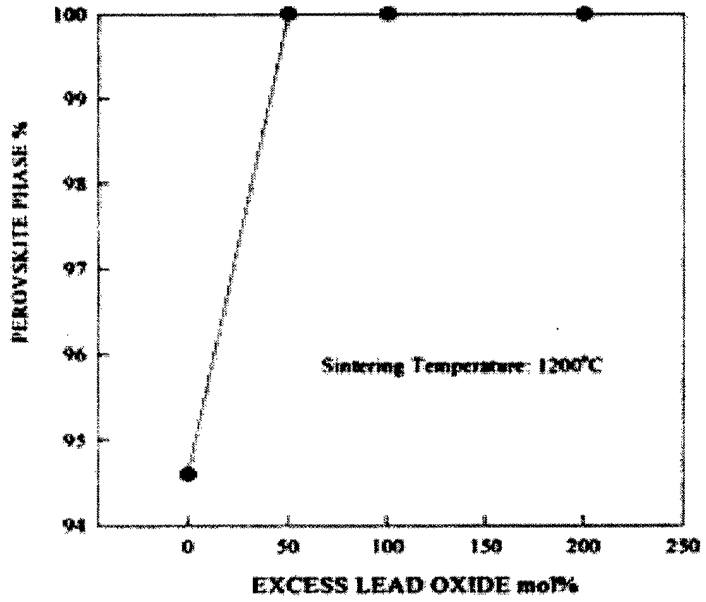

The effect of excess lead oxide on perovskite phase formed in PMN ceramics sintered at 1200°C for 2 h.

- **Single phase PMN powders have been prepared in the molten salt of potassium chlorate at temperatures of 900°C and above for 2 h when 100 mol % PbO excess was added in the starting composition.**
- **Too much excess lead oxide (e.g. 200 mol %) and a too high reaction temperature lead to the occurrence of exaggerated grain growth and the formation of faceted cubical particles, although the molten salt-derived powders exhibit litter particle agglomeration.**
- **The excess lead oxide enhances the formation of perovskite phase and promotes grain growth in sintered PMN ceramics, when it occurs at grain boundaries and grain junctions. This however degrades the dielectric properties of molten salt-derived PMN ceramics.**

Microcomposite particles $Sr_3Ti_2O_7$–$SrTiO_3$

- **Microcomposite particles $Sr_3Ti_2O_7$–$SrTiO_3$ with an epitaxial core–shell structure were prepared by the hydrothermal treatment of $Sr_3Ti_2O_7$ core particles.**
- **The $Sr_3Ti_2O_7$ core particles synthesized in a fused salt had a plate-like morphology with a well developed [001] plane of the Ruddlesden–Popper type crystal structure.**
- **The particles after hydrothermal treatment have an anisotropic morphology and a core–shell microcomposite structure: the plate-like $Sr_3Ti_2O_7$ particles covered with $SrTiO_3$ fine particulates and thin layers.**

Tsuguto Takeuchi , Toshihiko Tani, Toshikazu Satoh - Solid State Ionics 108 (1998) 67–71

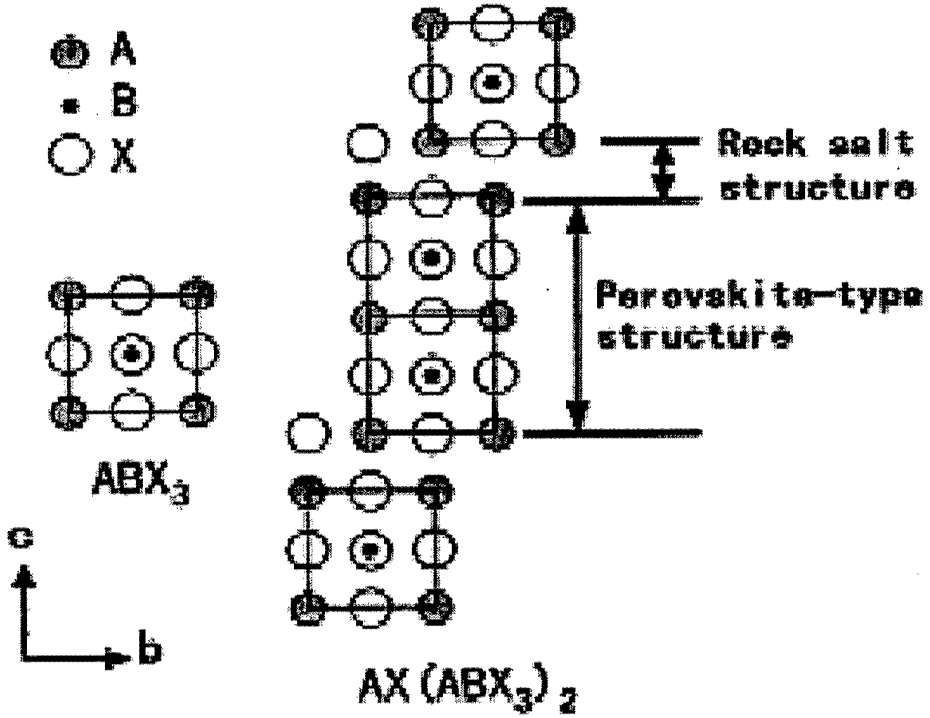

The $Sr_3Ti_2O_7$ has a Ruddlesden–Popper type structure (one of layered perovskite-type structure) and plate-like particles can be synthesized with the developed [001] plane by a molten salt synthesis.

- The atomic configuration in the [001] plane of a Ruddlesden–Popper type structure is similar to that in the [001] plane of a perovskite-type structure, as schematically shown.
- Especially, the lattice mismatch between $Sr_3Ti_2O_7$ and $SrTiO_3$ is only 0.1%, which suggests the possible formation of $SrTiO_3$ on the developed surface of $Sr_3Ti_2O_7$ with epitaxy.

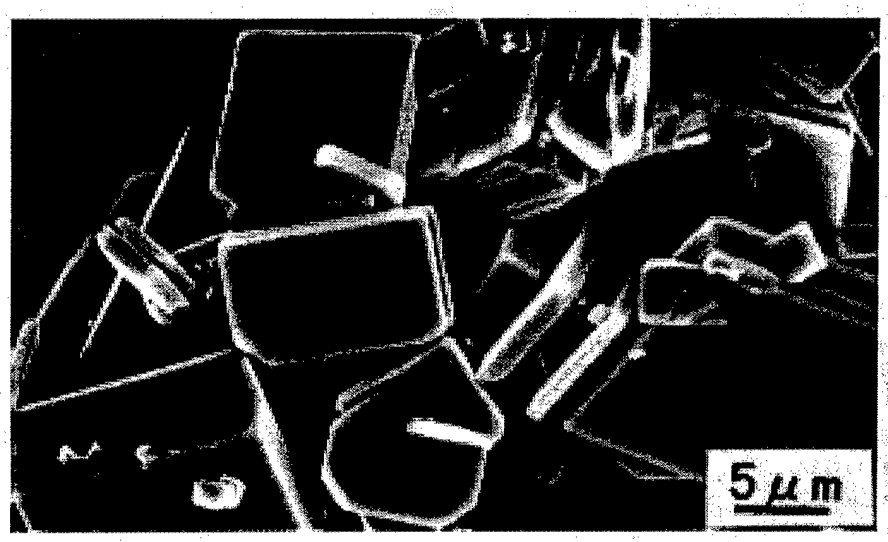

The plate-like particles have a smooth and well-developed rectan gular plane with a side length of 20–30 mm and an aspect ratio (side length / thickness) of about 10.

Plate-like $Sr_3Ti_2O_7$ core particles prepared by molten salt synthesis.

•$SrCO_3$ and TiO_2 (3:2 molar ratio) mixed for 24 h in ethanol with media of zirconia balls. The slurry was dried and then an equal weight of salts (50 mo % KCl and 50mol % NaCl) was mixed with the dried powder by a mortar and pestle for 30 min.

•The mixture was heated in a Pt crucible at 1200°C for8 h and cooled in air.

•The products were washed with hot deionized water several times in order to remove the salts.

Synthesis of SWNTs and MWNTs by a molten salt method

- Method to obtain the single-walled and multi-walled carbon nanotubes

- Electrolytic conversion of graphite to carbon nanotubes in fused NaCl at 810 °C.

- Filling of the nanotubes is also possible if elements are added in the salt solution.

J.B. Bai A.-L. Hamon , A. Marraud , B. Jouffrey , V. Zymla - Chemical Physics Letters 365 (2002) 184–188

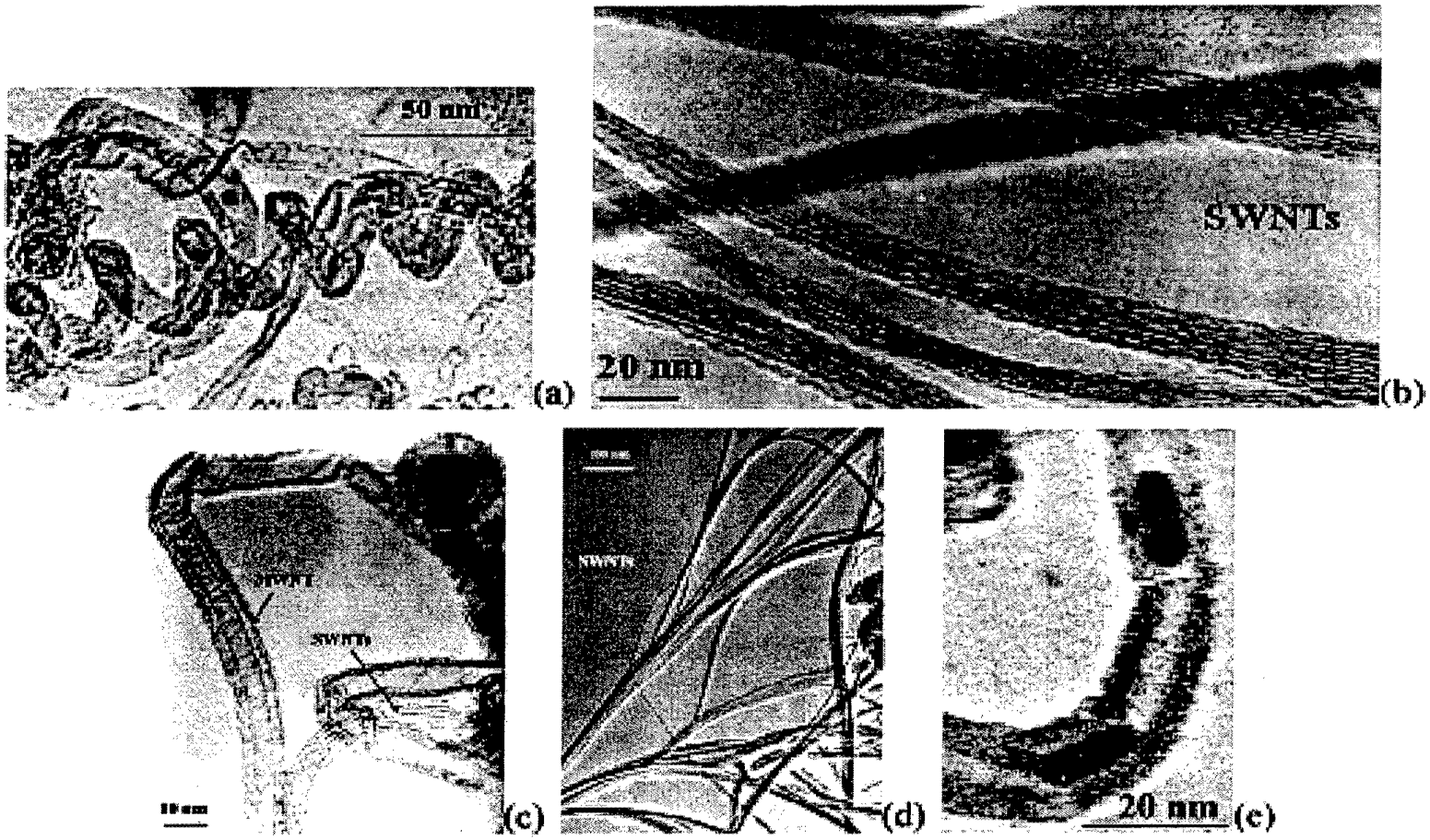

TEM imaging of the various morphologies of nanotubes.

PROCESSING, MICROSTRUCTURE AND MECHANICAL BEHAVIOR OF DIRECTIONALLY-SOLIDIFIED EUTECTIC CERAMIC OXIDES

V. M. Orera, J. I. Peña, R. I. Merino, A. Larrea,
J. LLorca, J. Y. Pastor, P. Poza,
J. Martínez, A. Ramírez, M. López, J. Quispe

Institute of Materials Science of Aragon
Universidad of Zaragoza / CSIC

CSIC

Department of Materials Science
Polytechnic University of Madrid

Department of Physics of Condensed Matter
University of Seville

OUTLINE

- **Motivation and Introduction**
- **Processing**
- **Microstructure**
  - Morphology
  - Phase distribution & composition
- **Residual stresses**
  - Experimental results
  - Stress generation and relaxation
- **Microstructure stability**
- **Mechanical behavior**
  - Ambient temperature properties
  - Toughening mechanisms
  - High temperature strength
- **Conclusions**

Why structural materials for high temperature?

- Higher temperatures in thermal engines lead to
  - Better efficiency and performance
  - Cleaner emissions

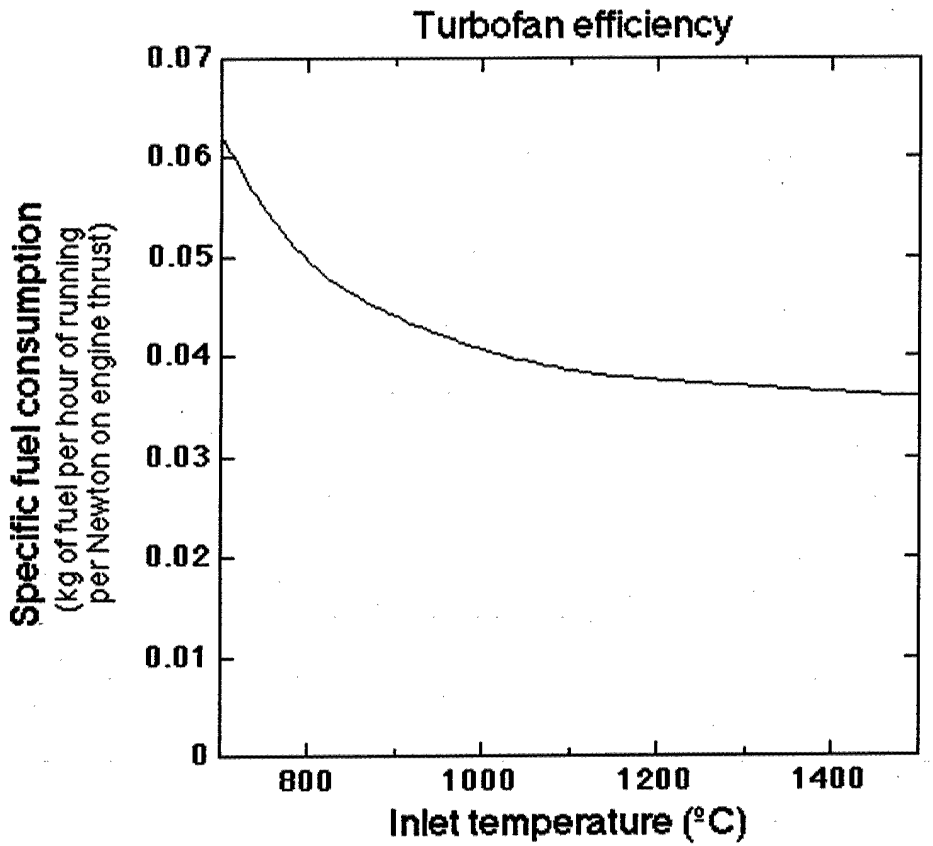

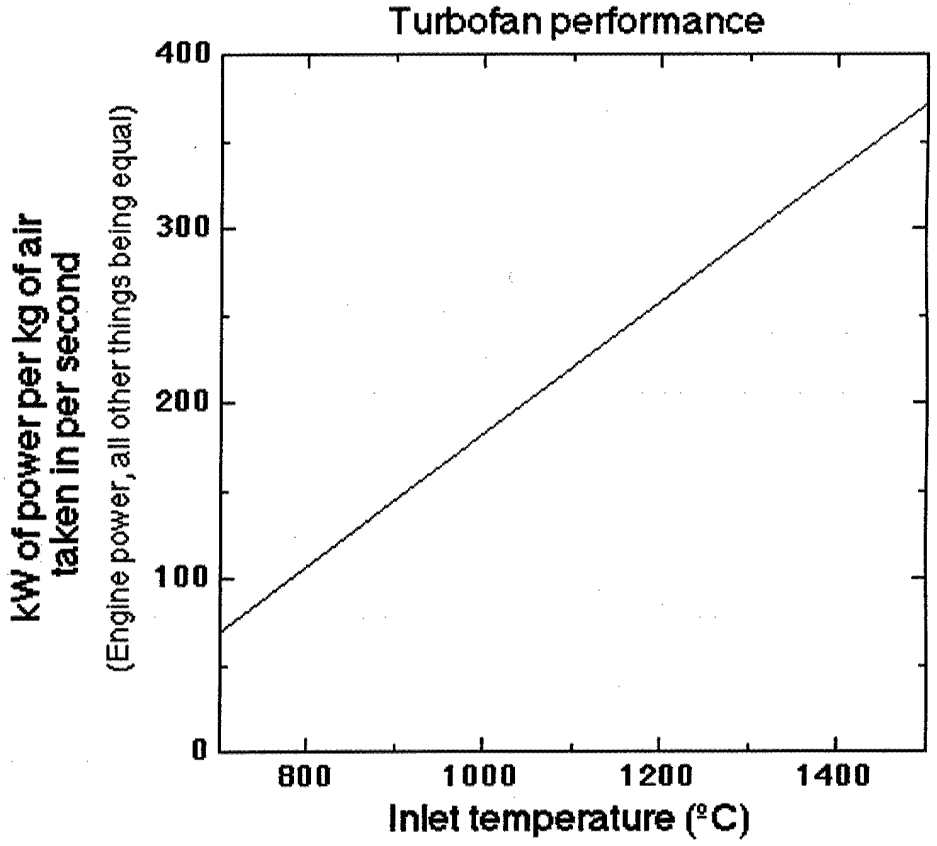

Basic requirements for high temperature structural materials

- High melting point
- Mechanical properties
- Microstructure stability
- Oxidation resistance

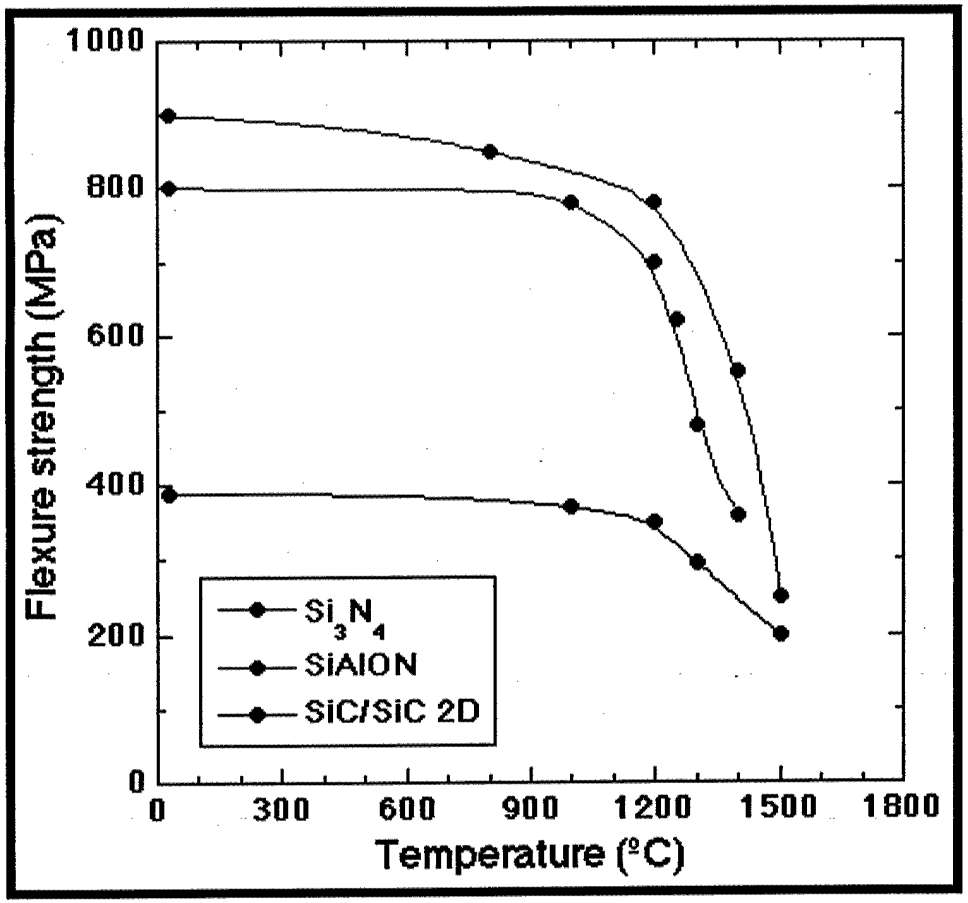

SiC- and Si_3N_4-based ceramics undergo severe oxidation above 1400°C

Directionally-solidified eutectic oxides

- Eutectic composites
  - Fine microstructure
  - Excellent bonding between phases
  - Clean interface
  - Stable up to near the eutectic temperature
- Directional solidification
  - Composite highly textured along growth direction
- Oxides
  - Chemically stable in oxidizing environments

The best mechanical properties have been obtained so far in the Al_2O_3/c-ZrO_2(Y_2O_3) system.
Flexure strength > 1.1 GPa, toughness = 7.8 MPa $m^{1/2}$

History

1970-1980 [1]	<600MPa at RT but good retention up to 1850K (524 MPa)
1990-1995[2-5]	1.0-1.5 GPa at RT
1995-	Sayir et al.[6] found tensile strength from 1.2 GPa at RT to 800 MPa at 1673K

[1] C.O. Hulse and J.A. Batt UARL N910803, (1974)
[2] V.A. Borodin et al. J. Cryst. Growth 104 (1990) 148
[3] J. Homeny & J.J. Nick, Mater. Sci. Eng. A117 (1990) 123
[4] H. E. Bates, Ceram. Eng. Sci Proc. 13 (1992) 190
[5] E. L. Courtright et al. Ceram. Eng. Sci Proc. 14 (1993) 671
[6] A. Sayir & S.C. Farmer, Acta Mater 48, 4691-7 (2000)

Objective: Production of melt growth composites Al_2O_3 - $ZrO_2(Y_2O_3)$ with optimized mechanical properties

- Study of the mechanical properties:

  Flexural and compressive strength & toughness.
  Retention at high T

Focus on

- Processing (Microstructure)

  Growth rate: **10- 1500mm/h**
  Rotation **200 to 0 rpm**

- Influence of the Y_2O_3 amount in the zirconia phase

  From the Al_2O_3-ZrO_2 eutectic to the Al_2O_3-ZrO_2-Y_2O_3 peritectic, Y_2O_3 content, Y= 0 to 12.2% (mol Y_2O_3 / mol ZrO_2+ Y_2O_3)

- Role of the thermo-elastic residual stresses

Preparation Procedures:

Melt Grown Composites (MGC) using Directional Solidification (DS)

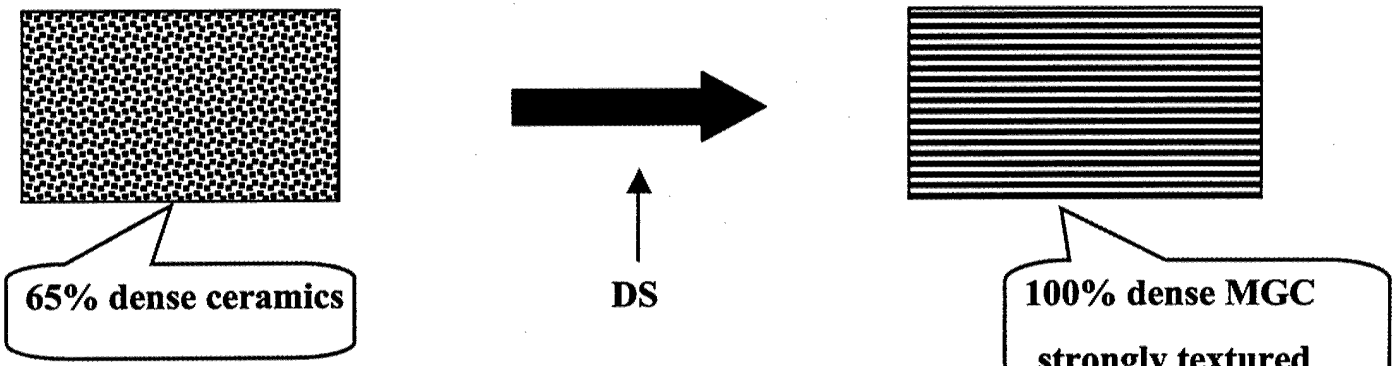

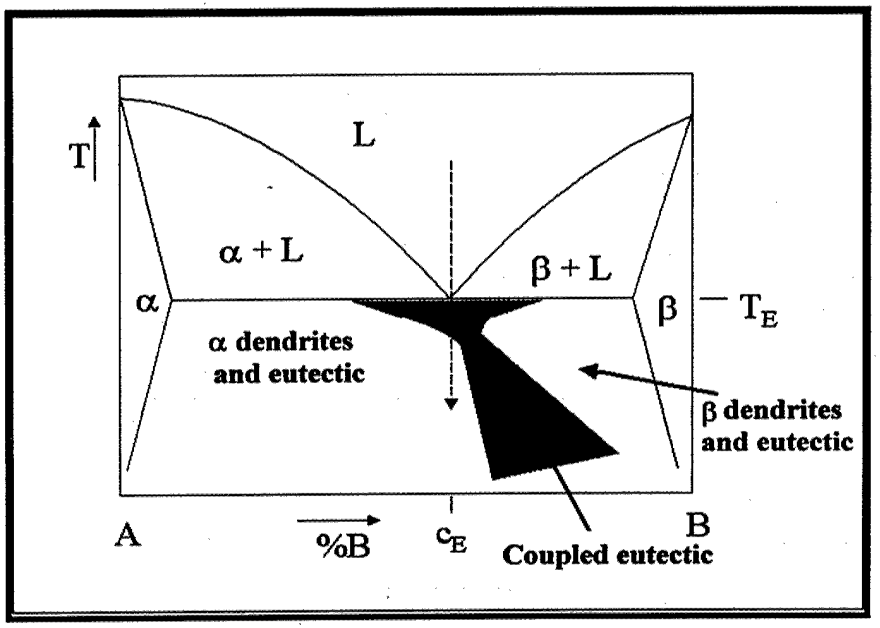

Laser Heated Float Zone: T_E =1860°C

Atmosphere: synthetic air

Upper rotation

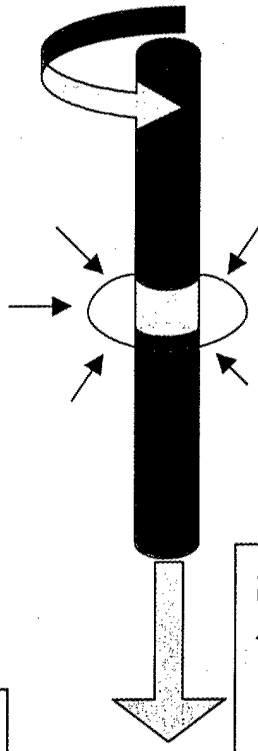

Concentric laser beam
- CW CO_2
- power ~ 70 watts

Lower rotation

Shift of the growing bar downward through the focused laser light

R = pulling rate
= growth rate

Rods <2 mm diameter and up to 100 mm length

Conciliate the mechanical measurements size needs with the growth constraints

- Flexural strength rods ≈ 1mm diameter
- Compression experiments & toughness > 2mm
- High axial thermal gradients ⟶ Large radial gradients ⟶ cracks more frequent in bars with larger radius

High speed rotation induces melt homogeneity and decreases lateral gradient effects but it is problematic for narrow samples

Conclusion:

None or low speed rotation (banding) for samples around 1mm and 200 rpm precursor rotation for larger samples

Al_2O_3 /c-$ZrO_2(Y_2O_3)$ eutectic

Microstructure versus solidification rate. G ≈ 600 °C/m

R = 10 mm/h

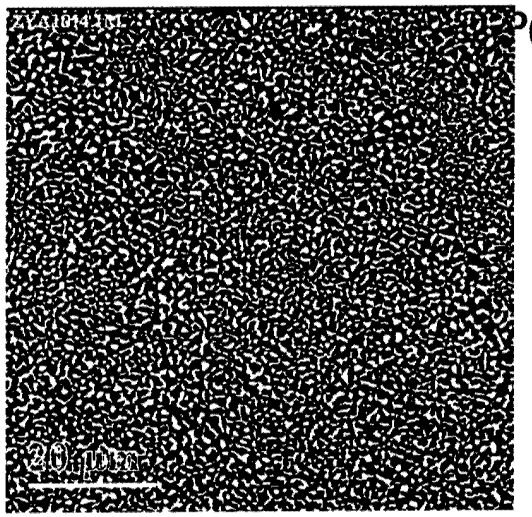

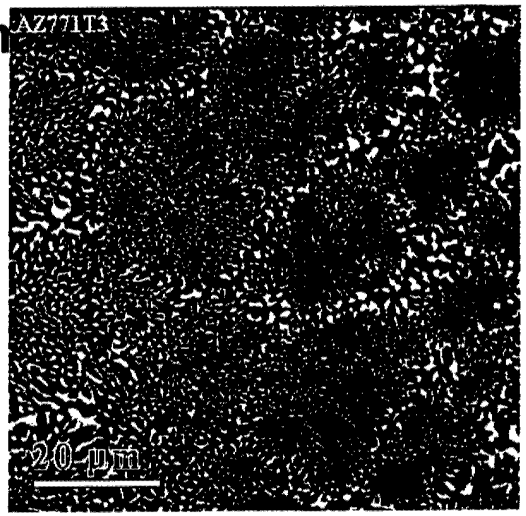

R = 100 mm/h

R = 300 mm/h

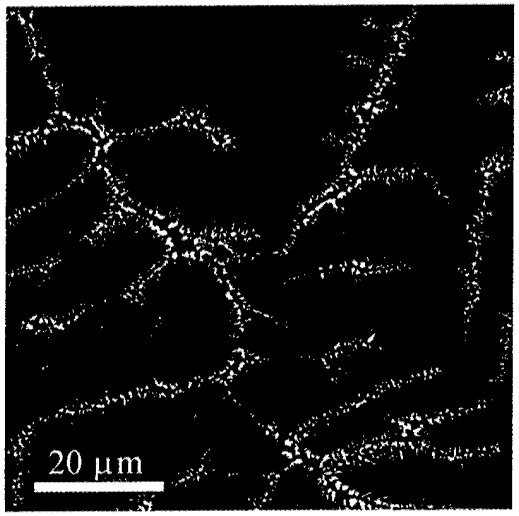

R = 1500 mm/h

Transverse

Samples with colony structure

It was induced at R > 30 mm/h as the Al_2O_3 phase leads the growth due to its high entropy of fusion ($\Delta S = 5.7R$).

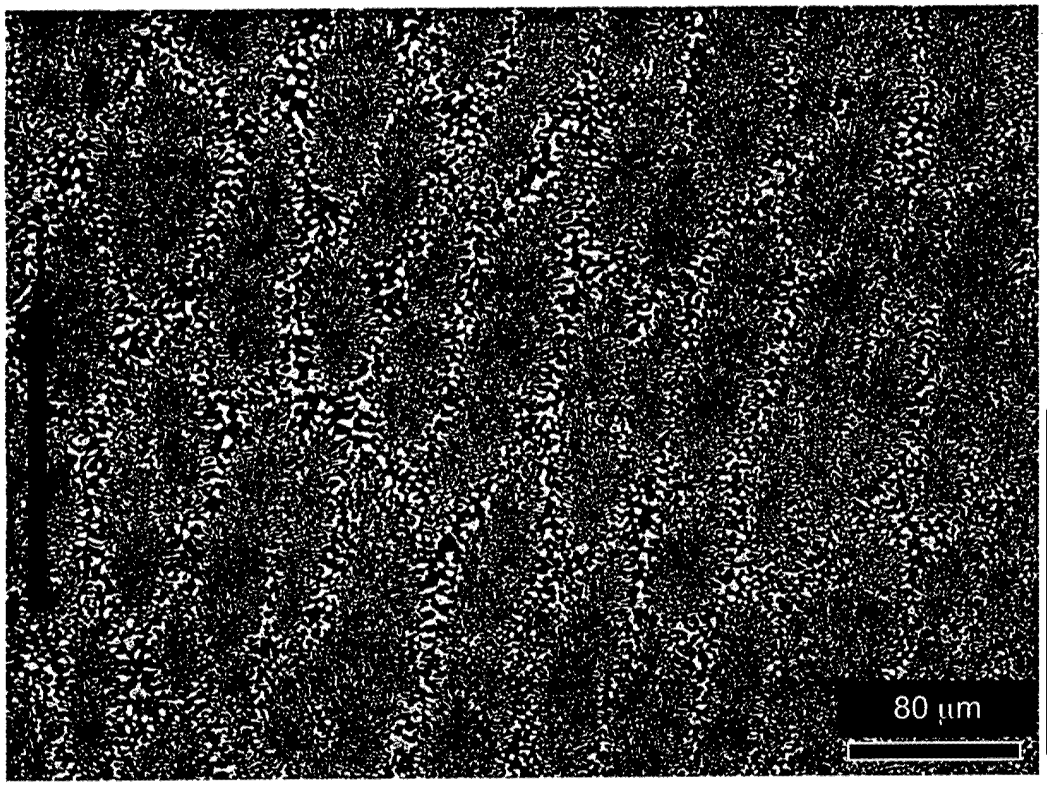

Longitudinal

Composition
α-Al_2O_3 ≈ 70% vol.
ZrO_2 (Y_2O_3) ≈ 30% vol.

Colonies
Diameter 31±10 μm
Aspect ratio ≈ 3
Colony boundary 13±4 μm

Al_2O_3/ c - $ZrO_2(Y_2O_3)$ Crystallographic orientation relationships

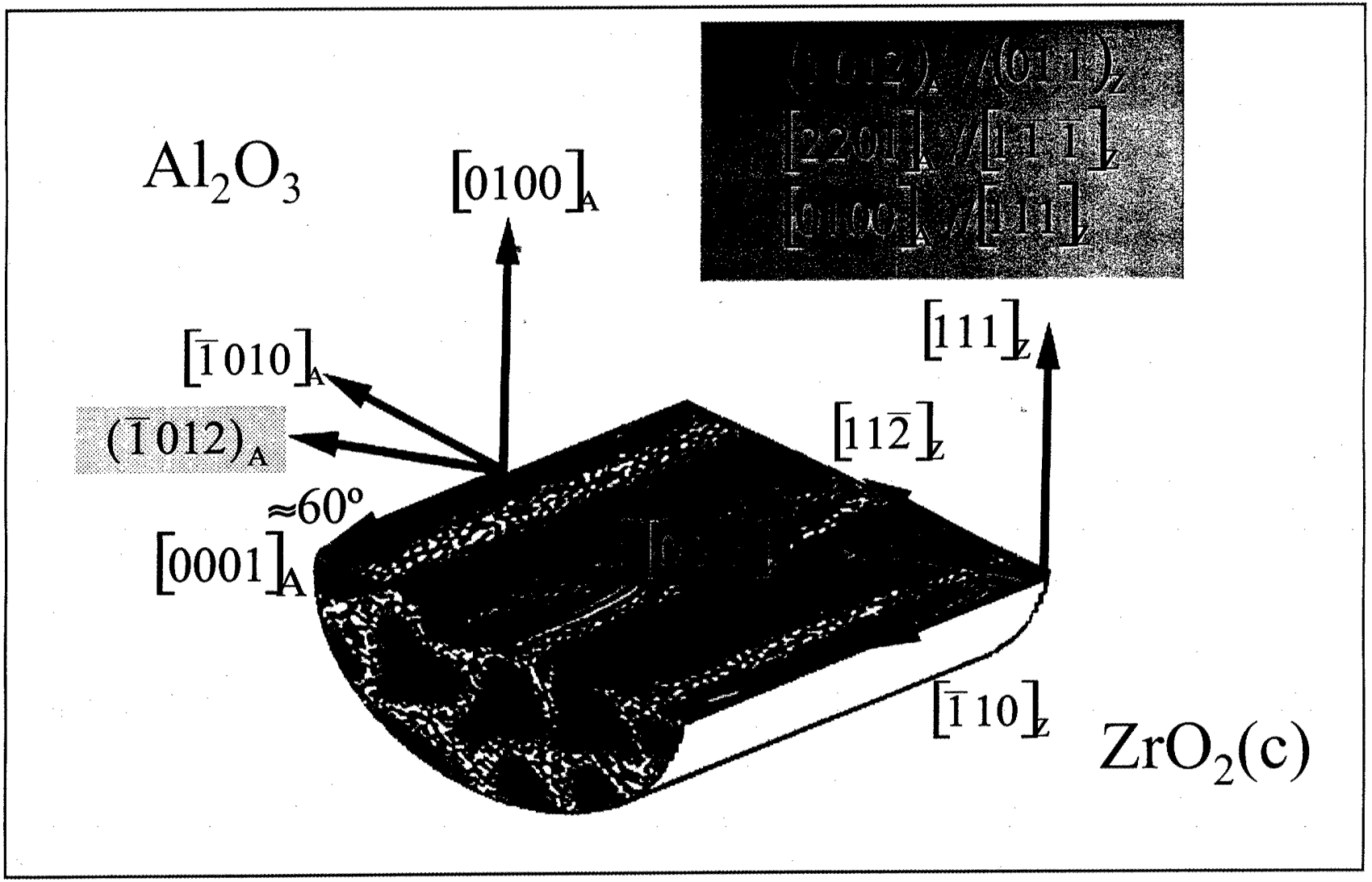

Interpenetrating structure:
Highly homogeneous 3d network

It was induced at V = 10 mm/h by the coupled growth of both phases (Al_2O_3 and ZrO_2)

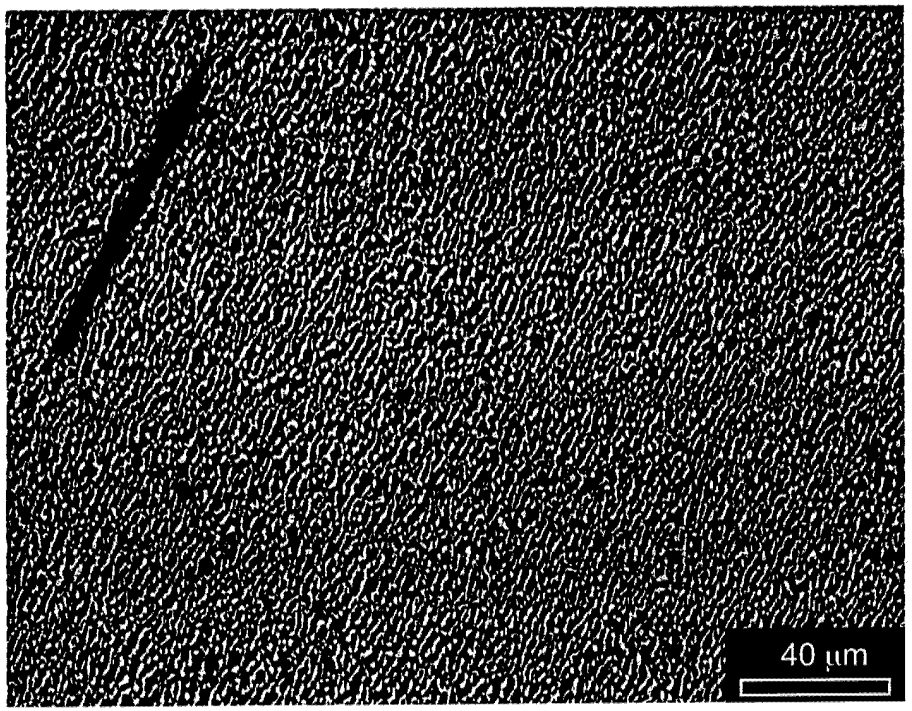

Composition
α-Al_2O_3 ≈ 70% vol.
ZrO_2 (Y_2O_3) ≈ 30% vol.

Fine dispersion of $ZrO_2(Y_2O_3)$ platelets embedded into the Al_2O_3 matrix

Interpenetrating structure

Aspect ratio and interlamellar spacing

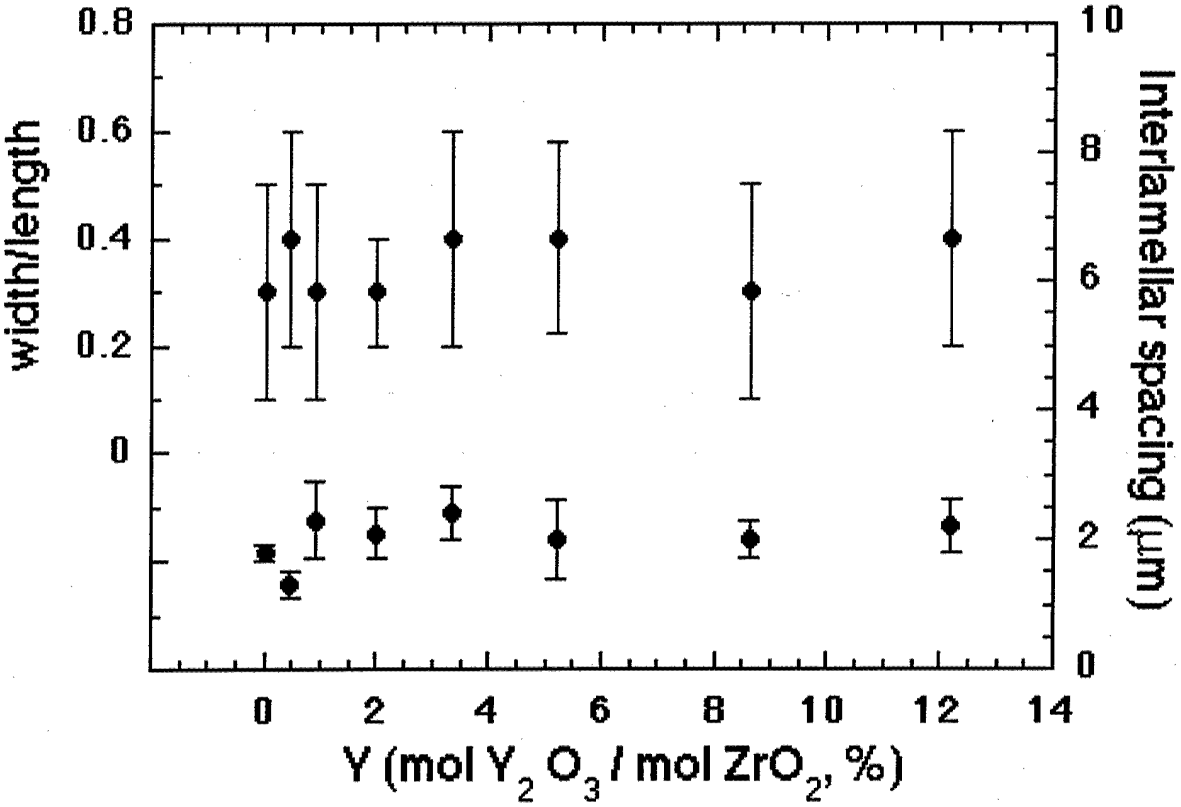

Influence of the Y_2O_3 amount in the zirconia phase

From the Al_2O_3-ZrO_2 eutectic to the Al_2O_3-ZrO_2-Y_2O_3 peritectic, Y_2O_3 content, Y= 0 to 12.2% (mol Y_2O_3 / mol ZrO_2+ Y_2O_3)

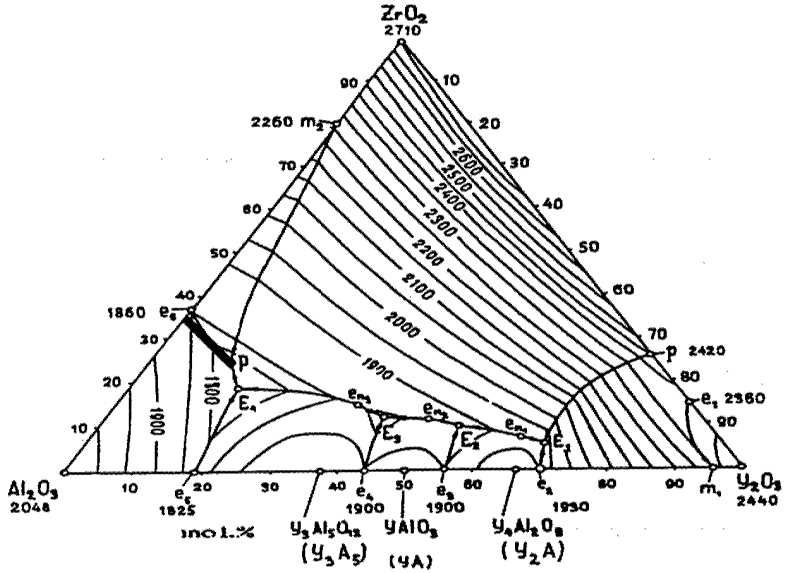

Fig. 5. Projection of the liquidus surface for the system Al_2O_3–ZrO_2–Y_2O_3.

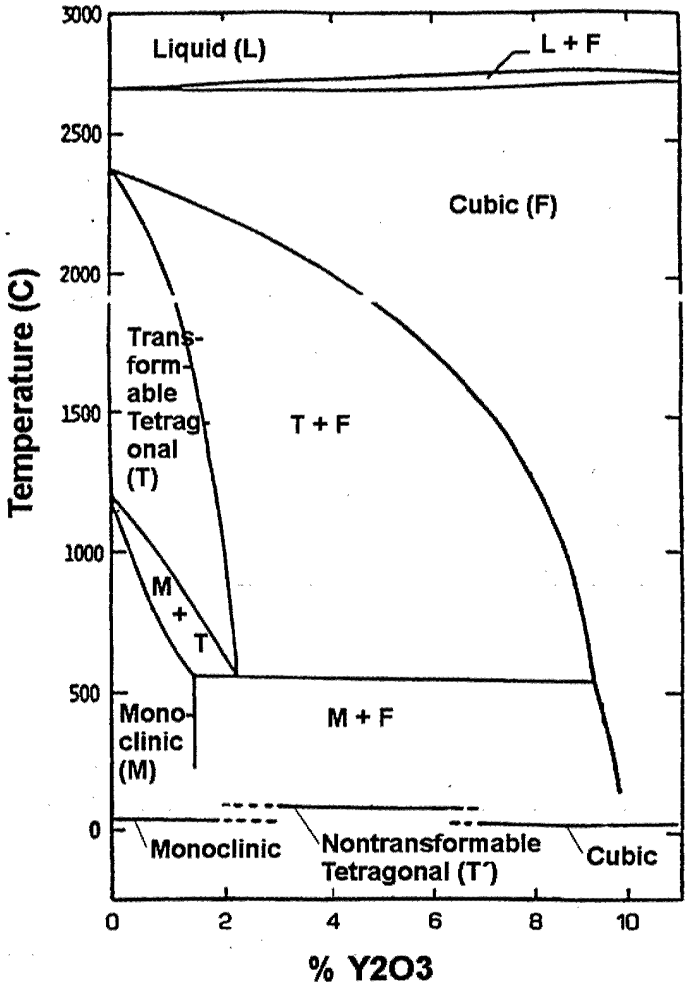

ZrO_2 phase volume fraction
X-ray diffraction

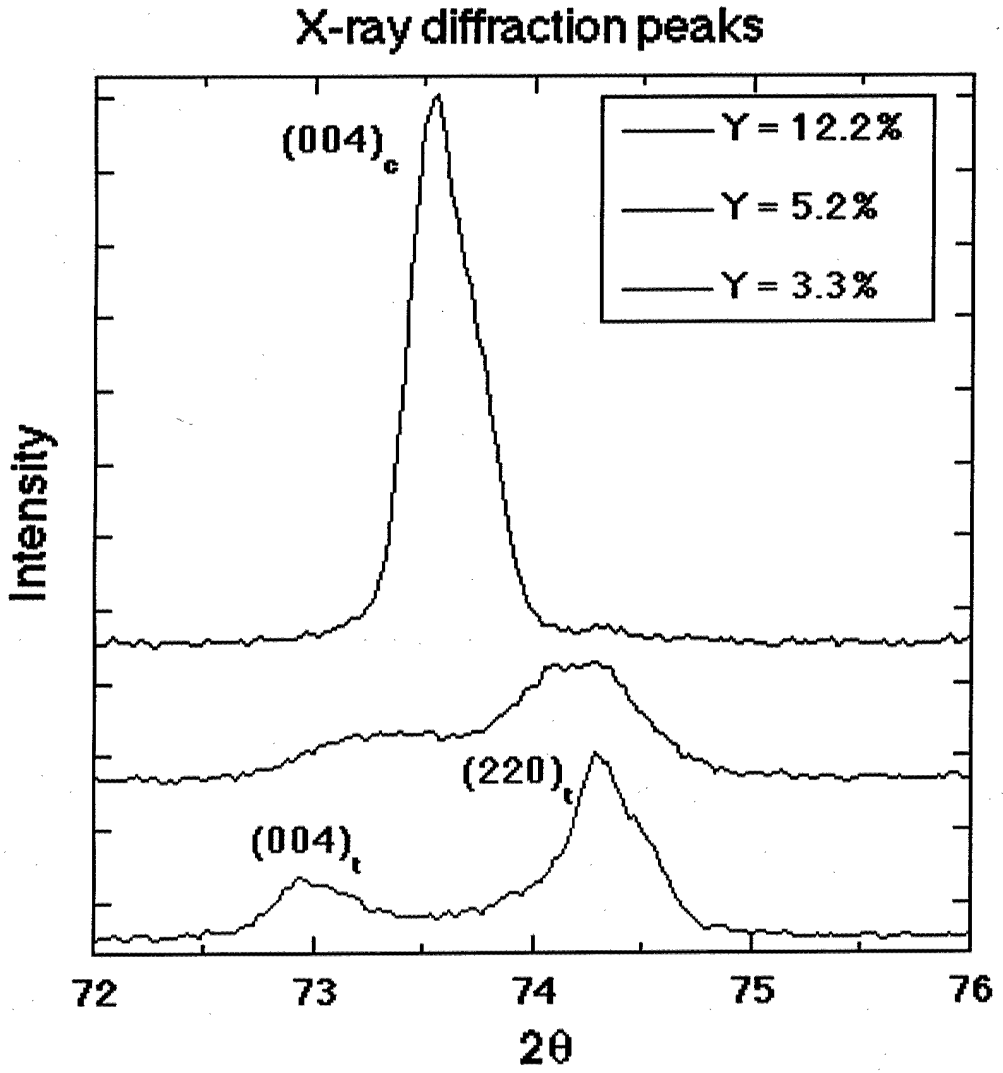

X-ray diffraction showed that the c/a ratio of (t) ZrO_2 decreased with Y

Non-transformable (t') and (t'') ZrO_2 phases are present

ZrO_2 phase volume fraction

Raman spectroscopy

$Y > 3.3\%$

$X_c + X_t = 1$

$X_t = I_{260} / I_{260}(Y=3.3)$

$Y < 3.3\%$

$X_m + X_t = 1$

$X_t / X_m = I_{260} / 1.8 I_{177}$

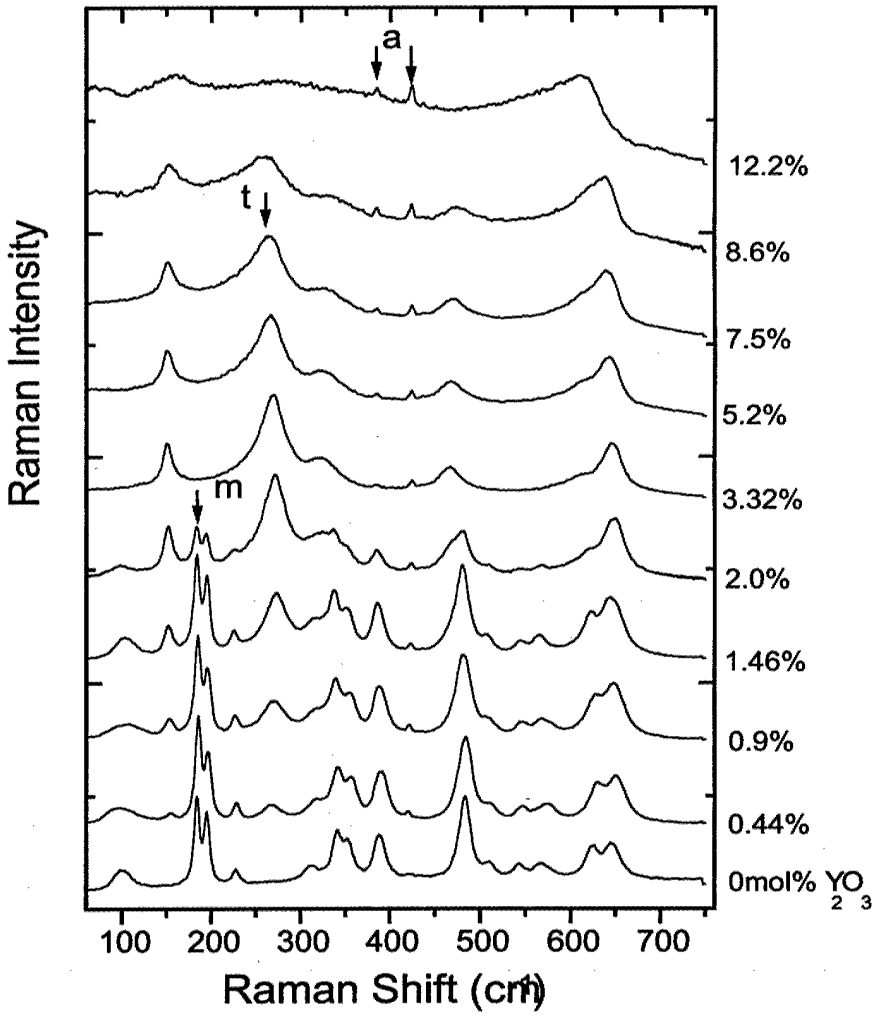

ZrO_2 phase volume fraction

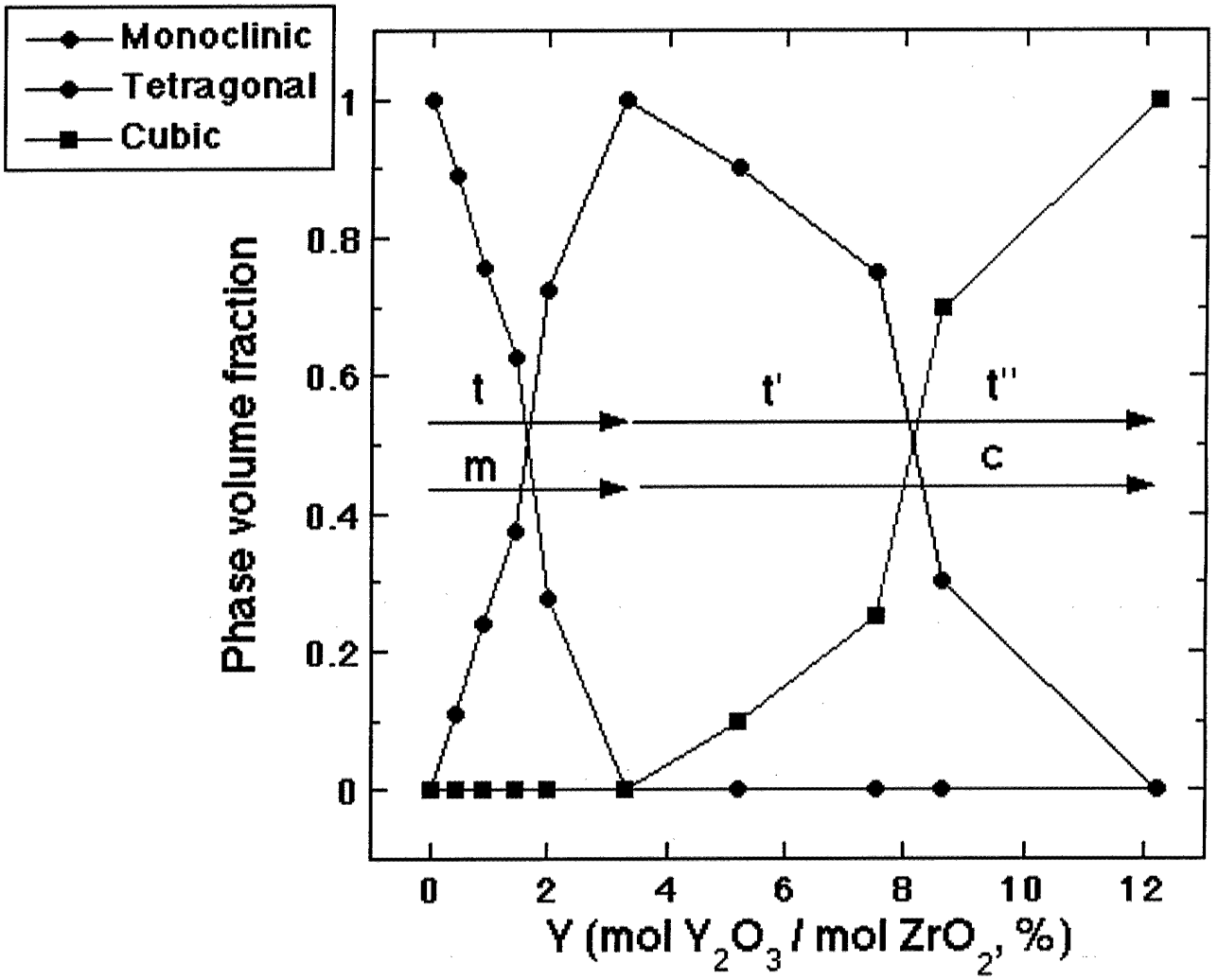

Piezo-spectroscopy of R1 and R2 lines in Al_2O_3

Residual stresses in Al_2O_3 can be computed from the shift in R1 and R2 peaks using the piezospectroscopic tensors in ruby.

$$\Delta R_1(cm^{-1}) = 3.26(\sigma_{11}+\sigma_{22}) + 1.53\,\sigma_{33}$$

$$\Delta R_2(cm^{-1}) = 2.73(\sigma_{11}+\sigma_{22}) + 2.16\sigma_{33}$$

(σ in GPa)

· Assumptions

- The alumina c-axis is parallel to the rod axis.

- The piezospectroscopic effect is isotropic in the alumina basal plane.

- the stress state in the eutectic is transversally isotropic

Inhomogeneous distribution of residual stresses

Al_2O_3-ZrO_2 (x %mol Y_2O_3)

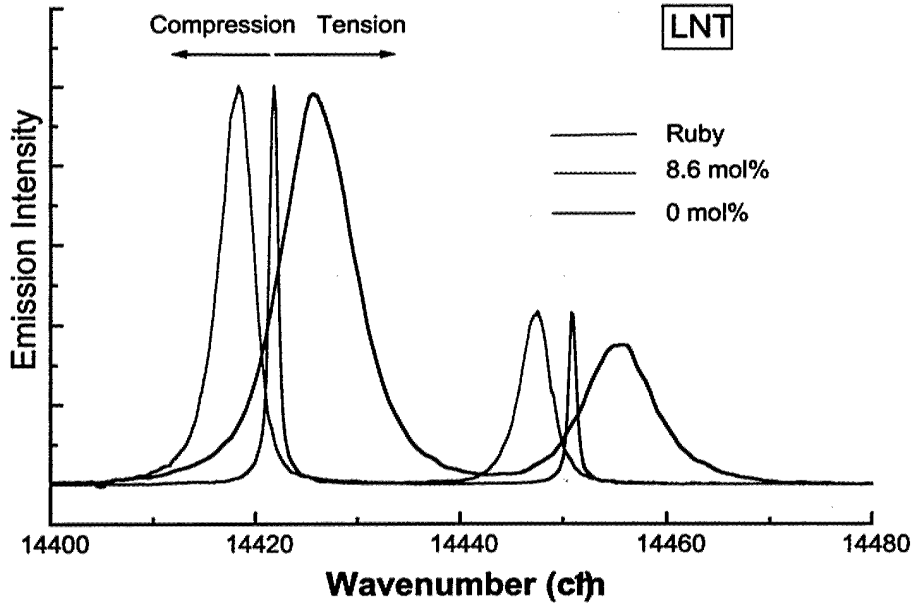

Residual stresses at ambient temperature

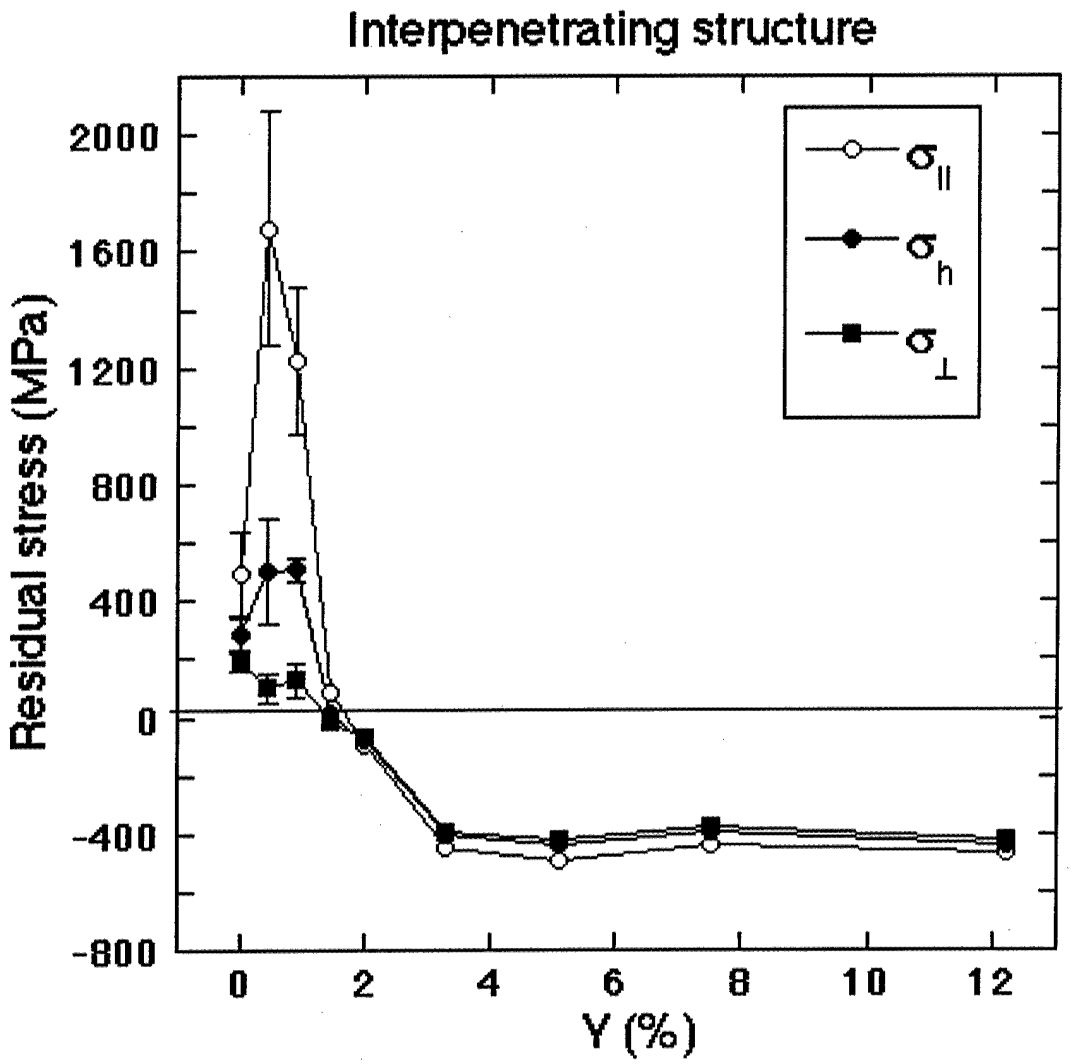

Residual stresses as a function of temperature

Hydrostatic residual stresses in the alumina phase vs temperature

- ■ AZE with Monoclinic zirconia, Martensitic
- ▲ AZE with "c or t" zirconia, Thermo-elastic

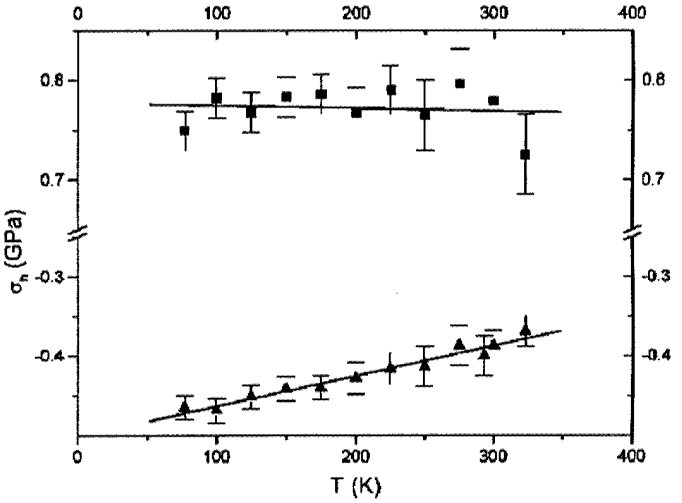

Thermo-elastic stresses depend on the CTE misfit, T_0 stress free temperature and K* an effective elastic modulus

$$\sigma(T) = K^* \varepsilon(T) = K^* \int_T^{T_0} (\acute{a}_A - \acute{a}_Z) dT$$

with $\alpha_A - \alpha_Z = -3.15 \times 10^{-6} + 1 \times 10^{-10} T - 5.5 \times 10^{-13} T^2$

T_0 = 1270 ± 35 K, K* = 118 ± 2.7 GPa in agreement with a model of spherical ZrO_2 particles in a Al_2O_3 matrix (97.5 GPa)

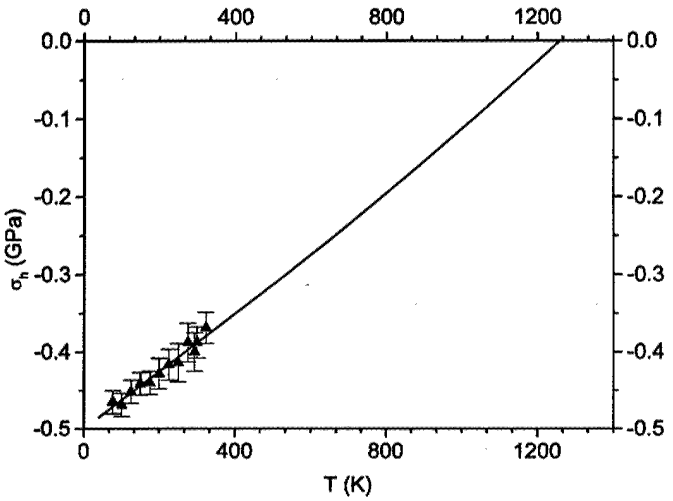

Self-consistent modeling
Hypotheses

- Alumina matrix: Transversally isotropic solid
  c-axis parallel to the rod axis
  $\alpha_a = 9.2\ 10^{-6}\ K^{-1}$ (c axis, average from 0 to 1000°C))
  $\alpha_a = 8.0\ 10^{-6}\ K^{-1}$ (m/a axis)

- Zirconia inclusions:
  Randomly distributed ellipsoids aligned in the rod axis
  Aspect ratio ≈ 3
  Isotropic, same elastic constants for **m**, **t**, and **c** phases
  $\alpha_m = 7.5\ 10^{-6}\ K^{-1}$
  $\alpha_c = \alpha_t = 12.65\ 10^{-6}\ K^{-1}$
  t --> **m** transformation at 950 °C ($\Delta V = 4.67\%$)

- Stress free temperature: 1150 °C

Comparison with experiments
No stress relaxation

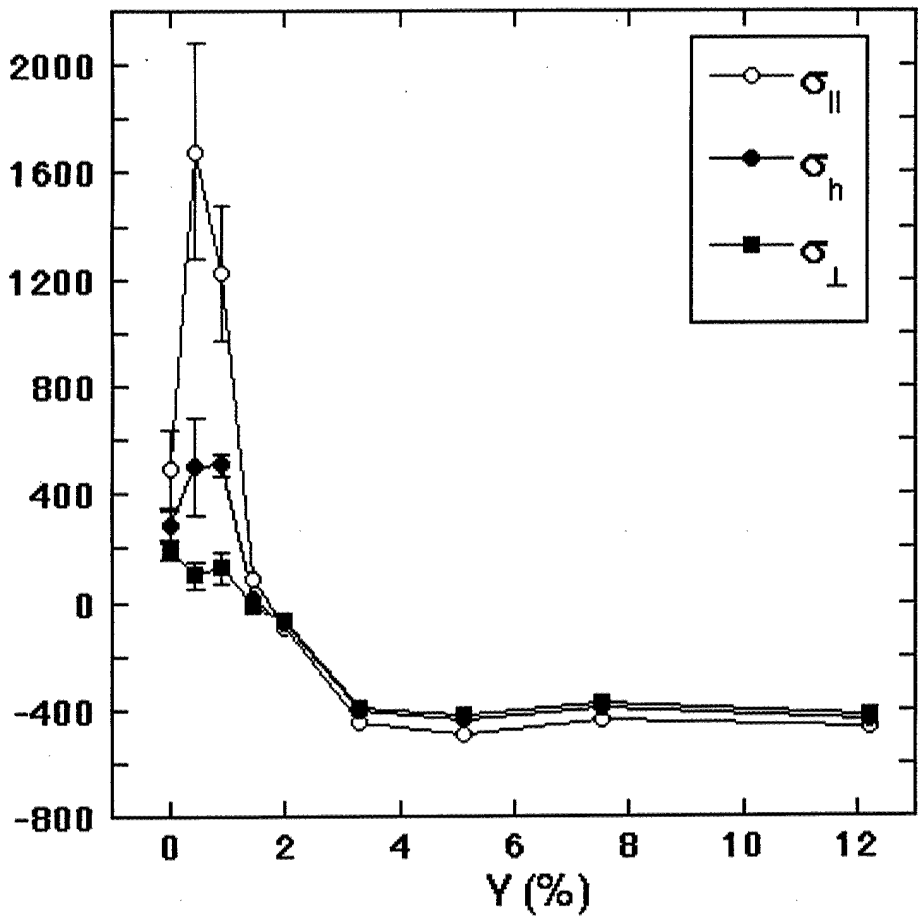

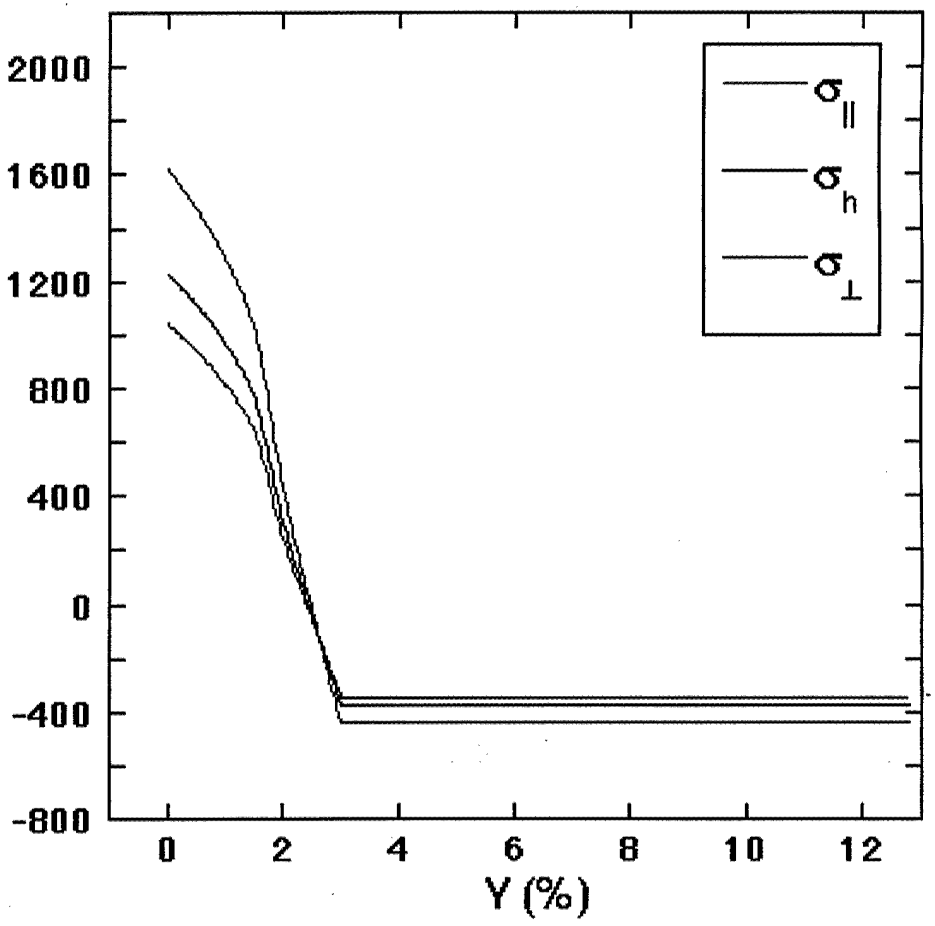

Comparison with experiments
stress relaxation in the Al_2O_3 basal plane

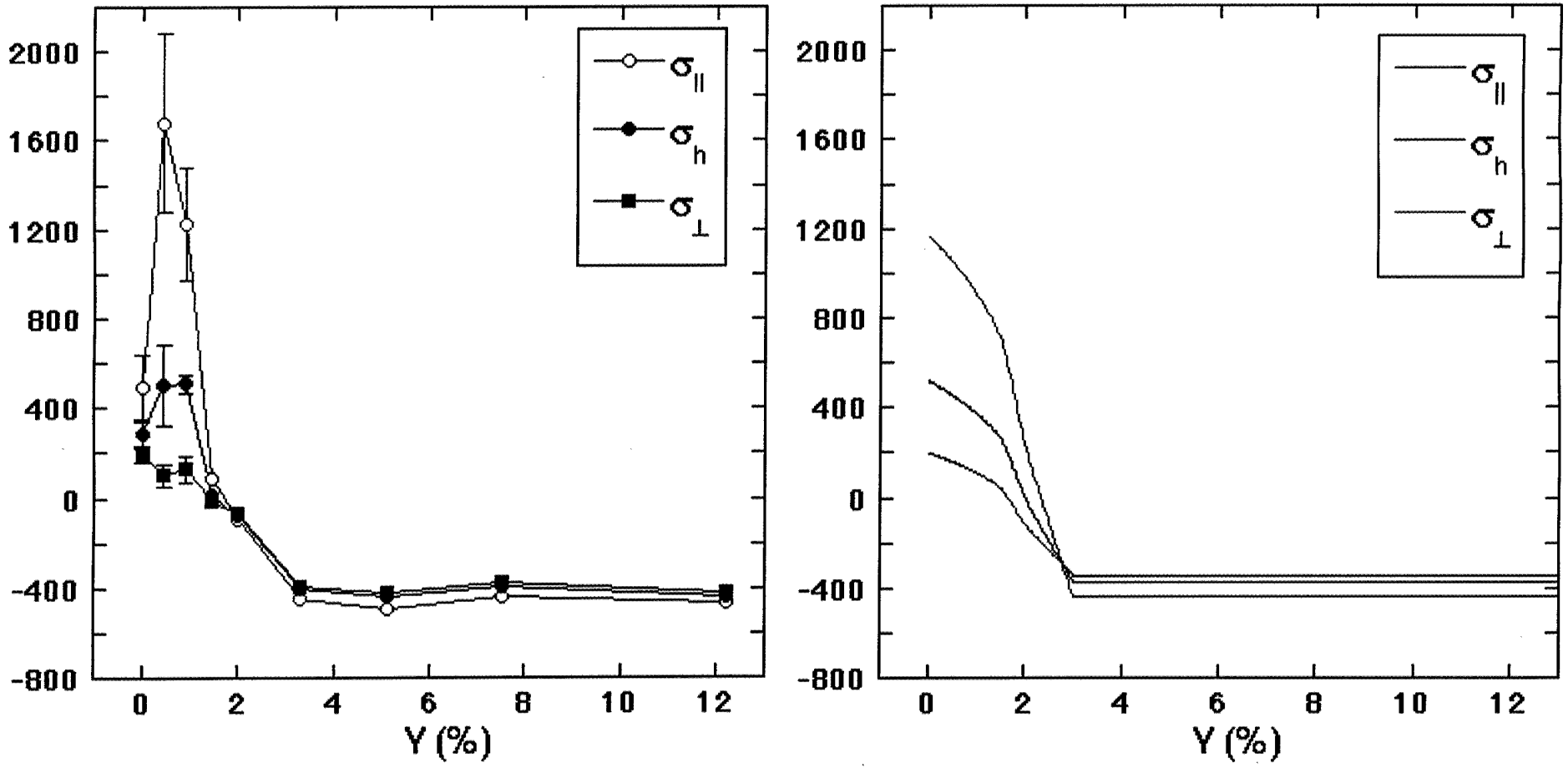

Toughening mechanisms

Y=10%

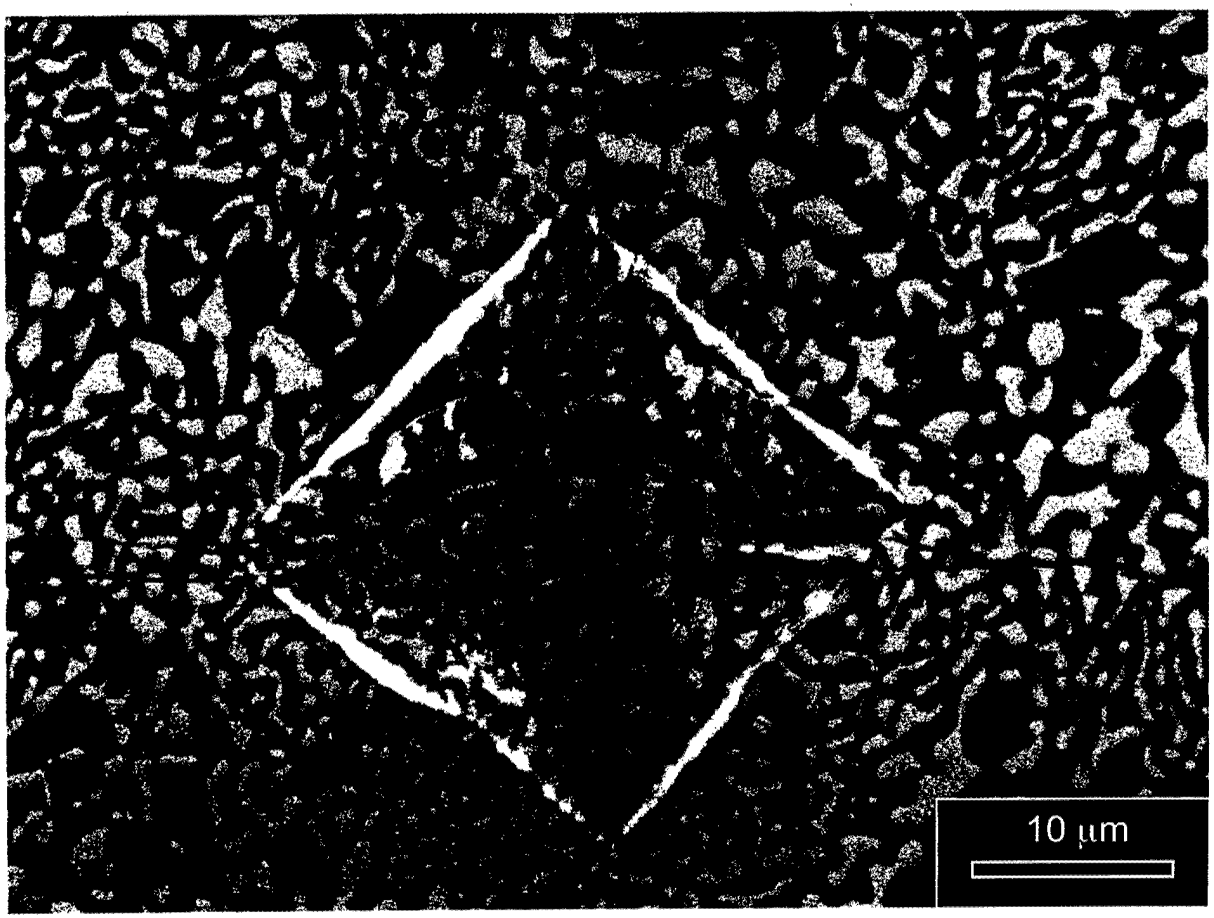

Toughening mechanisms

Crack arrest and overlapping

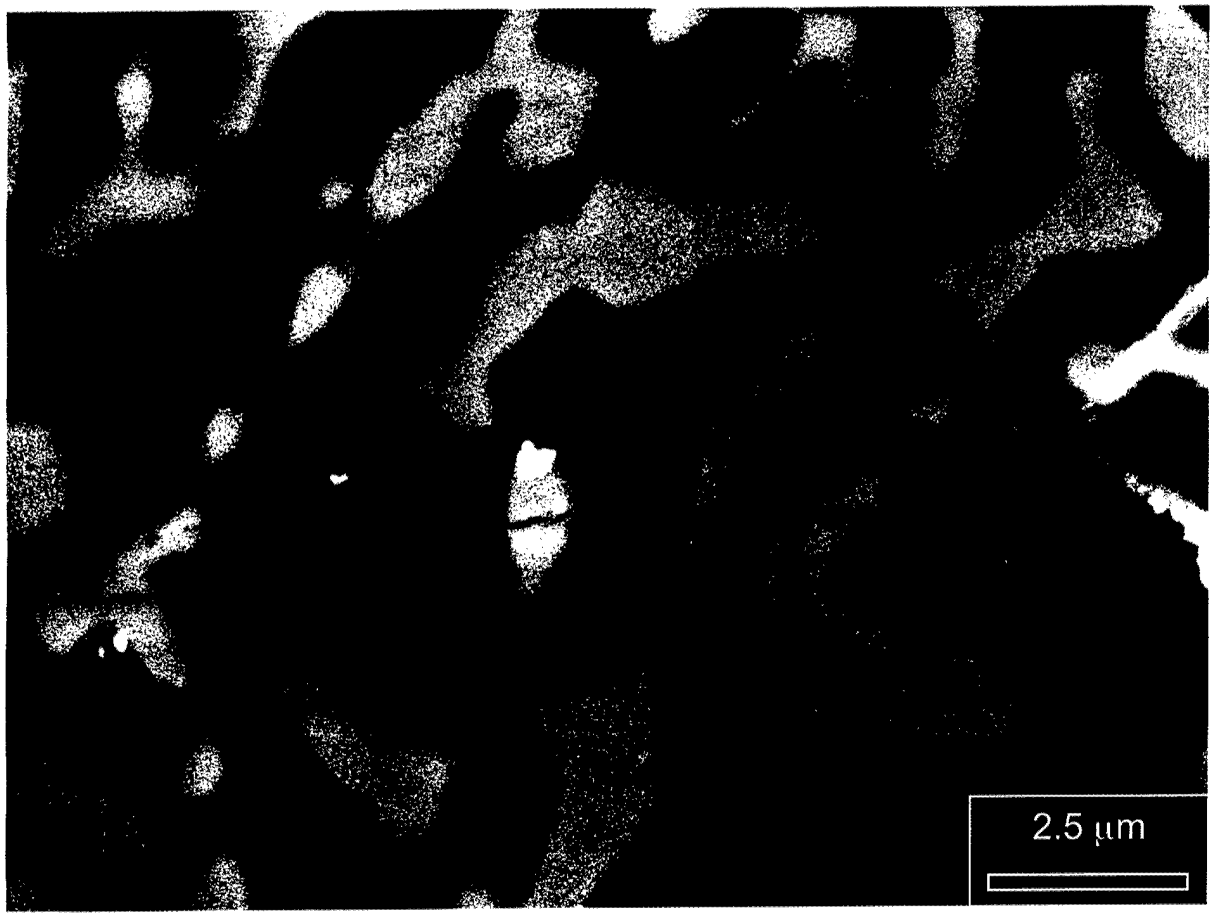

Causes

- Phases and interfaces with different crack growth resistance.
- Compressive residual stresses in Al_2O_3.

Toughening mechanisms

Effect of residual stresses

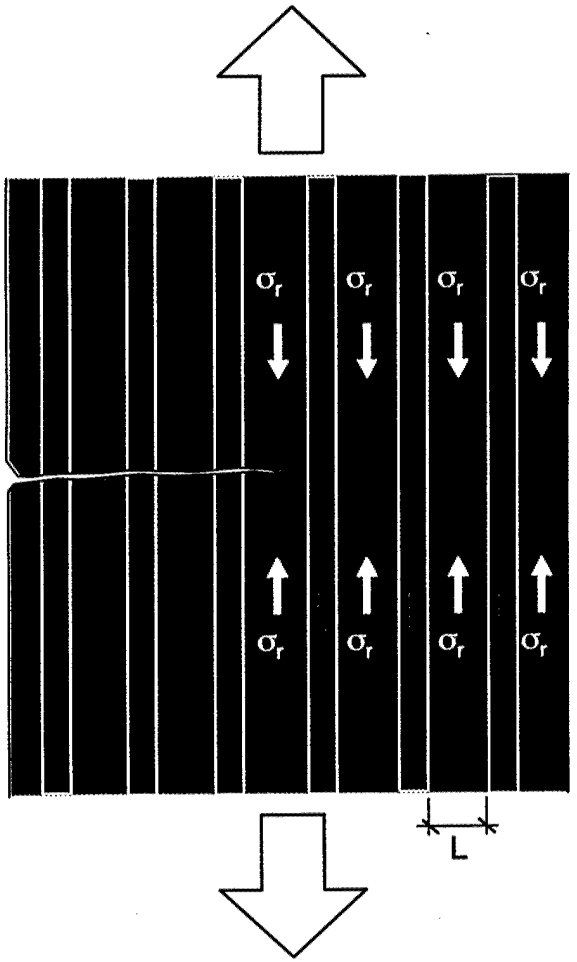

$$\Delta K_C = 2\sigma_r \sqrt{\frac{2L}{\pi}} = 1.6 \text{ MPa}\sqrt{\text{m}}$$

σ_r = 450 MPa, L = 5 μm

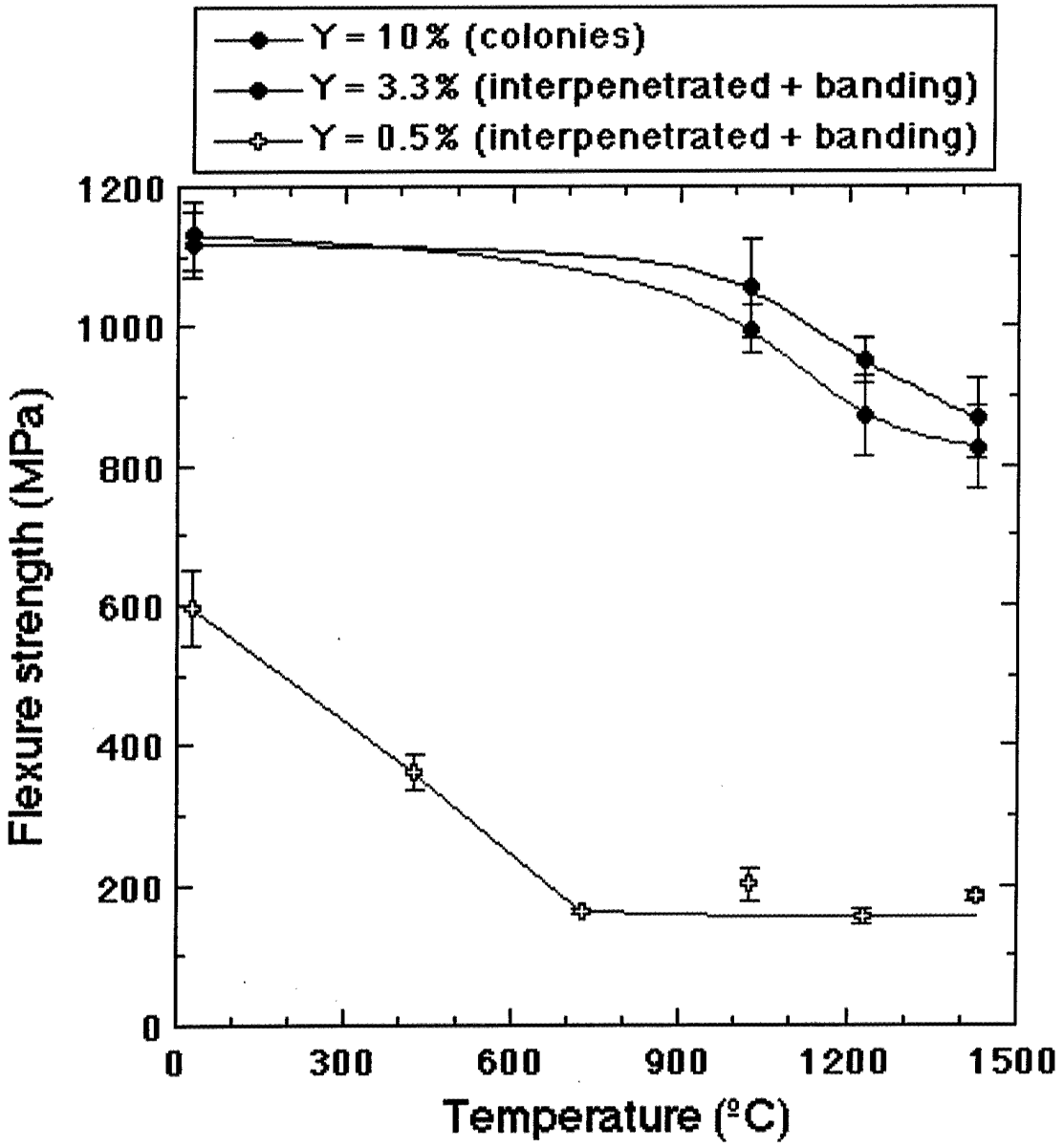
Y = 10% (colonies)
Y = 3.3% (interpenetrated + banding)
Y = 0.5% (interpenetrated + banding)
Flexure strength (MPa)
1200
1000
800
600
400
200
0
0
300
600
900
1200
1500
Temperature (ºC)

High temperature flexure strength
Mechanisms of strength reduction

Y=3.3%

- No changes in microstructure or critical defects
- Release of residual stresses --> lower toughness

Y=12.3%

- No changes in microstructure or critical defects
- Poor creep resistance of cubic ZrO_2
- Release of residual stresses --> lower toughness

Y=0.5%

- Crack propagation at the ZrO_2-Al_2O_3 interface induced by:
  - m --> t transformation between 700-900°C
  - thermal residual stresses

CONCLUSIONS

- Al_2O_3-$ZrO_2(Y_2O_3)$ eutectic oxides were processed using the laser-heated float zone method.

  - The microstructure of the composite (colonies vs interpenetrating) was controlled by changing the growth parameters.
  - The residual stresses and the crystalline structure of ZrO_2 can be controlled by changing the Y_2O_3 content.

- Mechanical properties of Al_2O_3-ZrO_2 eutectic oxides

  - Excellent strength (> 1.5 GPa) at 300 K.
  - Excellent toughness (7.8 MPa.$m^{1/2}$) at 300 K.
  - Fine microstructure stable up to 1800 K.
  - Very high strength retention at 1700 K (>800 MPa).
    Presumably > 1GPa?

Microcracking

Crack nucleation in Al_2O_3 - ZrO_2(m)

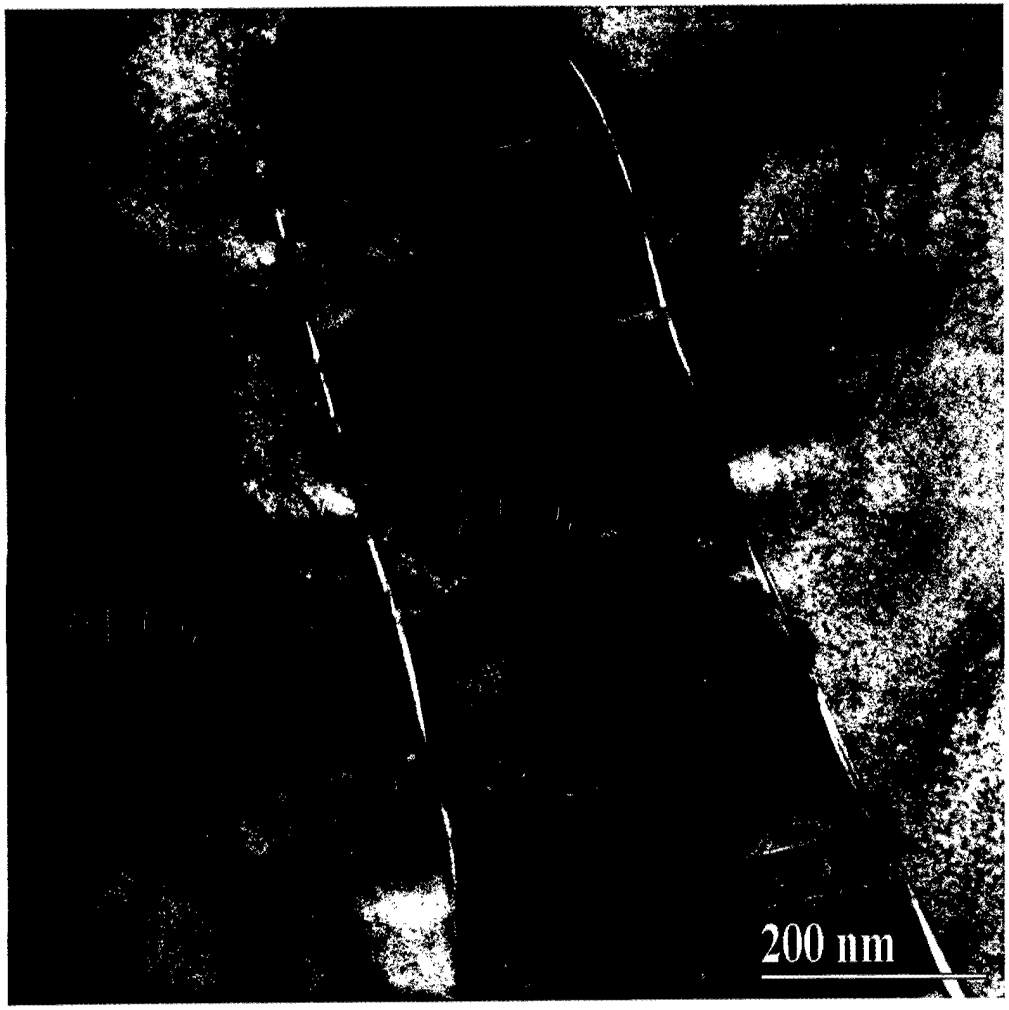

Cracks nucleate at the Al_2O_3-ZrO_2 interface as a result of the t --> m transformation

Microcraking
Crack growth Al_2O_3 - ZrO_2(m)

Cracks propagate upon cooling into the Al_2O_3 phase, which is under tensile residual stresses.

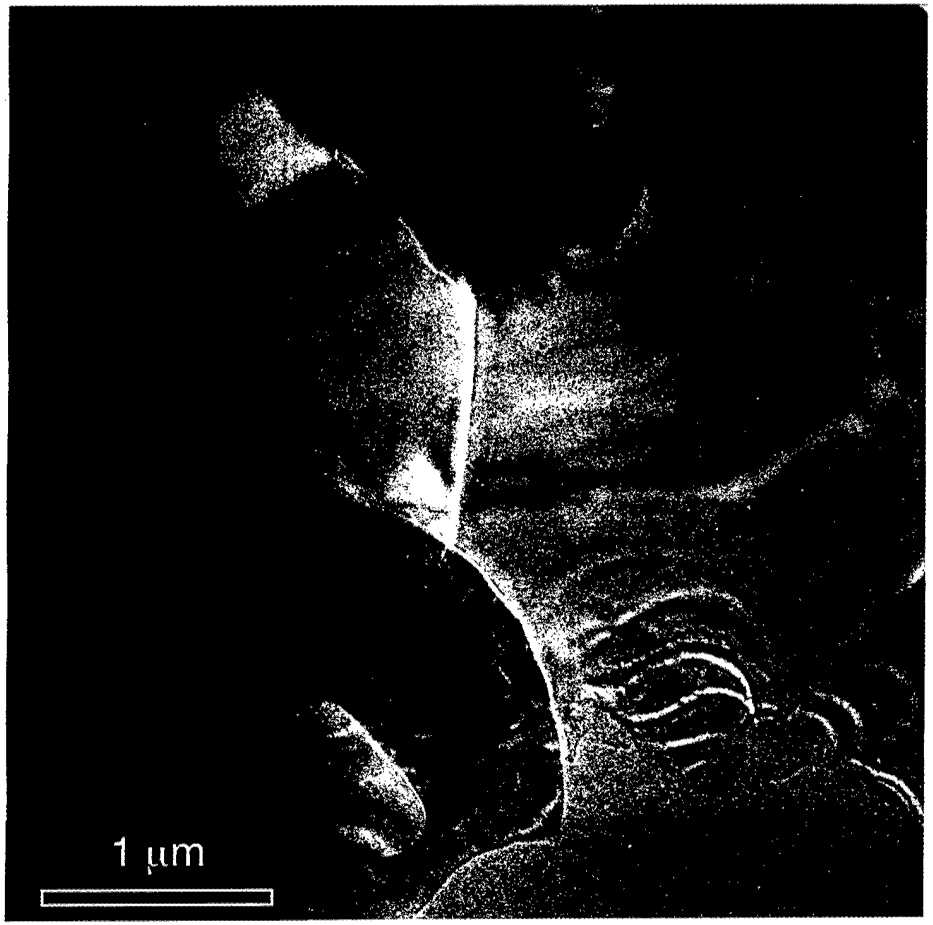

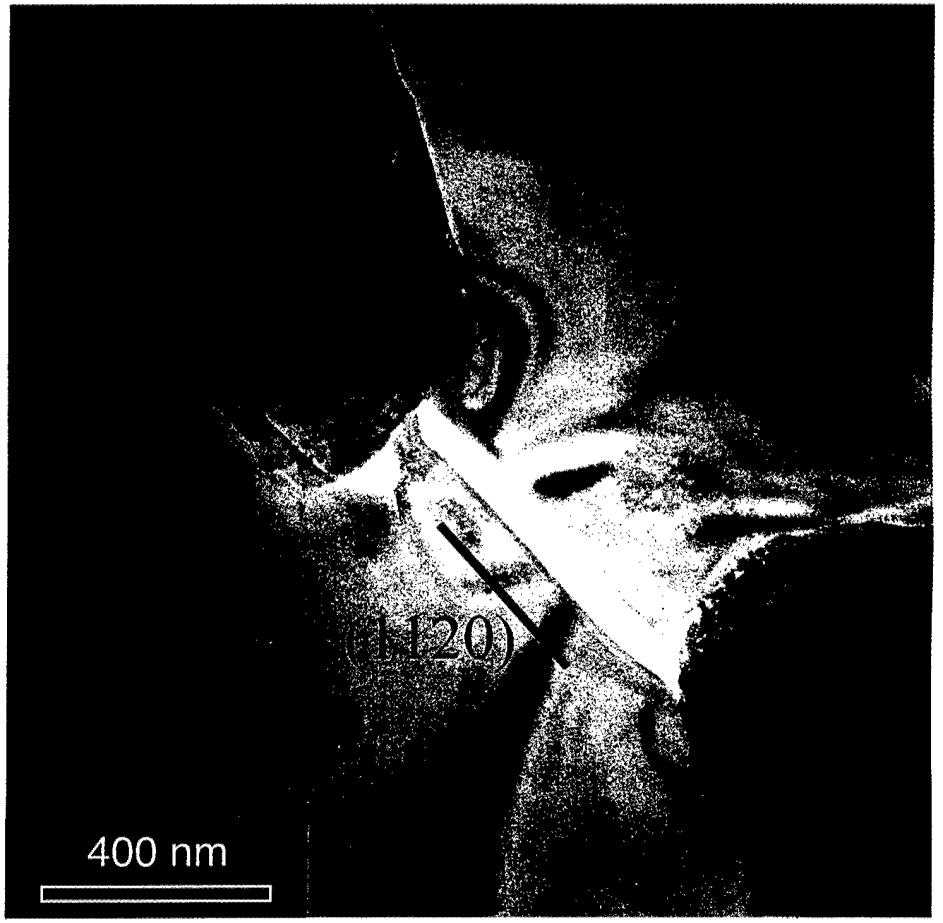

Mechanical testing techniques

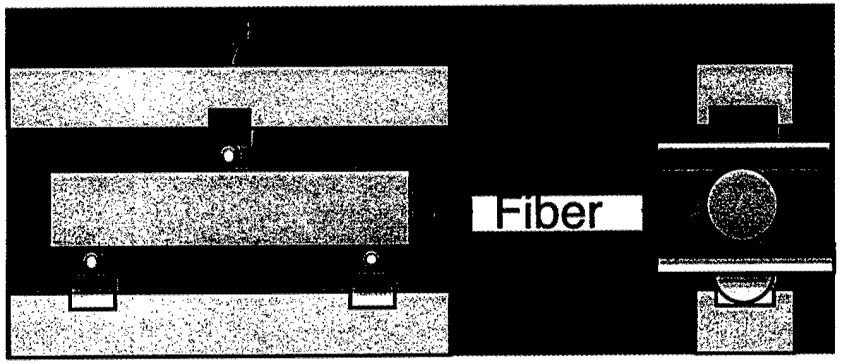

Flexure strength

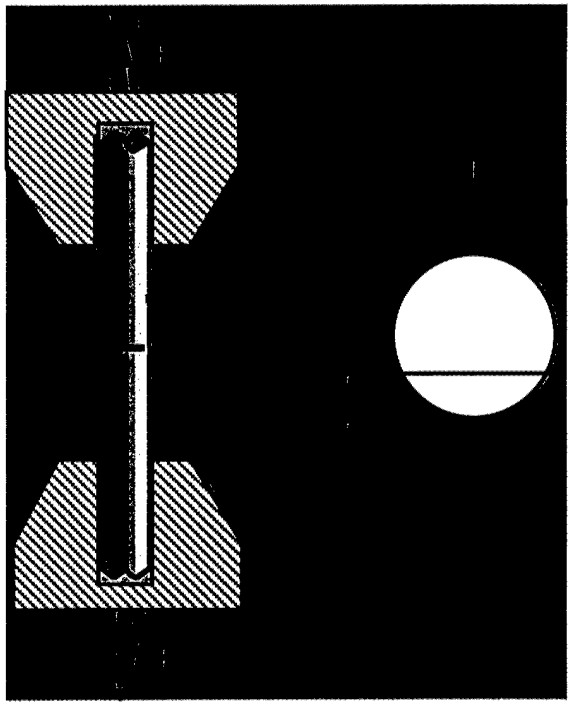

Fracture toughness

Ambient temperature

Colony structure (Y=10%)

E (GPa)	σ_f (MPa)	K_c (MPa$\sqrt{m}$)
343 ± 7	1130 ± 50	7.8 ± 0.3

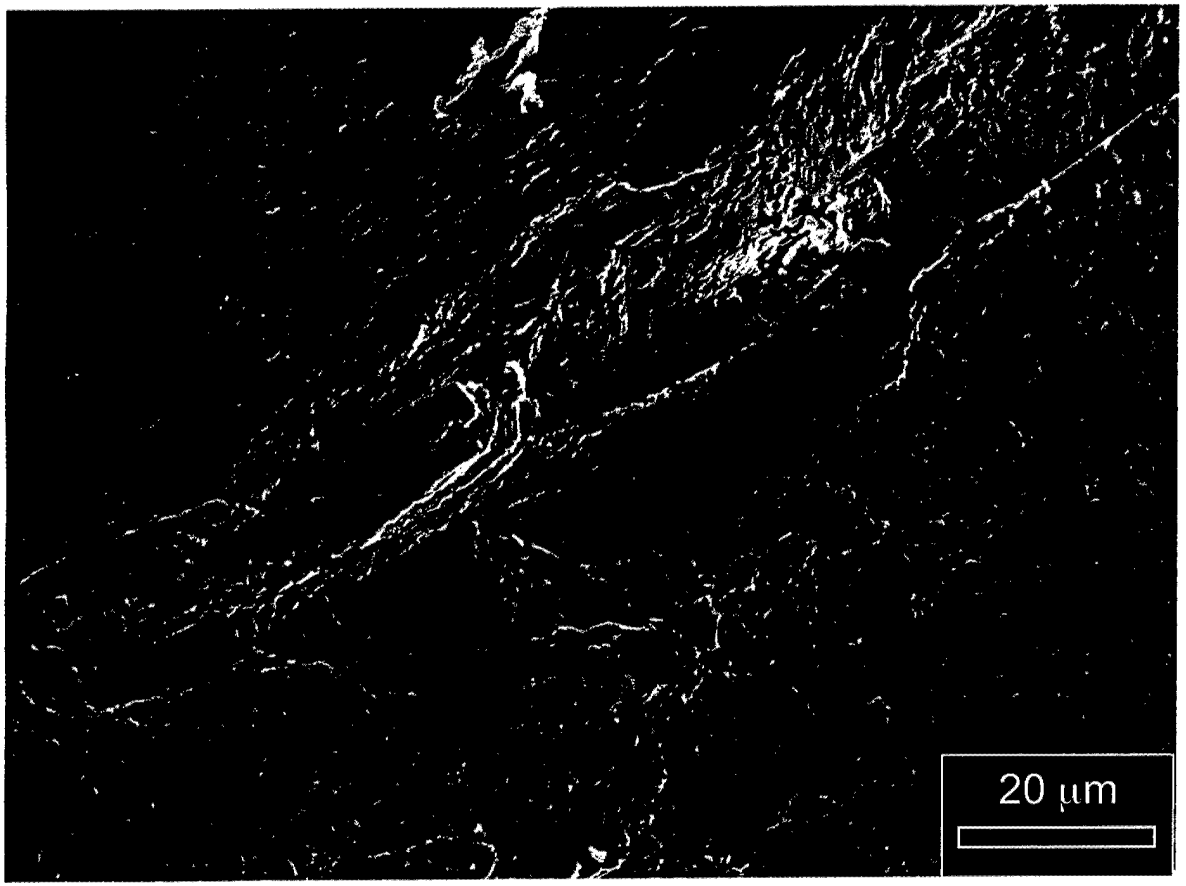

$$a_c = \frac{1}{\pi}\left[\frac{K_C}{0.65\ \sigma_f}\right]^2$$

$$a_c = 36\ \mu m$$

Ambient temperature flexure strength

Interpenetrating structure (banding)

Y(%)	0.5	3.3	12.2
σ_f (GPa)	0.6 ± 0.1	1.15 ± 0.08	1.13 ± 0.05
ZrO_2	mono	tetragonal	cubic

Y=0.5%:

- Low strength due to tensile residual stresses in Al_2O_3 and microcracking

Y=3.3 and 12.3:

- Excellent strength limited by inhomogeneities induced by banding
- No effect of t --> m transformation when Y=3.3%

Ambient temperature strength

Interpenetrating structure (homogeneous)

Y(%)3.312.2

$ZrO^{2}1$

σ

σ

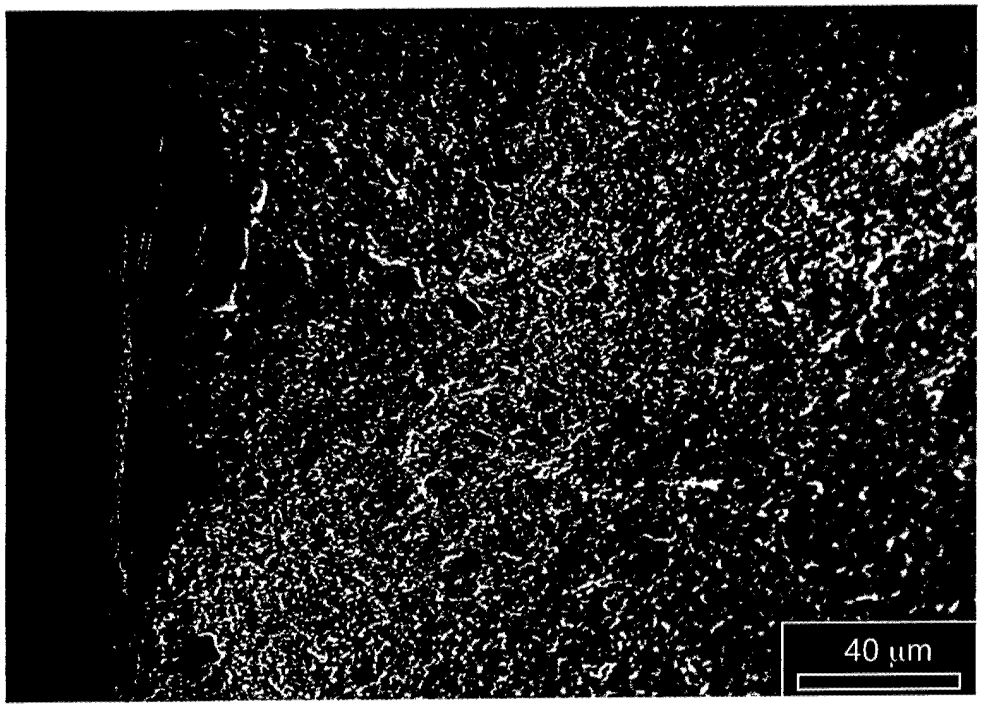

The critical defect of the homogeneous, interpenetrating structures are smaller

Microstructure - flexure strength

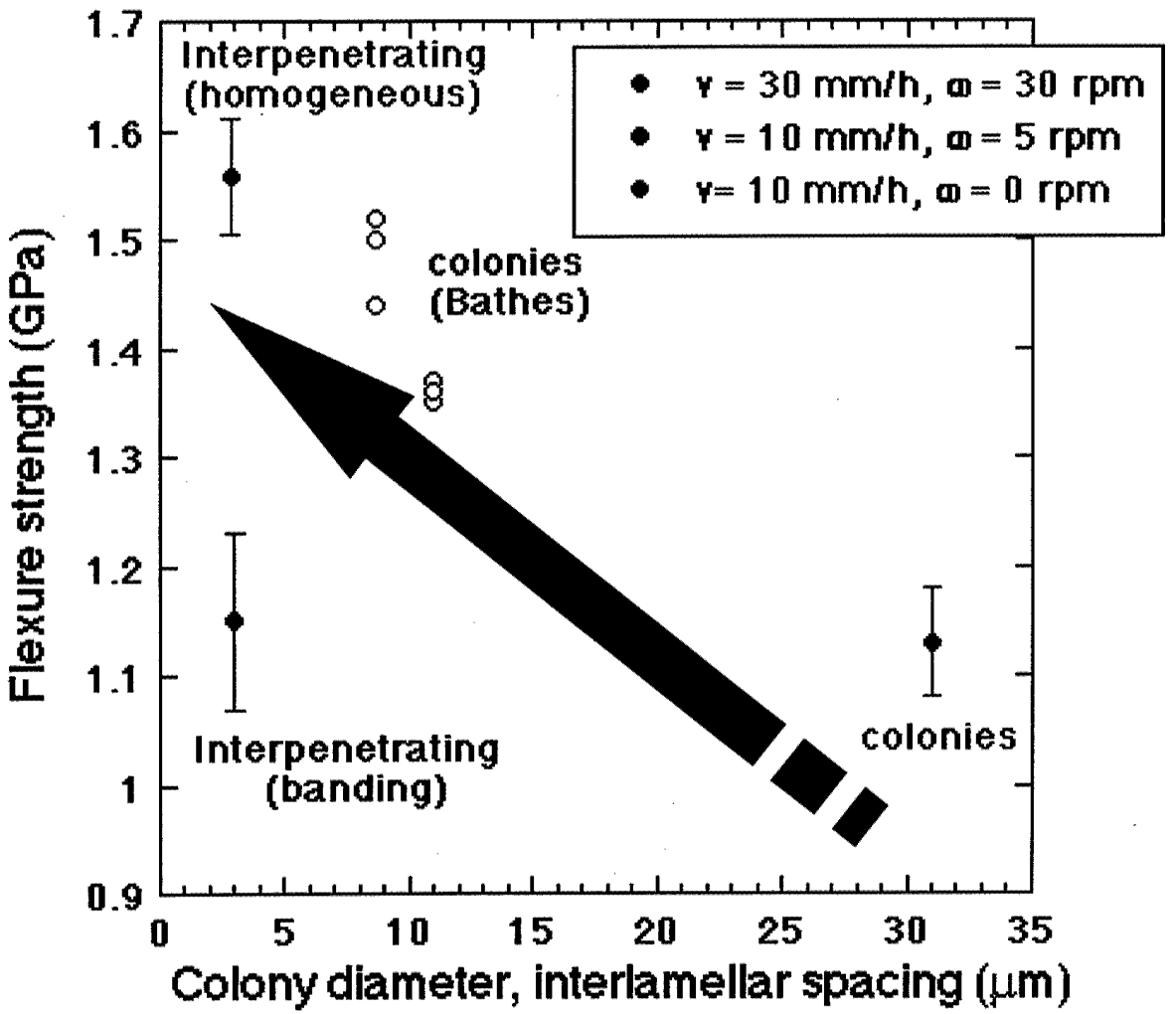

NANOSTRUCTURED MATERIALS BASED ON ALUMINA

L. Mazerolles, D. Michel, T. di Costanzo
CECM-CNRS UPR 2801
15 rue G. Urbain
94407 Vitry Cedex, France

J.-L. Vignes
LIMHP-CNRS UPR1311
99 avenue J.-B. Clément
93430 Villetaneuse, France

Z. Huang, D. Jiang
Shanghai Institute of Ceramics, Chinese Academy of Sciences, The State Key Laboratory of High Performance Ceramics & Superfine Microstructure
1295 Dingxi Road
Shanghai 200050, China

ABSTRACT

Alumina and alumina-based compounds were prepared using high specific surface area Al_2O_3 monoliths obtained by a novel preparation method. Impregnation with either liquid or vapor species followed by a thermal treatment under air or a reducing atmosphere leads to nanostructured spinels, mullite, Al_2O_3-metal or Al_2O_3-oxide composites.

INTRODUCTION

Many technological applications require materials with a controlled microstructure or/and chemical composition. In addition, low density or/and high specific surface area are needed for catalysts, sensors, filtration membranes, composites. Alumina and alumina-based compounds like spinel Al_2MgO_4 or mullite $Al_6Si_2O_{13}$ are of special interest because of their thermal stability and mechanical properties. This paper describes the synthesis of these compounds and various Al_2O_3-metal or Al_2O_3-oxide composites with nanometric grain size starting from porous alumina precursors.

NANOMETRIC ALUMINA AND SiO_2-MODIFIED ALUMINA

The starting materials are monolith alumina preforms consisting of nanometric amorphous or γ-aluminas. In particular, we have used porous monolithic samples obtained by room temperature oxidation of Al plates through a liquid mercury layer [1]. The composition and the structure of hydrated alumina filaments produced by this way were described by Pinel and Bennett [2]. The new process that we have developed produces shaped alumina monoliths at a typical rate of about 10 $mm.h^{-1}$ and the growth can be maintained during tens of hours. These alumina samples have a very light density ranging from 0.01 to 0.05×10^3 $kg.m^{-3}$ depending on the growth conditions.

After a dehydration treatment at 400°C, Al_2O_3 amorphous monoliths are obtained with a nanostructure consisting of tangled filaments of about 5 nm diameter with large voids between them (fig. 1). The material crystallises first into γ-alumina at 870°C and then transforms into θ-alumina above 1100°C. The average grain size is about 10 nm and the density remains very low ($< 0.1x10^3$ kg.m^{-3}). At 1200°C-1250°C, transformation into α-alumina occurs which leads to a microstructure with 200-300 nm grain size (fig. 2). Density increases by about one order of magnitude at the θ → α transition and above 1350°C densification occurs by sintering of the α alumina phase. Thus, various alumina samples with a controlled porosity can be prepared by adapting the thermal cycle.

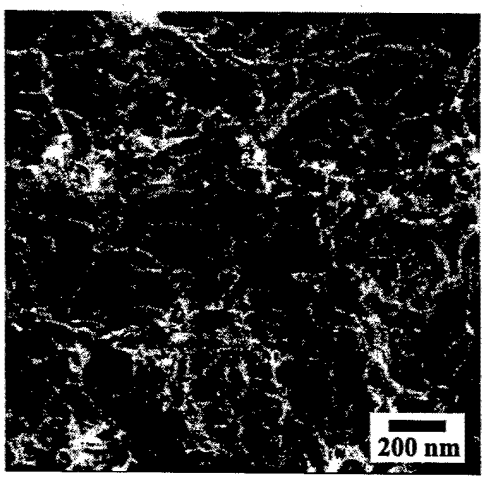

Figure 1 : raw alumina sample (second electron SEM image)

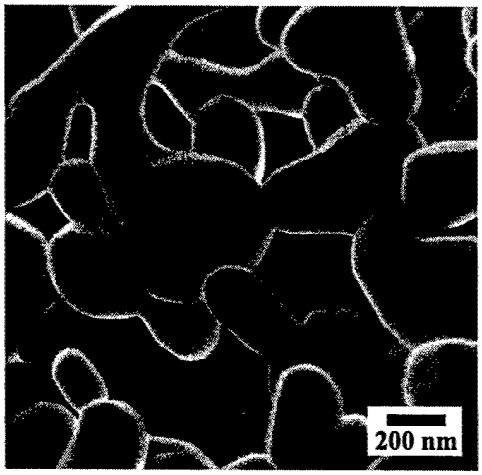

Figure 2 : after annealing at 1200°C (second electron SEM image)

The very high porosity of starting hydrated raw monoliths allows a rapid and homogeneous impregnation by gaseous species. In particular, a flow of silicon alkoxides diffusing inside the porous network is hydrolysed by the hydrated alumina surface. A remarkable modification of the thermal behaviour of alumina is obtained when a low amount of silica (about 6%°weight SiO_2) is incorporated by this way using trimethylethoxysilane (TMES). Without Si addition, the specific surface area of the raw material ranges between 300 and 420 m^2.g^{-1} depending on preparative conditions. After crystallization, the specific surface area stays relatively high (around 100 m^2.g^{-1}) and considerably decreases towards 5 m^2.g^{-1} at the θ→α transformation. Silica addition delays the transformation into α-Al_2O_3 up to 1400°C instead of 1200°C without silica addition. This chemical modification stabilizes aluminas with high specific surface area at higher temperature as shown on Figure 3.

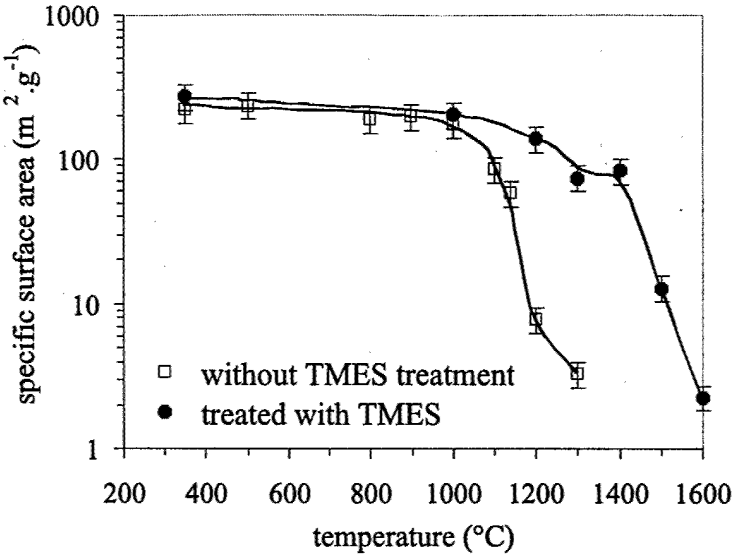

Figure 3 : Variation of the specific surface area versus temperature (4 hours annealing) for porous alumina impregnated or not by TMES.

NANOSTRUCTURED ALUMINA COMPOUNDS

a) nanometric mullite:

Similarly, silica can be incorporated using tetraethoxysilane (TEOS) vapour. This alkoxide with four hydrolysable functions permits higher silica additions than TMES. In particular, for the composition of mullite $3Al_2O_3$-$2SiO_2$, nanometric mullite monoliths are obtained after reaction. The average crystallite size determined from XRD line broadening is 10 nm at 1000°C and 30 nm at 1200°C (fig. 4). Transmission electron microscopy (TEM) images show that this size corresponds to crystalline particles (fig.5).

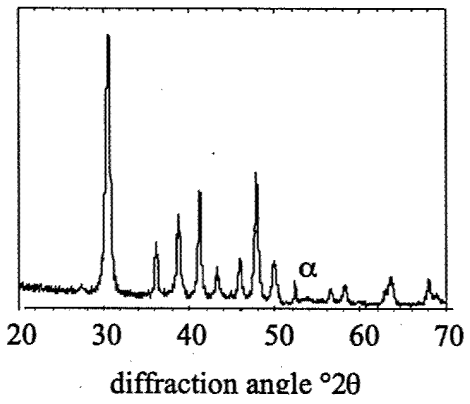

Figure 4 : X ray diffraction pattern of nanometric mullite prepared at 1200°C

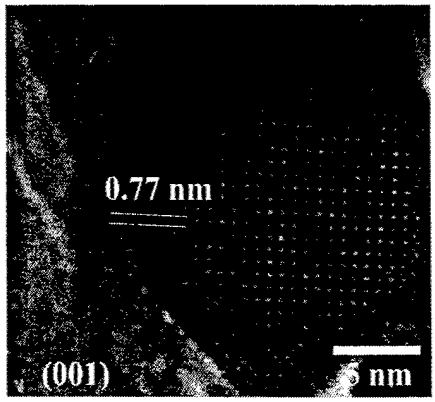

Figure 5 : HRTEM image of a mullite nanocrystal prepared at 1200°C

b) nanometric spinels:

Liquid impregnation is another way for chemical species to be introduced. After absorption of aqueous solutions of divalent metal salts by porous alumina preforms, calcination in air at low temperature (200-500°C) leads to nanometric MO particles (M= Mg, Ni). A subsequent heating treatment produces the reaction with alumina to form MAl_2O_4 spinel phases. For example, after impregnation of a porous alumina with a 300 nm grain size (fig. 2) with a magnesium nitrate solution, MgO is observed after annealing at 500°C, spinel appears at 900°C and the reaction is completed at 1200°C. After treatment at 1200°C, the spinel samples keeps the same microstructure as that of starting α-Al_2O_3. However, the transformation of each corundum grain into spinel produces aggregated spinel crystallites with a size around 100 nm. Similar behaviours and microstructures are obtained for $NiAl_2O_4$ and $CoAl_2O_4$ porous samples [3].

If the raw hydrated alumina is treated by TMES as previously exposed, spinels are formed at a lower temperature after a similar impregnation by Mg or Ni nitrate and annealing. Reaction into spinels occurs in that case at a finer scale. The reaction starts at 700°C and is completed at 1000°C in 4 hours for $MgAl_2O_4$ and $NiAl_2O_4$. This process allows to obtain nanometric spinels (fig. 6) with a microstructure similar to that of figure 1. The crystallite size stays in the range of 10 nm up to 1000°C (fig. 7). These samples display a high specific surface area which is higher than 40 $m^2.g^{-1}$ for preparation at temperatures of 700°C to 1100°C.

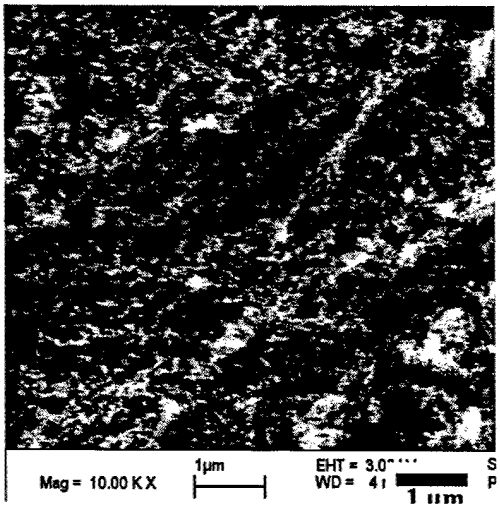

Figure 6 : SEM image of a nanometric $NiAl_2O_4$ spinel prepared at 1000°C

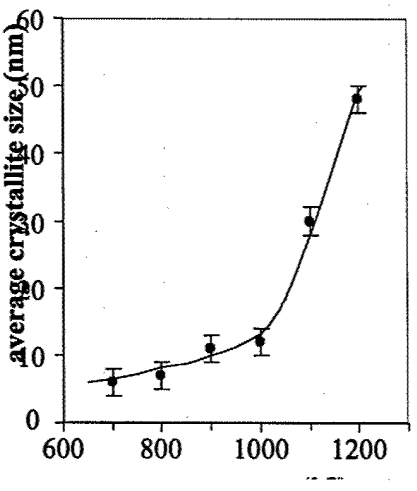

Figure 7 : Average crystallite size of $MgAl_2O_4$ spinel after 4 hour annealing

Al_2O_3-OXIDE and Al_2O_3-METAL NANOCOMPOSITES.

Particles of various oxides (TiO_2, ZrO_2, CeO_2) were introduced on alumina preforms by liquid impregnation of salt solutions. The size of crystallites covering porous aluminas is in the range of 5 to 20 nm depending on conditions of calcination and crystallisation [3-4]. This technique has been also used to prepare WO_3/Al_2O_3 and MoO_3/ Al_2O_3 catalysts for cracking and skeleton isomerization of hexenes [5-6].

The reduction of nickel or cobalt oxides dispersed in γ or α alumina under dihydrogen or a CO/CO_2 buffer atmosphere gives metal-ceramic composite samples. Another route used was to reduce the spinel formed by the reaction discussed previously. Depending on the preparative route, the temperature of reduction (between 650 and 1025°C) and the oxygen partial pressure (between 10^{-13} to 10^{-20} atm), metallic particles have a size distribution varying from 10 nm to 100 nm [7]. These composites consist of Ni or Co particles dispersed in a submicronic α alumina porous matrix or in a nanometric γ or θ phase (fig. 8).

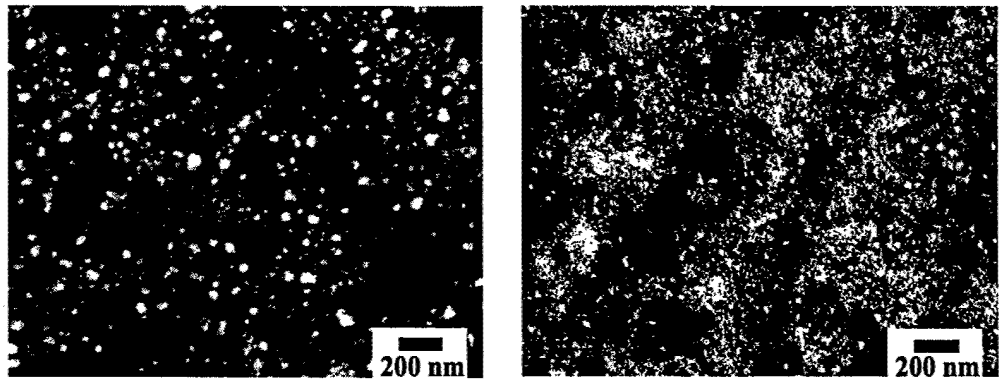

Figure 8 : Nanocomposites consisting of Ni particles dispersed in γ alumina obtained by reduction of NiO at 700°C under a CO/CO_2 controlled oxygen pressure ($pO_2 = 10^{-20}$atm). Left part : 10% volume Ni, right part: 5volume% Ni. Backscattered electron SEM images.

CONCLUSIONS

This paper presents various examples of preparation of nanostructured porous materials based on alumina. The insertion of chemical species by gaseous and liquid absorption into porous preforms followed by a thermal treatment leads to the synthesis of alumina compounds with a nanometric or submicronic microstructure. Metal-alumina nanocomposites can also be prepared by this way and recently carbon nanotubes were grown inside such aluminas from cracking of an organic precursor [8].

ACKNOWLEDGMENTS

The work on metal-ceramic nanocomposites was achieved thanks to the support of the French-Chinese Association for Scientific and Technological Research (AFCRST) within the framework of the Advanced Research Programme on Materials PRA MX00-07.

REFERENCES

[1] J.-L. Vignes, L. Mazerolles, D. Michel, "A novel method for preparing porous alumina objects" *Key Eng. Mater.*, **132-136** 432-435 (1997)

[2] M. R. Pinel, J. E. Bennett, "Voluminous oxidation of aluminium by continuous dissolution in a wetting mercury film" *J. Mater. Sci.*, **7** 1016-1026 (1972)

[3] L. Mazerolles, D. Michel, J.-L. Vignes, T. Di Costanzo, "New Developments in nanometric porous mullite, spinel and aluminas", *Ceramic Transactions,* 135, 227-39, The American Ceramic Society, Westerville, OH, USA (2002)

[4] T. Di Costanzo, C. Frappart, L. Mazerolles, J.-C. Rouchaud, M. Fedoroff, D. Michel, M. Beauvy, J.-L. Vignes , "Fixation of various wastes in porous monolithic aluminas", *Ann. Chim. Mat. (in French)* , 26 (2), 67-78 (2001)

[5] V. Logie, G. Maire, D. Michel and J.-L. Vignes, "Skeletal isomerization of hexenes on tungsten oxide supported on porous α-alumina", *J. Catalysis*, 188, 90-101 (1999)

[6] F. Di-Grégorio, V. Keller, T. Di Costanzo, J.-L. Vignes, D. Michel and G. Maire, "Cracking and skeleton isomerization of hexenes on acidic MoO_3-WO_3/α-Al_2O_3 oxide", *Applied Catalysis A*, 218, 13-24 (2001)

[7] Z. Huang, D. Jiang, D. Michel, L. Mazerolles, A. Ferrand, T. Di Costanzo, J.-L. Vignes, "Nickel-alumina nanocomposite powders prepared by novel in-situ chemical reduction", *J. Materials Research*, 17, 3177-3181 (2002)

[8] J. B. Bai, J.-L. Vignes, D. Michel, "A novel method for preparing preforms of porous alumina and carbon nanotubes by CDV", *Advanced Engineering Materials*, 4, 701-703 (2002)